Regression Discontinuity Designs Under Interference

Elena Dal Torrione[1], Tiziano Arduini[2], Laura Forastiere[1]

[1]Department of Biostatistics, Yale University
[2]Department of Economics and Finance, Tor Vergata University of Rome

Abstract

We extend the continuity-based framework to Regression Discontinuity Designs (RDDs) to identify and estimate causal effects under interference when units are connected through a network. Assignment to an "effective treatment," combining the individual treatment and a summary of neighbors' treatments, is determined by the unit's score and those of interfering units, yielding a multi-score RDD with complex, multidimensional boundaries. We characterize these boundaries and derive assumptions to identify boundary causal effects. We develop a distance-based nonparametric estimator and establish its asymptotic properties under restrictions on the network degree distribution. We show that while direct effects converge at the standard rate, the rate for indirect effects depends on the number of scores fixed at the cutoff. Finally, we propose a variance estimator accounting for network correlation and apply our method to PROGRESA data to estimate the direct and indirect effects of cash transfers on school attendance.

Keywords: Causal inference, regression discontinuity, interference, networks, local polynomials, statistical dependence.

1 Introduction

In a Regression Discontinuity Design (RDD), the treatment assignment is determined by whether an observed variable— known as "score" or "forcing" variable—exceeds a given cutoff. For instance, in conditional cash transfer (CCT) programs, eligibility for financial aid hinges on the household's poverty index relative to a predetermined threshold (e.g. Battistin and Rettore, 2008; Attanasio et al., 2021). Beyond CCT programs, RDDs have been applied across diverse domains, including education (e.g., Jacob and Lefgren, 2004), the labour market (e.g., Battistin and Rettore, 2002), and medicine, where eligibility for treatment is often determined by clinical thresholds such as age for vaccination (Basta and Halloran, 2019).

The deterministic nature of the RDD assignment mechanism violates the overlap assumption and prevents the use of covariate adjustment methods, common in observational studies (e.g. Hernan and Robins, 2023). However, since its early development (Hanh et al., 2001; Lee, 2008), the analysis of RDDs has relied on an assumption of continuity of the outcome regression functions to allow the identification of the average treatment effect at the cutoff. RDDs have gained renewed interest in recent years, leading to significant methodological advancements (e.g., Díaz and Zubizarreta, 2023; Imbens and Wager, 2019; Calonico et al., 2014; Kolesár and Rothe, 2018).

However, the role of interference in RDDs remains underexplored. Interference arises whenever the "treatment" on one unit affects the outcome of another unit (Cox, 1958), a common occurrence in settings where units interact physically or socially. Interference can affect RDD settings. Exploiting the two-stage partial population design, Angelucci and De Giorgi (2009) show that the Mexican PROGRESA/Oportunidades program increased consumption levels among ineligible households through informal loans from beneficiaries, while Lalive and Cattaneo (2009) find spillover effects on school attendance among ineligible children living in villages assigned to the program due to social interactions. Interference can also emerge in health and education interventions with eligibility cutoffs. In public health, providing vaccines to eligible individuals can indirectly protect ineligible individuals by lowering the community viral load. In education, retaining students based on standardized test score can affect other students' academic performance through classroom dynamics.

While interference is sometimes viewed as a nuisance when estimating treatment effects (e.g., Sobel, 2006), spillover effects have been recognized to be of substantive interest. Positive spillover effects can be leveraged to achieve cost-effective interventions: designing optimal policies allocating financial aid to a targeted subset of families can increase overall school attendance in a village through beneficial spillover effects (e.g. Viviano, 2024), and partial vaccination can achieve community-wide immunity (Halloran and Struchiner, 1995). Conversely, negative spillovers, such as reduced employability among those excluded from job training programs (Crépon et al., 2013), highlight the need for preventive measures to preserve policy effectiveness.

The literature on causal inference under interference has grown rapidly in recent years. A common assumption is partial interference, which allows interference within clusters but not across clusters (Sobel, 2006). Partial interference is used in two-stage randomized experiments to estimate direct and spillover effects (Hudgens and Halloran, 2008; Liu and Hudgens, 2014; Baird et al., 2018). In observational studies, inverse-probability-weighted (IPW) estimators have also been derived under the partial interference assumption (Tchetgen Tchetgen and VanderWeele, 2012; Perez-Heydrich et al., 2014; Papadogeorgou et al., 2019). Other works have analyzed more complex interference mechanisms, such as when units are connected through a network, in experimental studies (Bowers et al., 2013; Aronow and Samii, 2017; Athey et al., 2015; Leung, 2020; Viviano et al., 2025) and observational studies (Sofrygin and van der Laan, 2017; Forastiere et al., 2021, 2022; Ogburn et al., 2022). In experimental studies with network interference, several methods of analysis have been used, such as randomization tests (Bowers et al., 2013; Athey et al., 2015; Basse et al., 2019), IPW-type estimators and cell-means estimators (Aronow and Samii, 2017; Vazquez-Bare, 2022), and regression-based approaches (Leung, 2020). While approaches to observational studies on networks include generalized propensity score-based estimators (Forastiere et al., 2021, 2022), IPW estimators (Liu et al., 2016), targeted maximum likelihood estimator (TMLE) (Sofrygin and van der Laan, 2017; Ogburn et al., 2022), and graph neural networks (GNN) (Leung and Loupos, 2023), little attention has been paid to interference in the context of RDDs.

This paper develops a methodological framework that extends the continuity-based RDD paradigm to accommodate interference. We formalize interference via exposure mappings (Sofrygin and van der Laan, 2017; Aronow and Samii, 2017; Forastiere et al., 2021), defined over specified interference sets (e.g., networks or clusters), allowing each unit's potential outcome to depend on a bivariate "effective treatment", i.e., the binary individual treatment and a spillover exposure, resulting from applying the exposure mapping to the neighbors' treatments.

Our framework's key feature is that, although each unit is characterized by a single score, interference induces a multiscore structure: the effective treatment assignment becomes a deterministic function of both the individual score and the scores of units within the interference set. As a result, RDDs under interference can be reframed and analyzed as a multiscore RDD characterized by multidimensional boundaries, allowing us to build on and extend existing methodological tools from the literature on multivariate RDDs (Imbens and Zajonc, 2011; Keele and Titiunik, 2015). Unlike in standard multivariate RDDs, however, these boundaries arise from the interference mechanism and the RDD individual treatment rule, rather than being given ex ante. Within this framework, we provide a characterization of these multivariate boundaries and define new causal estimands, i.e., boundary direct effects at a given spillover exposure and boundary indirect effects comparing values of the spillover exposure. We further define the overall direct effect at the cutoff and an overall indirect effect of having one treated neighbor. We provide identification results by extending the standard RDD continuity assumptions. In addition, we show that the traditional RDD approach identifies the overall direct effect at the cutoff, even if interference is not accounted for.

We propose an estimation method that collapses multivariate scores into a univariate distance from the boundary, which is then used as the running variable in a local polynomial regression. Our estimator builds on the distance-based approach commonly used in multivariate RDDs (e.g. Keele and Titiunik, 2015). To our knowledge, however, the distance-based estimator in multivariate RDDs has not yet received a formal analysis in the literature. Our results thus offer theoretical insights of independent interest for multivariate RDDs beyond interference, especially in settings with complex multiscore structures. We show that the convergence rate of our estimator is determined by the codimension of the effective treatment boundary, that is, by the number of individual and neighbors' score components fixed at the cutoff. Our analysis shows that direct effects can be estimated at the same convergence rate as standard no-interference RDD estimators, whereas indirect effect estimators may converge more slowly. We also develop bias-corrected versions of these estimators. For estimation of the overall direct effect at the cutoff, we rely on the canonical local linear RDD estimator and show its convergence at the standard RDD rate. We further introduce a local polynomial estimator of the overall indirect effect, which can likewise be estimated at the standard RDD rate.

A characteristic of our setting is the dependence induced by network structures in both outcome and score variables, as well as by overlapping interference sets. In line with the literature on local polynomial estimation with dependent data, we establish that under a weak dependence condition limiting the growth rate of network links, our estimators maintain the same asymptotic distribution as under independent data. Despite this result suggesting that inference may proceed as with i.i.d. data, we argue that network-induced dependence must be explicitly accounted for. In particular, the possible presence of a non-negligible fraction of individuals sharing the same distance measure and the fixed bandwidth perspective of bias-correction methods can distort conventional inference. We therefore develop a novel variance estimator that accounts for network-induced correlation. To the best of our knowledge, aside from Bartalotti and Brummet (2017)-who analyzes clustered settings where all units in a cluster lie on the same side of the cutoff- this is the first contribution to address network dependence in RDDs, even regardless of the presence of interference.

Our analysis is complemented by a simulation study and an empirical application using data from PROGRESA/Oportunidades, where we estimate the direct and indirect effects of the program on children's school attendance, defining interference sets by village, grade, and gender. We find an overall direct effect of about 0.07, closely matching the direct effects reported by Lalive and Cattaneo (2009) and Arduini et al. (2020). In contrast, the overall indirect effect is notably larger than the indirect effect of about 0.02 found in these studies. Importantly, our estimates capture local boundary effects within treated villages, whereas existing estimates, relying on on village-level randomization, compare eligible and ineligible individuals across treated and untreated villages, thus reflecting average effects over broader populations.

To our knowledge, the only works that address interference in RDDs are Aronow et al. (2017), Auerbach et al. (2024), and Borusyak and Kolerman-Shemer (2024). Aronow et al. (2017) propose a difference-in-means estimator for the average direct effect near the cutoff under a local randomization assumption. In contrast, our approach provides an identification and estimation strategy for direct and indirect effects within the continuity-based framework. Auerbach et al. (2024) analyzes a linear-in-means model where a unit's neighborhood consists of units with scores within a specified radius from that unit's score. Our framework instead defines interference sets based on a specified network structure rather than proximity in the score space, and does not impose linear-in-means assumptions on the potential outcome model. However, unlike linear-in-means models, which allow interference to decay with path distance, our framework restricts interference only within the interference set. Moreover, we formalize interference as a multiscore RDD, defining causal effects conditional on individual and neighborhood scores at boundaries where the effective treatment changes discontinuously, whereas Auerbach et al. (2024) focuses on the linear-in-means direct and spillover coefficients, which are functions of the individual score evaluated at the cutoff. Finally, Borusyak and Kolerman-Shemer (2024) studies RDDs where units' treatment status is an aggregate across multiple discontinuity events. Their estimation method recovers in a simple way a local marginal effects of changing the treatment of lower-level units on the upper-level units' outcome. In contrast, our formalization of interference as a multiscore RDD accommodates a richer set of direct and spillover effects, albeit with greater methodological complexity.

The paper is organized as follows: Section 2 introduces the notation and methodological framework; Section 3 illustrates our identifying assumptions and results; Section 4 describes our estimation method; Section 5 includes the simulation study; Section 6 provides the empirical illustration; and Section 7 concludes.

2 Framework

2.1 Interference

Let us consider a set $\mathcal{N}$ of n units, indexed by $i = 1, ..., n$. Such units are connected through a set of edges, or links, $\mathcal{E}$ with generic element $(i, j) = (j, i)$ representing the presence of a link between i and j. The pair $G = (\mathcal{N}, \mathcal{E})$ is an undirected network that can be represented by an adjacency matrix $\boldsymbol{A}$, with generic entry $A_{ij} = 1$ if unit i and j are linked and equal to 0 otherwise. Each unit is associated with a set of random variables, including a score variable $X_i \in \mathcal{X} \subseteq \mathbb{R}$, a binary treatment assignment $D_i \in \{0, 1\}$, and an outcome variable $Y_i \in \mathbb{R}$. We denote by $\boldsymbol{X}$, $\boldsymbol{D}$, and $\boldsymbol{Y}$ the n-vectors collecting the score, the treatment, and the outcome variables, respectively, for all n units. Let us denote as $Y_i(\boldsymbol{d})$, with $\boldsymbol{d} \in \{0, 1\}^n$, the potential outcome we would observe on unit i if the treatment vector were set to $\boldsymbol{d}$ in the sample $\mathcal{N}$. Because units are causally connected in this setting, in their most general form, potential outcomes depend on the complete treatment vector.

We introduce an interference assumption that restricts interference within specified *interference sets* and uses an *exposure mapping function* to describe the interference mechanism. Specifically, for each unit $i \in \mathcal{N}$ we define an interference set $\mathcal{S}_i \subseteq (\mathcal{N} \setminus \{i\})$. The interference set $\mathcal{S}_i$ may contain all units that are connected to i by a link in $\boldsymbol{A}$, i.e., the network neighborhood (network neighborhood interference, Forastiere et al. 2021). When units are grouped in clusters, such as villages, and schools, $\mathcal{S}_i$ can include only units in the same cluster as i (partial interference, Sobel 2006). This scenario is a particular case of neighborhood interference represented by a block-diagonal adjacency matrix. The interference set $\mathcal{S}_i$ can also be defined based on network (or cluster) features and covariates. For example, in school settings, children may interact more with classmates of the same gender (Shrum et al., 1988), so that $\mathcal{S}_i$ consists of individuals within the same school and gender group. We refer to elements of $\mathcal{S}_i$ generically as *neighbors* of i, and we let $\boldsymbol{D}_{\mathcal{S}_i}$ and $\boldsymbol{X}_{\mathcal{S}_i}$, with values $\boldsymbol{d}_{\mathcal{S}_i}$ and $\boldsymbol{x}_{\mathcal{S}_i}$, collect the treatments and the score variables of units in $\mathcal{S}_i$.

Additionally, we define the exposure mapping as a function that maps the treatment vector within $\mathcal{S}_i$ to an exposure value: $g : \{0,1\}^{|\mathcal{S}_i|} \to \mathcal{G}_i$, where $\mathcal{G}_i$ is a discrete space of equal or lower dimension than $\{0,1\}^{|\mathcal{S}_i|}$. Let $G_i \in \mathcal{G}_i$ be the resulting random variable, with $G_i = g(\boldsymbol{D}_{\mathcal{S}_i})$. Without loss of generality, we refer to G_i as the *neighborhood treatment*. Common examples of exposure mapping functions include the number or proportion of treated neighbors, $G_i = \sum_{j\in\mathcal{S}_i} D_j$ and $G_i = \frac{\sum_{j\in\mathcal{S}_i} D_j}{|\mathcal{S}_i|}$. Another type is the *one treated* exposure mapping, $G_i = \mathbb{1}\{\sum_{j\in\mathcal{S}_i} D_j > 0\}$, which takes value one if there is at least one treated unit in $\mathcal{S}_i$, and zero otherwise. Our definition also accommodates vector-valued exposure mappings that classify neighbors into types (e.g., parents, influencers), as in Qu et al. (2021), allowing outcomes to depend, for instance, on the proportion of treated units in each type. However, we require that the range $\mathcal{G}_i$ be discrete, and we therefore rule out continuously valued exposure mappings, such as weighted averages of neighbors' treatments with weights based on continuous covariates. We make the following assumptions.

Assumption 1 (Consistency)**.** *For all $i \in \mathcal{N}$, if $\boldsymbol{D} = \boldsymbol{d}$ then $Y_i = Y_i(\boldsymbol{d})$.*

Assumption 2 (Interference)**.** *For all $i \in \mathcal{N}$, and for all $\boldsymbol{D}$, $\boldsymbol{D}' \in \{0,1\}^n$ such that $D_i = D'_i$ and $g(\boldsymbol{D}_{\mathcal{S}_i}) = g(\boldsymbol{D}'_{\mathcal{S}_i})$, the following holds: $Y_i(\boldsymbol{D}) = Y_i(\boldsymbol{D}')$.*

Assumption 1 is the standard "consistency" assumption, which ensures that potential outcomes are well-defined by excluding multiple versions of the treatment. Assumption 2, "interference," is our interference assumption which allows the potential outcomes of unit i to depend on the treatments within $\mathcal{S}_i$, but not outside of it, and only through the exposure mapping. Assumption 1 and Assumption 2 together constitute an extended version of the SUTVA under which potential outcomes can be indexed by the value of the *individual treatment* D_i and by the value of the *neighborhood treatment* G_i. The tuple (D_i, G_i) is then a bivariate treatment where D_i is the binary treatment assigned to each unit i, and G_i is a summary of the treatment vector in the interference set. Following Manski (2013), we refer to this as *effective* *treatment*. Thus, under Assumptions 1 and 2, $Y_i(d, g)$ denotes the potential outcome of unit i if $D_i = d$ and if $G_i = g$, i.e., if the summary of treatment vector within the interference set of i has value g through the function $g(\cdot)$[1].

The number of potential outcomes for each unit under interference depends on the specification of the interference set and the exposure mapping. For instance, with one treated exposure mapping, G_i takes only two values. Finally, Assumption 2 implies that the interference sets and the exposure mapping are correctly specified.

We assume that the network $\boldsymbol{A}$ is fixed and constant during the study; it is not affected by the treatment vector $\boldsymbol{D}$ and is fully observed, ensuring that the interference sets are also observed and unaffected by the treatment. In addition, the data $(\boldsymbol{X}, \boldsymbol{D}, \{Y_i(d, g)\}_{i\in\mathcal{N},\, d\in\{0,1\},\, g\in\mathcal{G}_i})$ are jointly distributed according to $P(\boldsymbol{A})$, a data-generating distribution depending on $\boldsymbol{A}$, that is, we assume that we have access to a random draw of these variables from this distribution for our population of n connected units. Our approach, which treats potential outcomes as random variables, is known as a model-based perspective (Hernan and Robins, 2023), and is similar to, e.g., Ogburn et al. (2022), and Leung and Loupos (2023), who consider an interference setting where the observed data are generated from a random process conditional on the network.

2.2 Effective Treatment Rule

In RDDs, the treatment is assigned to each unit according to whether the individual score X_i exceeds a known cutoff c. We express the individual treatment assignment through the following *individual treatment rule*:

Assumption 3 (Individual treatment rule)**.** *For all $i \in \mathcal{N}$*

$$D_i = \mathbb{1}(X_i \geq c) = t(X_i) \tag{1}$$

Under Assumption 3 the treatment assignment is a deterministic function of the score variable, and only units scoring above the cutoff are assigned to the treatment. In

[1]Note that potential outcomes for units whose interference set is empty are not defined. In this work, we leave such potential outcomes undefined. However, other assumptions are possible, such as defining outcomes of the form $Y_i(d)$ for these units.

sharp RDDs, when the treatment receipt coincides with the assignment, the treatment receipt follows the same individual treatment rule as in (1) (e.g., Hanh et al., 2001). On the contrary, in fuzzy RDDs, when some units do not comply with the assignment, the treatment receipt is no longer a deterministic function of the score (Trochim, 1984). This paper focuses on the causal effect of the treatment assignment D_i, referred to as the intention-to-treat (ITT) effect in fuzzy settings. For simplicity, we still refer to D_i as the treatment variable.

Assumption 3 leads to the following property:

Property 1 (Non-probabilistic individual assignment)**.** *For all $i \in \mathcal{N}$, $\mathbb{P}(\,D_i = 1 \,|\, X_i = x_i\,) = 0$ for $x_i < c$ and $\mathbb{P}(\,D_i = 1 \,|\, X_i = x_i\,) = 1$ for $x_i \geq c$.*

With a non-probabilistic individual assignment, it is not possible to observe both treated and untreated units with the same value of the individual score X_i.

Crucially, the non-probabilistic nature of the individual assignment mechanism induces a non-probabilistic assignment mechanism of the effective treatment in our interference framework under interference. For each unit $j \in \mathcal{S}_i$, the treatment is assigned according to the individual treatment rule in Eq (1), i.e., $D_j = t(X_j)$. Therefore, G_i can be rewritten as follows:

$$G_i = g(\boldsymbol{D}_{\mathcal{S}_i}) = g(\{t(X_j)\}_{j \in \mathcal{S}_i}) = e(\boldsymbol{X}_{\mathcal{S}_i}) \tag{2}$$

Combining Eq (1) and Eq (2), we obtain a deterministic *effective treatment rule*:

$$(D_i, G_i) = (t(X_i), e(\boldsymbol{X}_{\mathcal{S}_i})) = \boldsymbol{F}(X_i, \boldsymbol{X}_{\mathcal{S}_i}) \tag{3}$$

From Eq. (3), it is clear that the effective treatment is governed by multiple scores. Therefore, RDDs under interference can be reframed as a "multiscore design" (Reardon and Robinson, 2012). As opposed to typical multiscore RDDs, where the individual treatment is assigned based on multiple individual scores (e.g., math and reading test scores, Matsudaira, 2008), here the first component of the effective treatment, the individual treatment D_i, is determined by the individual one-dimensional score X_i, and the second component, the neighborhood treatment G_i, is determined by the scores of units in the interference set $\boldsymbol{X}_{\mathcal{S}_i}$. Thus, the effective treatment is determined by multiple scores of the same variable on different units.

Let us define the multiscore space $\mathcal{X}_{i\mathcal{S}_i} \subseteq \mathbb{R}^{|\mathcal{S}_i|+1}$ as the space of all elements

$(x_i, \boldsymbol{x}_{\mathcal{S}_i})$. The effective treatment rule defines a partition of $\mathcal{X}_{i\mathcal{S}_i}$ into *effective treatment regions*, defined as

$$\mathcal{X}_{i\mathcal{S}_i}(d,g) = \{(x_i, \boldsymbol{x}_{\mathcal{S}_i}) \in \mathcal{X}_{i\mathcal{S}_i} : \boldsymbol{F}(x_i, \boldsymbol{x}_{\mathcal{S}_i}) = (d,g)\}$$

where the probability of receiving the effective treatment (d,g) is equal to one. Formally, we can state the following property of RDDs under interference, characterized by a non-probabilistic individual treatment assignment (Property 1) and an interference mechanism defined in Assumption 2.

Property 2 (Non-probabilistic effective treatment assignment)**.** *For all $i \in \mathcal{N}$, for all $d \in \{0,1\}$, and for all $g \in \mathcal{G}_i$*

$$\mathbb{P}(\, D_i = d, G_i = g \,|\, (X_i, \boldsymbol{X}_{\mathcal{S}_i}) = (x_i, \boldsymbol{x}_{\mathcal{S}_i})\,) = \begin{cases} 1 & (x_i, \boldsymbol{x}_{\mathcal{S}_i}) \in \mathcal{X}_{i\mathcal{S}_i}(d,g) \\ 0 & (x_i, \boldsymbol{x}_{\mathcal{S}_i}) \notin \mathcal{X}_{i\mathcal{S}_i}(d,g) \end{cases}$$

An immediate consequence of Property 2 is that conditional on the individual score X_i and neighborhood $\boldsymbol{X}_{\mathcal{S}_i}$ potential outcomes are independent of the effective treatment, as stated in the following property.

Property 3 (Unconfoundedness)**.** *For all $i \in \mathcal{N}$, for all $d \in \{0,1\}$ and for all $g \in \mathcal{G}_i$ it holds that $Y_i(d,g) \perp\!\!\!\perp D_i,\, G_i \,|\, X_i,\, \boldsymbol{X}_{\mathcal{S}_i}$.*

Therefore, conditional unconfoundedness, is an inherent characteristic of the RDD with interference under Assumption 2 resulting from the deterministic dependence of the effective treatment on X_i and $\boldsymbol{X}_{\mathcal{S}_i}$.

2.3 Effective Treatment Boundaries

The non-probabilistic effective treatment assignment results in a structural lack of overlap, as units with the same value of X_i and $\boldsymbol{X}_{\mathcal{S}_i}$ are never observed under different effective treatments. Therefore, unconfoundedness cannot be exploited directly as in other observational studies with interference (Perez-Heydrich et al., 2014; Papadogeorgou et al., 2019; Ogburn et al., 2022; Forastiere et al., 2021, 2022). However, as in no-interference multiscore RDDs, causal effects can be identified at common boundary points between effective treatment regions. We next characterize these boundaries, while identification results are presented in Section 3.

Formally, the boundary of a region $\mathcal{X}_{i\mathcal{S}_i}(d,g)$, denoted by $\bar{\mathcal{X}}_{i\mathcal{S}_i}(d,g)$, is the set of points $(x_i, \boldsymbol{x}_{\mathcal{S}_i})$ such that for any $\epsilon > 0$, a neighborhood of radius ϵ around $(x_i, \boldsymbol{x}_{\mathcal{S}_i})$ contains elements in $\mathcal{X}_{i\mathcal{S}_i}(d,g)$ and in its complement, i.e. $\mathcal{X}_{i\mathcal{S}_i}(d,g)^c$. We define the *effective treatment boundary* $\bar{\mathcal{X}}_{i\mathcal{S}_i}(d,g\,|\,d',g')$ as the intersection of two such boundaries, $\bar{\mathcal{X}}_{i\mathcal{S}_i}(d,g\,|\,d',g') = \bar{\mathcal{X}}_{i\mathcal{S}_i}(d,g) \cap \bar{\mathcal{X}}_{i\mathcal{S}_i}(d',g')$, which captures the set of points where a small change in the score vector induces a change in effective treatment from (d,g) to (d',g'). For example, Figure 1 depicts the multiscore space for a unit with one neighbor, $\mathcal{S}_i = \{j\}$, and $G_i = D_j$. Here, the multiscore space $\mathcal{X}_{i\mathcal{S}_i}$, represented on the Cartesian plane with X_i on the $x-$axis and X_j on the $y-$axis, is partitioned into four effective treatment regions where the effective treatment boundary is either a segment (e.g., between the top-left and bottom-left treatment regions) or the point (c,c) (between the bottom-left and top-right regions).

The geometry of $\bar{\mathcal{X}}_{i\mathcal{S}_i}(d,g\,|\,d',g')$ depends on the interference set and the exposure mapping. Figure 2 illustrates two scenarios for a unit with two neighbors ($\mathcal{S}_i = \{j,k\}$): one under the "one treated" exposure mapping and the other under the "sum of treated" mapping. Here, the complete multiscore space $\mathcal{X}_{i\mathcal{S}_i}$ is three-dimensional, but for clarity, we represent the effective treatment regions for $D_i = 0$ by fixing X_i at $x_i < c$. With the "one treated" exposure mapping, there are two effective treatment regions (for $D_i = 0$), and their boundary consists of two intersecting segments. With the "sum of treated" exposure mapping, (for $D_i = 0$) there are three effective treatment regions, separated pairwise by segments, except for $\mathcal{X}_{i\mathcal{S}_i}(0,2)$ and $\mathcal{X}_{i\mathcal{S}_i}(0,0)$, where the boundary is (c,c).

Identifying $\bar{\mathcal{X}}_{i\mathcal{S}_i}(d,g\,|\,d',g')$ may be challenging in high dimensions. In such settings, even determining whether two regions are adjacent, i.e., whether their boundaries intersect, may not be obvious. For example, suppose G_i is the sum of treated neighbors, and consider the boundary between $\mathcal{X}_{i\mathcal{S}_i}(0,3)$ and $\mathcal{X}_{i\mathcal{S}_i}(0,7)$ for a unit with 10 neighbors. Understanding whether boundary points between these regions exist and identifying them is not trivial. We address this by providing an explicit characterization of the effective treatment boundary as the set of points where one or more inequalities describing the effective treatment regions switch direction.

Let $\mathcal{D}_{i\mathcal{S}_i}(d,g) = \{(d_i, \boldsymbol{d}_{\mathcal{S}_i}) \in \mathcal{D}_{i\mathcal{S}_i}\ s.t.\,(d_i, g(\boldsymbol{d}_{\mathcal{S}_i})) = (d,g)\}$, with generic element $\boldsymbol{d}^{d,g}_{i\mathcal{S}_i} = (d_i, \boldsymbol{d}_{\mathcal{S}_i})^{d,g}$, the set of individual and neighbors' treatment that yield the effective treatment (d,g). Then the effective treatment boundary $\bar{\mathcal{X}}_{i\mathcal{S}_i}(d,g\,|\,d',g')$ can be written as $\bar{\mathcal{X}}_{i\mathcal{S}_i}(d,g\,|\,d',g') = \bigcup_{\mathcal{D}_{i\mathcal{S}_i}(d,g)\times\mathcal{D}_{i\mathcal{S}_i}(d',g')} \ell(\boldsymbol{d}^{d,g}_{i\mathcal{S}_i}, \boldsymbol{d}^{d',g'}_{i\mathcal{S}_i})$, with the set-valued function ℓ :

$\mathcal{D}_{i\mathcal{S}_i}(d,g) \times \mathcal{D}_{i\mathcal{S}_i}(d',g') \to \mathcal{X}_{i\mathcal{S}_i}$ being

$$\ell(\boldsymbol{d}_{i\mathcal{S}_i}^{d,g}, \boldsymbol{d}_{i\mathcal{S}_i}^{d',g'}) = \left\{ (x_i, \boldsymbol{x}_{\mathcal{S}_i}) \in \mathcal{X}_{i\mathcal{S}_i} \;\middle|\; \forall z \in (\{i\} \cup \mathcal{S}_i), \begin{cases} x_z \geq c & d_z^{d,g} = d_z^{d',g'} = 1 \\ x_z \leq c & d_z^{d,g} = d_z^{d',g'} = 0 \\ x_z = c & d_z^{d,g} \neq d_z^{d',g'} \end{cases} \right\} \tag{4}$$

(see Supplementary Material S.1 for the derivation). The effective treatment boundary $\bar{\mathcal{X}}_{i\mathcal{S}_i}(d,g\,|\,d',g')$ can be identified by applying $\ell(\cdot)$ to each pair of elements $\boldsymbol{d}_{i\mathcal{S}_i}^{d,g}$ and $\boldsymbol{d}_{i\mathcal{S}_i}^{d',g'}$ and taking the union of the resulting sets. For example, when in our empirical application (Section 6) we compare $G_i = 1$ (having all treated neighbors) to $G_i = 0$ (having no treated neighbor) for untreated units ($D_i = 0$) with 4 neighbors, we must identify the boundary $\bar{X}_{i\mathcal{S}_i}(0,1\,|\,0,0)$ between the regions corresponding to the effective treatment values $\mathcal{D}_{i\mathcal{S}_i}(0,1) = (0,1,1,1,1)$ and $\mathcal{D}_{i\mathcal{S}_i}(0,0) = (0,0,0,0,0)$, respectively. Our procedure yields the boundary $\bar{X}_{i\mathcal{S}_i}(0,1\,|\,0,0) = \{(x_i, \boldsymbol{x}_{\mathcal{S}_i}) \in \mathcal{X}_{i\mathcal{S}_i} : x_i \leq c$ and $x_j = c$ for $j \in \mathcal{S}_i\}$, that is, including untreated units with all neighbors at the cutoff.

The characterization of $\bar{\mathcal{X}}_{i\mathcal{S}_i}(d,g\,|\,d',g')$ via $\ell(\cdot)$ implies that $\bar{\mathcal{X}}_{i\mathcal{S}_i}(d,g\,|\,d',g')$ is always non-empty. Moreover, $\bar{\mathcal{X}}_{i\mathcal{S}_i}(d,g\,|\,d',g')$ can be written as a finite union of linear pieces $\ell(\boldsymbol{d}_{i\mathcal{S}_i}^{d,g}, \boldsymbol{d}_{i\mathcal{S}_i}^{d',g'})$, each associated with a specific number of score components fixed at the cutoff, which we denote by $s_{\ell(\boldsymbol{d}_{i\mathcal{S}_i}^{d,g}, \boldsymbol{d}_{i\mathcal{S}_i}^{d',g'})} = \sum_{z\in(\{i\}\cup\mathcal{S}_i)} \mathbb{1}(d_z^{d,g} \neq d_z^{d',g'})$. Specifically, each linear piece is a $(|\mathcal{S}_i|+1-s_{\ell(\cdot)})$-dimensional submanifold of $\mathcal{X}_{i\mathcal{S}_i}$ with codimension $s_{\ell(\cdot)}$, defined as the difference between the dimension of $\mathcal{X}_{i\mathcal{S}_i}$, i.e., $|\mathcal{S}_i|+1$, and that of the linear piece. Consequently, $\bar{\mathcal{X}}_{i\mathcal{S}_i}(d,g\,|\,d',g')$ admits a well-defined surface measure, allowing us to define boundary average causal effects as integrals over $\bar{\mathcal{X}}_{i\mathcal{S}_i}(d,g\,|\,d',g')$. Formally, $\bar{\mathcal{X}}_{i\mathcal{S}_i}(d,g\,|\,d',g')$ is a $(|\mathcal{S}_i|+1-\bar{s}_i)$-rectifiable set (see Appendix S.2 for the definition), with dimension $|\mathcal{S}_i|+1-\bar{s}_i$ and codimension $\bar{s}_i$, where $\bar{s}_i$ is the minimal value of $s_{\ell(\cdot)}$ across all score configurations generating boundary pieces between effective treatment regions, i.e., $\bar{s}_i = \min_{\mathcal{D}_{i\mathcal{S}_i}(d,g)\times\mathcal{D}_{i\mathcal{S}_i}(d',g')} s_{\ell(\boldsymbol{d}_{i\mathcal{S}_i}^{d,g}, \boldsymbol{d}_{i\mathcal{S}_i}^{d',g'})}$. For example, in Figure 1, $\mathcal{X}_{i\mathcal{S}_i}$ is 2-dimensional and the boundary $\bar{\mathcal{X}}_{i\mathcal{S}_i}(0,0|0,1)$ is the 1-dimensional $(2-1)$ piece where $X_i < 0$ and $X_j = c$. In Figure 2, the multiscore space is 3-dimensional, and the boundary $\bar{\mathcal{X}}_{i\mathcal{S}_i}(0,0|0,1)$ is formed by two planar pieces, where either $X_j = c$ or $X_k = c$, both 2-dimensional $(3-1)$, and their intersection, where $X_j = X_k = c$, of dimension 1 $(3-2)$. Hence, the union of these pieces forms a subset of dimension $3-1=2$, with $\bar{s}_i = 1$. As shown in Section 4, the dimension of $\bar{\mathcal{X}}_{i\mathcal{S}_i}(d,g\,|\,d',g')$ crucially determines via $\bar{s}_i$ the convergence rate of the proposed distance-based local polynomial estimators.

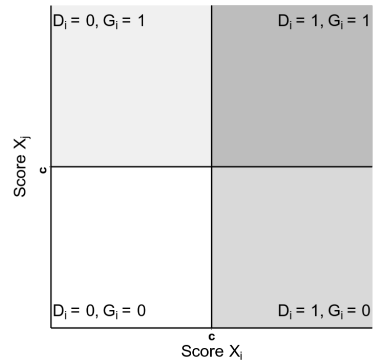

Figure 1: Score space for unit i with interference set $\mathcal{S}_i = \{j\}$ and $G_i = D_j$.

Figure 2: Score space for unit i with interference set $\mathcal{S}_i = \{j, k\}$ fixing $X_i = x_i$ with $x_i < c$.

2.4 Causal Estimands

Here, for simplicity, we concentrate on the case where units have equally-sized interference sets and homogeneous effective treatment boundaries, as well as homogeneous outcome and score distributions. That is, $|\mathcal{S}_i|$, $\bar{s}_i$, $\mathbb{E}[Y_i(d,g) \mid (X_i, \boldsymbol{X}_{\mathcal{S}_i}) = (x_i, \boldsymbol{x}_{\mathcal{S}_i})]$, and $f(x_i, \boldsymbol{x}_{\mathcal{S}_i})$ are homogeneous across units. Our main causal estimand of interest is the *boundary average causal effect*, defined as the difference in the average potential outcomes under different effective treatments at the effective treatment boundary:

$$\tau_{d,g|d',g'}\big(\bar{\mathcal{X}}_{i\mathcal{S}_i}(d,g \,|\, d',g')\big) = \mathbb{E}[\,Y_i(d,g) - Y_i(d',g') \,|\, (X_i,\, \boldsymbol{X}_{\mathcal{S}_i}) \in \bar{\mathcal{X}}_{i\mathcal{S}_i}(d,g \,|\, d',g')\,] \tag{5}$$

with $d, d' \in \{0,1\}$, $g, g' \in \mathcal{G}_i$. Here, the expectation is taken with respect to the distribution of potential outcomes conditional on the individual and neighborhood score being at the boundary and on the network under our model-based perspective.

Boundary average causal effects can be written as weighted averages of causal effects across the effective treatment boundary:

$$\tau_{d,g|d',g'}\big(\bar{\mathcal{X}}_{i\mathcal{S}_i}(d,g\,|\,d',g')\big) = \frac{\int_{\bar{\mathcal{X}}_{i\mathcal{S}_i}(d,g\,|\,d',g')} \tau_{d,g|d',g'}(x_i, \boldsymbol{x}_{\mathcal{S}_i}) f(x_i, \boldsymbol{x}_{\mathcal{S}_i}) d\mathcal{H}^{|\mathcal{S}_i|+1-\bar{s}}}{\int_{\bar{\mathcal{X}}_{i\mathcal{S}_i}(d,g\,|\,d',g')} f(x_i, \boldsymbol{x}_{\mathcal{S}_i}) d\mathcal{H}^{|\mathcal{S}_i|+1-\bar{s}}} \tag{6}$$

where $f(x_i, \boldsymbol{x}_{\mathcal{S}_i})$ is the joint density of X_i and $\boldsymbol{X}_{\mathcal{S}_i}$ and $\tau_{d,g|d',g'}(x_i, \boldsymbol{x}_{\mathcal{S}_i}) = \mathbb{E}[\,Y_i(d,g) - Y_i(d',g')\,|\,(X_i, \boldsymbol{X}_{\mathcal{S}_i}) = (x_i, \boldsymbol{x}_{\mathcal{S}_i})\,]$, is the the average causal effect of the effective treatment (d,g) compared to (d',g') at a point $(x_i, \boldsymbol{x}_{\mathcal{S}_i})$[2]. The integral in (6) is taken with respect to the $|\mathcal{S}_i| + 1 - \bar{s}$-dimensional Hausdorff measure. Specifically, because $\bar{\mathcal{X}}_{i\mathcal{S}_i}(d,g\,|\,d',g')$ is a union of linear pieces, the integral can be written as a sum of integrals with respect to the $|S_i| + 1 - \bar{s}$-dimensional surface measure over each linear component (see Supplementary Material S.2 for more details).

We can further distinguish between boundary direct average effects and boundary indirect average effects. Specifically, *boundary direct average effects*, defined as

$$\tau_{1,g\,|\,0,g}\big(\bar{\mathcal{X}}_{i\mathcal{S}_i}(1,g\,|\,0,g)\big) = \mathbb{E}[\,Y_i(1,g) - Y_i(0,g)\,|\,(X_i\,, \boldsymbol{X}_{\mathcal{S}_i}) \in \bar{\mathcal{X}}_{i\mathcal{S}_i}(1,g\,|\,0,g)\,] \tag{7}$$

for $g \in \mathcal{G}_i$, isolate the (local) impact of the individual treatment for a fixed level of G_i. In contrast, *boundary indirect effects*, given by

$$\tau_{d,g\,|\,d,g'}(\bar{\mathcal{X}}_{i\mathcal{S}_i}(d,g\,|\,d,g')) = \mathbb{E}[\,Y_i(d,g) - Y_i(d,g')\,|\,(X_i\,, \boldsymbol{X}_{\mathcal{S}_i}) \in \bar{\mathcal{X}}_{i\mathcal{S}_i}(d,g\,|\,d,g')\,] \tag{8}$$

for $d \in \{0,1\}$, g, $g' \in \mathcal{G}_i$, capture the indirect effects of changing the neighborhood treatment G_i for a fixed level of the individual treatment.

For example, in our empirical application in Section 6, we estimate the direct boundary effect $\tau_{10|00}(\bar{\mathcal{X}}_{i\mathcal{S}_i}(10|00))$, which captures the impact of being eligible for the PROGRESA/Oportunidades program for individuals at the poverty threshold who have friends that are below the threshold. This effect reveals whether the program directly benefits children whose peers are situated below the eligibility cutoff. In contrast, the indirect boundary effect $\tau_{01|00}(\bar{\mathcal{X}}_{i\mathcal{S}_i}(01|00))$ measures the effect of having

[2]We refer to Appendix C.1 for discussion on the identification and estimation of causal effects at a point of the effective treatment boundary.

all eligible friends versus no eligible friends, for ineligible individuals whose peers are at the threshold. This estimand helps assess whether implementing such a program indirectly benefits those who are themselves ineligible but connected to eligible peers.

Furthermore, we define the *boundary overall direct effect* as

$$\tau_{1|0} = \sum_{g \in \mathcal{G}_i} \tau_{1,g\,|\,0,g}(\bar{\mathcal{X}}_{i\mathcal{S}_i}(1, g\,|\,0, g)) \cdot \mathbb{P}(\, G_i = g \,|\, X_i = c\,) \tag{9}$$

which averages boundary direct effects over the probability distribution of G_i conditional on X_i being equal to the cutoff. This effect can be written as a weighted average of point direct effects $\tau_{1,g|0,g}(x_i, \boldsymbol{x}_{\mathcal{S}_i}) = \mathbb{E}[\, Y_i(1, g) - Y_i(0, g') \,|\, (X_i, \boldsymbol{X}_{\mathcal{S}_i}) = (x_i, \boldsymbol{x}_{\mathcal{S}_i})\,]$ across the union of all boundaries of the type $\bar{\mathcal{X}}_{i\mathcal{S}_i}(1, g|0, g)$[3]. Thus, the boundary overall direct effect summarizes the effect of the individual treatment at the cutoff[4]. In the example in Figure 1, the overall direct effect at the cutoff corresponds to the boundary point direct effects averaged along the line $X_i = c$, the union of the boundaries $\bar{\mathcal{X}}_{i\mathcal{S}_i}(1, 1\,|\,0, 1)$ and $\bar{\mathcal{X}}_{i\mathcal{S}_i}(1, 0\,|\,0, 0)$.

Finally, we also define a *boundary overall indirect effect*, which can be considered a measure of the marginal effect of having an additional treated neighbor. We define the boundary overall indirect effect as

$$\begin{aligned}\tau_{indirect} = \sum_{d_i} \sum_{\boldsymbol{d}_{\mathcal{S}_i}} \sum_{\substack{\boldsymbol{d}'_{\mathcal{S}_i}: \\ d'_j \geq d_j \; \forall j \in \mathcal{S}_i, \\ \sum_{j \in \mathcal{S}_i} |d'_j - d_j| = 1}} & \mathbb{E}[\, Y_i(d_i, g(\boldsymbol{d}'_{\mathcal{S}_i})) - Y_i(d_i, g(\boldsymbol{d}_{\mathcal{S}_i})) \,|\, (X_i, \boldsymbol{X}_{\mathcal{S}_i}) \in \ell\big((d_i, \boldsymbol{d}'_{\mathcal{S}_i}), (d_i, \boldsymbol{d}_{\mathcal{S}_i})\big)\,] \\ & \cdot \mathbb{P}(\, D_i = d_i, \boldsymbol{D}'_{\mathcal{S}_i} = \boldsymbol{d}'_{\mathcal{S}_i} \,|\, \exists j \in \mathcal{S}_i : X_j = c\,)\end{aligned} \tag{10}$$

where $\ell(\cdot)$ is the function defined in Eq. (4). The overall indirect effect takes the

[3]Specifically, $\bar{\mathcal{X}}_{i\mathcal{S}_i}(1, g|0, g) = \{(x_i, \boldsymbol{x}_{\mathcal{S}_i}) \in \mathcal{X}_{i\mathcal{S}_i} \,:\, x_i = c\,, \boldsymbol{x}_{\mathcal{S}_i} \in \mathcal{X}_{\mathcal{S}_i}(g)\}$ where $\mathcal{X}_{\mathcal{S}_i}(g)$ is the set of all elements $\boldsymbol{x}_{\mathcal{S}_i}$ such that $e(\boldsymbol{x}_{\mathcal{S}_i}) = g$. The union of such boundaries across g then corresponds to $\{(x_i, \boldsymbol{x}_{\mathcal{S}_i}) \in \mathcal{X}_{i\mathcal{S}_i} \,:\, x_i = c\}$. It can be shown that $\tau_{1|0}$ can be equivalently written as

$$\tau_{1|0} = \sum_{g \in \mathcal{G}_i} \int_{\mathcal{X}_{\mathcal{S}_i}(g)} \mathbb{E}[\, Y_i(1, g) - Y(0, g) \,|\, X_i = c, \boldsymbol{X}_{\mathcal{S}_i} = \boldsymbol{x}_{\mathcal{S}_i}\,] \cdot \frac{f(c, \boldsymbol{x}_{\mathcal{S}_i})}{f(c)} d\boldsymbol{x}_{\mathcal{S}_i}$$

[4]The boundary overall direct effect is similar to the overall main effect defined by Forastiere et al. (2021), which is the average causal effect of the individual treatment marginalized over the (empirical) probability distribution of G_i. Here, however, the boundary overall direct effect is an average of boundary (conditional) direct effects over the probability distribution of G_i at the cutoff.

average of boundary indirect effects comparing neighborhood treatment vectors that differ by one treated neighbor marginalized over the distribution of the individual treatment and neighborhood treatment conditional on having at least one neighbor at the cutoff, that is, the probability of having the individual and neighbors' scores $(X_i, \boldsymbol{X}_{\mathcal{S}_i})$ with at least one neighbor at the cutoff. Note that the effective treatment boundary $\ell\big((d_i, \boldsymbol{d}'_{\mathcal{S}_i}), (d_i, \boldsymbol{d}_{\mathcal{S}_i})\big)$ has at the cutoff the score of the neighbor $j \in \mathcal{S}_i$ whose treatment is assumed to switch from 0 to 1 between $\boldsymbol{d}_{\mathcal{S}_i}$ and $\boldsymbol{d}'_{\mathcal{S}_i}$. This estimand appears cumbersome in its general form. However, it reduces to a simple form once we specify the interference set and exposure mappings. In the example of Figure 1, with a single treated unit, $\tau_{indirect}$ corresponds to a weighted average of the boundary indirect effects on $\bar{\mathcal{X}}_{i\mathcal{S}_i}(0, 1 \mid 0, 0)$ and $\bar{\mathcal{X}}_{i\mathcal{S}_i}(1, 1 \mid 1, 0)$—or, equivalently, to the weighted average of boundary point indirect effects along the line $X_j = c$, which constitutes the union of these boundaries. We discuss identification and estimation of this estimand in Supplemental Appendix C.2, where we also provide its form under specific exposure mappings.

Our definitions of causal effects assume equally-sized interference sets and homogeneity of the effective treatment boundaries, as well as identical outcomes and scores distribution. However, units may have different numbers of neighbors, and heterogeneous effective treatment boundaries, and the outcome and score distributions may depend on the network. Under such heterogeneity, causal effects are unit-specific and causal estimands should be defined as the average of expected potential outcomes across the sample units (e.g. Ogburn et al., 2022). We extend our analysis to account for such heterogeneity in the Supplemental Appendix A.

3 Identification

3.1 Identification of Boundary Average Causal Effects

Due to the lack of overlap (Property 1), at the boundary between two effective treatment regions $\bar{\mathcal{X}}_{i\mathcal{S}_i}(d, g \mid d', g')$, all units are either observed under effective treatment (d, g) or (d', g'). Therefore, at least one of the two conditional expectations in the definition of causal estimands in Eq. (5), which requires some form of extrapolation. Following the RDD literature (Imbens and Lemieux, 2008), we assume that units near the boundary, and thus having similar own and neighbor scores, also have similar potential outcomes on average. This idea is formalized by a continuity assumption on $\mathbb{E}[\,Y_i(d,g)\,|\,(X_i,\boldsymbol{X}_{\mathcal{S}_i})=(x_i,\boldsymbol{x}_{\mathcal{S}_i})\,]$ for all (d,g), which allows to use observation just on one side of the boundary to estimate the unobserved average potential outcomes. A key limitation of this continuity-based identification is that it can only identify local causal estimands, i.e., conditional on the individual and neighbors' scores lying on the boundary. This locality is a feature of RDDs, which rely on discontinuities in treatment assignment and cannot identify broader effects without stronger assumptions beyond continuity.

We now formalize our identification result. Let us first introduce the following notation, which we adapt from Imbens and Zajonc (2011). Let $l(p,q)$ be the Euclidean distance between two generic points p and q. Define the minimum distance of a point $(x_i,\boldsymbol{x}_{\mathcal{S}_i})\in\mathcal{X}_{i\mathcal{S}_i}$ from the effective treatment boundary $\bar{\mathcal{X}}_{i\mathcal{S}_i}(d,g\,|\,d',g')$ as $l^{min}_{d,g|d',g'}(x_i,\boldsymbol{x}_{\mathcal{S}_i})=\min_{\bar{\mathcal{X}}_{i\mathcal{S}_i}(d,g\,|\,d',g')} l\big((x_i,\boldsymbol{x}_{\mathcal{S}_i}),(\bar{x}_i,\bar{\boldsymbol{x}}_{\mathcal{S}_i})\big)$, and let

$$\mathcal{B}_\varepsilon(\bar{\mathcal{X}}_{i\mathcal{S}_i}(d,g\,|\,d',g'))=\{(x_i,\boldsymbol{x}_{\mathcal{S}_i})\in\mathcal{X}_{i\mathcal{S}_i}:l^{min}_{d,g|d',g'}(x_i,\boldsymbol{x}_{\mathcal{S}_i})\leq\epsilon\}$$

be the ϵ-neighborhood of $\bar{\mathcal{X}}_{i\mathcal{S}_i}(d,g\,|\,d',g')$, that is, the set of points within distance ϵ from $\bar{\mathcal{X}}_{i\mathcal{S}_i}(d,g\,|\,d',g')$. Lastly, let $\mathcal{B}^{d,g}_\varepsilon(\bar{\mathcal{X}}_{i\mathcal{S}_i}(d,g\,|\,d',g'))$ and $\mathcal{B}^{d',g'}_\varepsilon(\bar{\mathcal{X}}_{i\mathcal{S}_i}(d,g\,|\,d',g'))$ be the intersections of the effective treatment boundary ϵ-neighborhood with the effective treatment regions $\mathcal{X}_{i\mathcal{S}_i}(d,g)$ and $\mathcal{X}_{i\mathcal{S}_i}(d',g')$, respectively.
We make the following identifying assumptions, building on Imbens and Zajonc (2011).

Assumption 4 (Identification)**.** *Assume that X_i has bounded support. For all $i\in\mathcal{N}$, for all d, $d'\in\{0,1\}$ and for all g, $g'\in\mathcal{G}_i$:*

a) Score density positivity: $f(x_i,\boldsymbol{x}_{\mathcal{S}_i})>0$ for all $(x_i,\boldsymbol{x}_{\mathcal{S}_i})\in\mathcal{B}_\varepsilon(\bar{\mathcal{X}}_{i\mathcal{S}_i}(d,g\,|\,d',g'))$.

b) Outcome continuity: $\mathbb{E}[\,Y_i(d,g)\,|\,(X_i,\boldsymbol{X}_{\mathcal{S}_i})=(x_i,\boldsymbol{x}_{\mathcal{S}_i})\,]$ is continuous at all $(x_i,\boldsymbol{x}_{\mathcal{S}_i})\in\mathcal{X}_{i\mathcal{S}_i}$.

c) Score density continuity: $f(x_i,\boldsymbol{x}_{\mathcal{S}_i})$ is continuous at all $(x_i,\boldsymbol{x}_{\mathcal{S}_i})\in\mathcal{X}_{i\mathcal{S}_i}$.

d) Boundedness: $\big|\mathbb{E}[\,Y_i(d,g)\,|\,(X_i,\boldsymbol{X}_{\mathcal{S}_i})=(x_i,\boldsymbol{x}_{\mathcal{S}_i})\,]\big|$ and $f(x_i,\boldsymbol{x}_{\mathcal{S}_i})$ are bounded.

Combined with the extended SUTVA (Assumptions 1 and 2) and the RDD treatment assignment rule (Assumption 1), Assumption 4 enables the identification of average causal effects at the effective treatment boundary, as shown in the following theorem.

Theorem 1 (Identification)**.** *Suppose assumptions 1-4 hold. Then for all* $d,\ d' \in \{0,1\}$*,* $g,\ g' \in \mathcal{G}_i$

$$\begin{aligned}\tau_{d,g|d',g'}\big(\bar{\mathcal{X}}_{i\mathcal{S}_i}(d,g\,|\,d',g')\big) = &\lim_{\epsilon\to 0}\mathbb{E}[\,Y_i\,|\,(X_i,\boldsymbol{X}_{\mathcal{S}_i}) \in \mathcal{B}^{d,g}_{\varepsilon}(\bar{\mathcal{X}}_{i\mathcal{S}_i}(d,g\,|\,d',g'))\,] \\ &-\lim_{\epsilon\to 0}\mathbb{E}[\,Y_i\,|\,(X_i,\boldsymbol{X}_{\mathcal{S}_i}) \in \mathcal{B}^{d',g'}_{\varepsilon}(\bar{\mathcal{X}}_{i\mathcal{S}_i}(d,g\,|\,d',g'))\,]\end{aligned} \tag{11}$$

Proof. See Supplementary Material S.1.

Theorem 1 states that the boundary average causal effect $\tau_{d,g|d',g'}\big(\bar{\mathcal{X}}_{i\mathcal{S}_i}(d,g\,|\,d',g')\big)$ is identified by taking the difference between the limits of the conditional expectations of the observed outcomes on $\mathcal{B}^{d,g}_{\varepsilon}(\bar{\mathcal{X}}_{i\mathcal{S}_i}(d,g\,|\,d',g'))$ and $\mathcal{B}^{d',g'}_{\varepsilon}(\bar{\mathcal{X}}_{i\mathcal{S}_i}(d,g\,|\,d',g'))$ as ϵ shrinks to zero. This result relies on Assumptions 4. Specifically, Assumption 4.a) ensures well-defined conditional expectations near an effective treatment boundary by requiring a non-null score density near that boundary. Assumption 4.b) extends the continuity requirement from standard multivariate RDDs and enables the approximation of unobserved potential outcome expectations at boundary points using sufficiently close observations, thereby restoring a form of overlap. This assumption implies that individuals sharing similar scores and also having neighbors with similar scores have, in turn, similar potential outcome expectations. In our application, when estimating the effect of having all versus no neighbors eligible among the ineligible, it means that individuals with the same poverty index and neighbors just above or below the cutoff have comparable expected outcomes. Although untestable and more restrictive than the standard RDD continuity assumption, this assumption's plausibility can be assessed, for example, by checking for covariate balance near the boundary, as significant imbalances may cast doubt on its validity. Since boundary effects are weighted averages of point effects with weights determined by the scores density, Assumption 4.c) ensures that the weighting scheme is also continuous on each side of the effective treatment boundary. This guarantees that a change in the distribution of the baseline score variables does not spuriously determine the difference in the potential outcomes' conditional expectations. For instance, this assumption would be violated in PROGRESA/Oportunidades if ineligible individuals with all eligible peers had a different poverty index distribution—such as a higher concentration of lower values—than those with no eligible peers. In principle, this assumption can also be assessed empirically by estimating the score density near the boundary, though this would often require multivariate methods. Finally, Assumption 4.d) is a technical condition allowing the interchange of the limit and integral operators.

3.2 Identification of Boundary Overall Direct Effects

In no-interference RDDs, the local average causal effect at the cutoff is identified as the difference between the right and left limit of the observed outcome regression functions as X_i approaches the cutoff c. In our framework, such an identification strategy does not identify the average causal effect at the cutoff as potential outcomes of the form $Y_i(1)$ and $Y_i(0)$ are ill-defined under interference. However, the following theorem shows that the identification strategy used in standard RDDs identifies the boundary overall direct effect at the cutoff provided that Assumptions 1-4 hold.

Theorem 2 (Identification of boundary overall direct effect)**.** *Under assumptions 1-4*

$$\tau_{1|0} = \lim_{x_i \downarrow c} \mathbb{E}[\, Y_i \mid X_i = x_i \,] - \lim_{x_i \uparrow c} \mathbb{E}[\, Y_i \mid X_i = x_i \,]$$

Proof. See Supplementary Material S.1.

$\lim_{x_i \downarrow c} \mathbb{E}[\, Y_i \mid X_i = x_i \,] - \lim_{x_i \uparrow c} \mathbb{E}[\, Y_i \mid X_i = x_i \,]$ is precisely the quantity that identifies the average treatment effect at the cutoff in the standard RDD without interference. This result crucially relies on Assumption 4.c (score density continuity), which ensures that the distribution of $\boldsymbol{X}_{\mathcal{S}_i}$ conditional on X_i is balanced on each side of the cutoff c. This, in turn, implies that the (conditional) distribution of G_i is equal on each side of the cutoff.

4 Estimation

In no-interference RDDs, the average causal effect at the cutoff is typically estimated using local polynomial regression, which fits Y_i on a low-order polynomial of the centered score $(X_i - c)$ on each side of the cutoff using observations within a fixed bandwidth h_n (Hanh et al., 2001). However, estimating boundary average effects in our setting is more complex due to the multidimensional nature of the effective treatment boundaries.

Several estimation strategies for multivariate RDDs without interference reduce the multivariate score to a one-dimensional variable and then apply univariate local polynomial techniques using this variable as the one-dimensional score[5]. This is done either by subsetting the data by treatment region (frontier estimation) (Matsudaira, 2008) or by computing a summary score (binding approach) (Reardon and Robinson, 2012). A widely used method in this class is the distance-based approach, which replaces the multivariate score with the shortest Euclidean distance of each unit to the treatment boundary (Dell, 2010; Keele and Titiunik, 2015). The distance-based method offers several advantages. Unlike frontier estimation, it estimates effects over the entire treatment boundary without subsetting the data, and unlike the binding approach, it applies to more general boundary shapes. Moreover, its local non-parametric approach potentially avoids the misspecification pitfalls of a global model and retains the visually appealing properties of univariate RDDs (Imbens and Zajonc, 2011).

We adapt the distance-based local polynomial estimator to our framework for estimating boundary average effects, and derive its asymptotic properties. To our knowledge, the distance-based local polynomial estimator in multivariate RDDs has not, to date, received a thorough formal analysis. The only exception is the recent work of Cattaneo et al. (2025), which studies causal effects at boundary points in settings without interference. In contrast, we develop an asymptotic theory for distance-based estimators of aggregate interference effects over treatment boundaries, where distance is measured from the entire boundary rather than individual points. Furthermore, while conventional multivariate RDDs typically feature boundaries of dimension $d-1$ (with d denoting the dimension of the forcing variable), we consider effective treatment boundaries of dimension $|\mathcal{S}_i| + 1 - \bar{s}$, where $\bar{s}$ may exceed one. Under homogeneity in the interference-set size and in the outcome and score distributions, we show that the distance-based local polynomial estimators converge at rate $nh_n^{2p+2+\bar{s}}$, where $\bar{s}$ depends on the causal estimand and p denotes the polynomial degree. Finally, we extend our analysis to the case of heterogeneous effective treatment boundaries and heterogeneous outcome and score distributions (Supplemental Appendix A).

For the boundary overall direct effect, $\tau_{1|0}$, we propose using the standard RDD

[5] Alternatives to these methods include, for example, integrating numerically estimates of point effects, obtained by multiple local linear regression, over the treatment boundary (Imbens and Zajonc, 2011)

local polynomial estimator, as justified by our identification result in Theorem 2. In the Supplemental Appendix C.2, we show that the overall indirect effect $\tau_{indirect}$ can be estimated via univariate local polynomial regression using as the one-dimensional regressor the score of the neighbor closest to the cutoff.

A key characteristic of our setting is the statistical dependence in the data, which may arise from interference among observations with overlapping interference sets and from network-induced correlations in outcomes and scores. For example, in networks linked observations tend to be more similar, a phenomenon known as homophily (McPherson et al., 2001). Standard asymptotic theories for local polynomial estimators based on i.i.d. data, are therefore not applicable. However, kernel estimators have been shown to be asymptotically equivalent to their counterparts with independent data under forms of weak dependence. Bartalotti and Brummet (2017) establish this result for clustered RDDs where all units within a cluster lie on one side of the cutoff, while Masry and Fan (1997) and Jenish (2012) show similar equivalence for time- and spatially-dependent data modeled as random fields on Euclidean lattices. However, a generic network is not necessarily embeddable in an Euclidean lattice (Kojevnikov et al., 2021). Therefore, we develop a new asymptotic theory that builds on Leung (2020) under restrictions on the growth of network links. We establish the asymptotic equivalence with the independent data case when units do not share the same distance variable. However, dependence is non-vanishing when units have the same distance variable, which can occur with overlapping interference sets. In addition, data dependence can affect the distribution of the estimator in finite samples with non-zero bandwidth. We develop a variance estimator that is robust to these sources of dependence. This will also be applied to the the standard RDD local polynomial estimator for the boundary overall direct effect, $\tau_{1|0}$.

4.1 Potential Outcome Model

We write potential outcomes for generic (d, g) as

$$Y_i(d, g) = m_{d,g}(X_i, \boldsymbol{X}_{\mathcal{S}_i}) + \epsilon_{i,d,g}, \quad i = 1, ..., n \tag{12}$$

where $m_{d,g}(x_i, \boldsymbol{x}_{\mathcal{S}_i}) = \mathbb{E}[\,Y_i(d, g)\,|\,(X_i, \boldsymbol{X}_{\mathcal{S}_i}) = (x_i, \boldsymbol{x}_{\mathcal{S}_i})\,]$ and $\epsilon_{i,d,g}$ is an error term with $\mathbb{E}[\,\epsilon_{i,d,g}\,|\,X_i, \boldsymbol{X}_{\mathcal{S}_i}\,] = 0$. By design, $m_{d,g}(x_i, \boldsymbol{x}_{\mathcal{S}_i})$ is only observed within the effective treatment region $\mathcal{X}_{i\mathcal{S}_i}(d, g)$. Under consistency the observed outcome is $Y_i =$

$m(X_i, \boldsymbol{X}_{\mathcal{S}_i}) + \epsilon_i$ where $m(X_i, \boldsymbol{X}_{\mathcal{S}_i}) = \sum_{d,g} \mathbb{1}((X_i, \boldsymbol{X}_{\mathcal{S}_i}) \in \mathcal{X}_{i\mathcal{S}_i}(d,g)) \cdot m_{d,g}(X_i, \boldsymbol{X}_{\mathcal{S}_i})$ is the observed outcome conditional expectation, and $\epsilon_i = \sum_{d,g} \mathbb{1}((X_i, \boldsymbol{X}_{\mathcal{S}_i}) \in \mathcal{X}_{i\mathcal{S}_i}(d,g)) \cdot \epsilon_{i,d,g}$. Identification of effects at the effective treatment boundary therefore relies on the continuity assumption of $m_{d,g}(x_i, \boldsymbol{x}_{\mathcal{S}_i})$ (see Section 3)

Here, dependence may arise through G_i due to overlapping interference sets and through scores and error terms correlated over the network. We model this dependence for the collection of random variables $\{(\{Y_i(d,g)\}_{d,g}, X_i, \boldsymbol{X}_{\mathcal{S}_i}, D_i, G_i)\}_{i=1}^n$ using *dependency neighborhoods*, determined by the network $\boldsymbol{A}$[6]. The dependency neighborhood of a unit i is a collection of indices of observations potentially dependent on observation i. Formally, a collection of random variables $\{Z_i\}_{i=1}^n$ has dependency neighborhoods $\boldsymbol{N}_i \subseteq \{1, ..., n\}$, $i = 1, \ldots, n$, if $i \in \boldsymbol{N}_i$, and Z_i is independent of $\{Z_j\}_{j \notin \boldsymbol{N}_{i,n}}$ (Ross, 2011).

Assumption 5 (Dependency neighborhoods)**.** *$\{(\{Y_i(d,g)\}_{d,g}, X_i, \boldsymbol{X}_{\mathcal{S}_i}, D_i, G_i)\}_{i=1}^n$ has dependency neighborhoods $\boldsymbol{N}_i \subseteq \{1, ..., n\}$, $i = 1, \ldots, n$, where $\boldsymbol{N}_i$ is a function of $\boldsymbol{A}$.*

Letting $O_i = (Y_i, X_i, \boldsymbol{X}_{\mathcal{S}_i}, D_i, G_i)$ be the observed data for unit $i = 1, ..., n$, then, under Assumption 5, $\{O_i\}_{i=1}^n$ also has a dependency neighborhood $\boldsymbol{N}_i$. Dependency neighborhoods can be represented by a *dependency graph* $\boldsymbol{W}$, a binary $n \times n$ matrix with entry $W_{ij} = 1$ if $j \in \boldsymbol{N}_i$ and $W_{ij} = 0$ otherwise. The dependency graph determines the amount of independent information available in the data as by construction, for any two disjoint subsets $I_1, I_2 \subseteq \{1, ..., n\}$ where $W_{ij} = 0$ for all $i \in I_1$ and $j \in I_2$ we have $\{O_i : i \in I_1\} \perp\!\!\!\perp \{O_j : j \in I_2\}$.

The results in this Section do not depend on the exact form of $\boldsymbol{W}$, but only on certain restrictions on its empirical degree distribution (see Subsection 4.3). However, inference requires knowledge of $\boldsymbol{W}$, whose form will generally depend on the data-generating distribution and the assumed interference mechanism[7].

[6] Under our model-based perspective outcome, scores and treatments are sampled from a data-generating distribution conditional on $\boldsymbol{A}$. Given the deterministic assignment rule, the randomness of the treatment thus arises from the randomness of the score.

[7] For instance, $\boldsymbol{N}_i$ can contain observations that are two links away in the network (e.g. Leung, 2020; Ogburn et al., 2022), which is consistent with network neighborhood interference when the score and error variables are i.i.d.

4.2 Distance-based Estimator

We now introduce our distance-based estimation method for the boundary average causal effect $\tau_{d,g|d',g'}\big(\bar{\mathcal{X}}_{i\mathcal{S}_i}(d,g\,|\,d',g')\big)$. The approach reduces the multivariate score $(X_i, \boldsymbol{X}_{\mathcal{S}_i})$ to the shortest Euclidean distance to the effective treatment boundary and performs a local polynomial estimation using this distance as the one-dimensional score (e.g. Keele and Titiunik, 2015).

Let $c = 0$ without loss of generality and let $\tilde{X}_{i,d,g,d',g'} = l^{min}_{d,g|d',g'}(X_i, \boldsymbol{X}_{\mathcal{S}_i})$ be minimum Euclidean distance from $\bar{\mathcal{X}}_{i\mathcal{S}_i}(d,g\,|\,d',g')$ of a random point $(X_i, \boldsymbol{X}_{\mathcal{S}_i})$. with realization $\tilde{x}_{i,d,g,d',g'}$. The distance-based linear local regression estimator uses this one-dimensional distance variable $\tilde{X}_{i,d,g,d',g'}$.

The estimation of the boundary average effects will not rely on the direct estimation of $m(X_i, \boldsymbol{X}_{\mathcal{S}_i})$ but on the estimation of $\mu(\tilde{X}_{i,d,g,d',g'}) = \mathbb{E}[\,Y_i\,|\,\tilde{X}_{i,d,g,d',g'}, D_i, G_i\,]$, the expectation of the observed outcome conditional on the one-dimensional distance variable and the effective treatment assignment. Taking the expectation of model (12) with respect to $\tilde{X}_{i,d,g,d',g'}$ and D_i, G_i yields

$$Y_i = \mu(\tilde{X}_{i,d,g,d',g'}) + u_{i,d,g,d',g'}, \quad i = 1, ..., n \tag{13}$$

where $u_{i,d,g,d',g'} = m(X_i, \boldsymbol{X}_{\mathcal{S}_i}) - \mu(\tilde{X}_{i,d,g,d',g'}) + \epsilon_i$.

For convenience, let us denote $\tilde{X}_{i,d,g,d',g'}$ by $\tilde{X}_i$ when it is not ambiguous. The outcome regression functions of interest are $\mu_{d,g}(\tilde{x}_i) = \mathbb{E}[\,Y_i\,|\,\tilde{X}_i = \tilde{x}_i, D_i = d, G_i = g\,]$ and $\mu_{d',g'}(\tilde{x}_i) = \mathbb{E}[\,Y_i\,|\,\tilde{X}_i = \tilde{x}_i, D_i = d', G_i = g'\,]$. Let $\mu_{d,g}(0) = \lim_{\tilde{x}_i \to 0^+} \mu_{d,g}(\tilde{x}_i)$ and $\mu_{d',g'}(0) = \lim_{\tilde{x}_i \to 0^+} \mu_{d',g'}(\tilde{x}_i)$. Here, the cutoff point $\tilde{x}_i = 0$ represents the effective treatment boundary $\bar{\mathcal{X}}_{i\mathcal{S}_i}(d,g\,|\,d',g')$. The idea is to approximate in a flexible way the regression functions $\mu_{d,g}(\tilde{x}_i)$ and $\mu_{d',g'}(\tilde{x}_i)$ close to $\tilde{x}_i = 0$ to estimate $\mu_{d,g}(0)$ and $\mu_{d',g'}(0)$, and the target estimand $\tau_{d,g|d',g'}\big(\bar{\mathcal{X}}_{i\mathcal{S}_i}(d,g\,|\,d',g')\big) = \mu_{d,g}(0) - \mu_{d',g'}(0)$.

Assuming that the regression functions $\mu_{d,g}(\tilde{x}_i)$ and $\mu_{d',g'}(\tilde{x}_i)$ are at least twice differentiable at the cutoff, a first-order Taylor expansion of the functions around $\tilde{x}_i = 0$ yields

$$\mu_{d,g}(\tilde{x}_i) \approx \mu_{d,g}(0) + \mu^{(1)}_{d,g}(0) \cdot \tilde{x}_i, \quad \mu_{d',g'}(\tilde{x}_i) \approx \mu_{d',g'}(0) + \mu^{(1)}_{d',g'}(0) \cdot \tilde{x}_i \tag{14}$$

where $\mu^{(q)}_{d,g}(0)$ and $\mu^{(q)}_{d',g'}(0)$ denote the q^{th} derivative of $\mu_{d,g}(\tilde{x}_i)$ and $\mu_{d',g'}(\tilde{x}_i)$ in $\tilde{x}_i = 0$.

To simplify exposition, here we focus on a local linear estimator. However, in the

Supplementary Material, S.3, results are stated for polynomials with generic degree p. Setting $\beta_{d,g}(0) = [\mu_{d,g}(0), \mu^{(1)}_{d,g}(0)]^T$ and $\beta_{d',g'}(0) = [\mu_{d',g'}(0), \mu^{(1)}_{d',g'}(0)]^T$, the distance-based local linear estimators for $\beta_{d,g}(0)$ and $\beta_{d',g'}(0)$ are obtained as

$$\begin{aligned}\hat{\beta}_{d,g,p}(h_n) &= \operatorname*{arg\,min}_{\boldsymbol{b}\in\mathbb{R}} \sum_i \mathbb{1}(D_i = d, G_i = g)(Y_i - \boldsymbol{r}_p(\tilde{X}_i)^T \boldsymbol{b})^2 \cdot K_{h_n^s}(\tilde{X}_i) \\ \hat{\beta}_{d',g',p}(h_n) &= \operatorname*{arg\,min}_{\boldsymbol{b}\in\mathbb{R}} \sum_i \mathbb{1}(D_i = d, G_i = g)(Y_i - \boldsymbol{r}_p(\tilde{X}_i)^T \boldsymbol{b})^2 \cdot K_{h_n^s}(\tilde{X}_i)\end{aligned} \tag{15}$$

where h_n is a positive bandwidth and $K_{h_n}(u) = K(u/h_n)/h_n$ for a given kernel function $K(\cdot)$. We assume that the kernel function has support $[-1, 1]$ and is positive, symmetric, and continuous, as is common in RDD literature (e.g., Calonico et al., 2014).[8]

We now introduce some useful notation, adapting the notation in Calonico et al. (2014). Let us set $\boldsymbol{Y} = [Y_1, ..., Y_n]^T$ and $\tilde{\boldsymbol{X}}_n = [\tilde{X}_1, ..., \tilde{X}_n]^T$, and let $r(u) = [1, u]$. We define $\tilde{X}(h_n) = [\boldsymbol{r}(\tilde{X}_1/h_n), ..., \boldsymbol{r}(\tilde{X}_n/h_n)]$, that is, the matrix containing the linear expansion of the distance variable, the diagonal weighting matrices $W_{d,g}(h_n)$ with generic diagonal element $w_{i,d,g}(h_n) = \mathbb{1}(D_i = d, G_i = g) \cdot K_{h_n}(\tilde{X}_i)$, and $W_{d',g'}(h_n)$ with generic diagonal element $w_{i,d',g'}(h_n) = \mathbb{1}(D_i = d', G_i = g') \cdot K_{h_n}(\tilde{X}_i)$. Finally, we define $\Gamma_{d,g}(h_n) = \tilde{X}(h_n)^T W_{d,g}(h_n)\tilde{X}(h_n)/n$ and $\Gamma_{d',g'}(h_n) = \tilde{X}(h_n)^T W_{d',g'}(h_n)\tilde{X}(h_n)/n$. Letting $H(h_n) = \text{diag}(1, h_n^{-1})$, for $h_n > 0$, the solutions to (15) are

$$\begin{aligned}\hat{\beta}_{d,g}(h_n) &= H(h_n)\Gamma^{-1}_{d,g}(h_n)\tilde{X}(h_n)^T W_{d,g}(h_n)\boldsymbol{Y}/n \\ \hat{\beta}_{d',g'}(h_n) &= H(h_n)\Gamma^{-1}_{d',g'}(h_n)\tilde{X}(h_n)^T W_{d',g'}(h_n)\boldsymbol{Y}/n\end{aligned} \tag{16}$$

The final estimator for $\tau_{d,g|d',g'}(\bar{\mathcal{X}}_{i\mathcal{S}_i}(d, g \mid d', g'))$ is given by the difference in the estimators of the intercepts of the transformed outcome regression functions

$$\hat{\tau}_{d,g|d',g'}(h_n) = \hat{\mu}_{d,g}(h_n) - \hat{\mu}_{d',g'}(h_n) \tag{17}$$

where $\hat{\mu}_{d,g}(h_n) = e_1^T \hat{\beta}_{d,g}(h_n)$ and $\hat{\mu}_{d',g'}(h_n) = e_1^T \hat{\beta}_{d',g'}(h_n)$ with $e_1 = [1, 0]^T$.

---

[8]Common choices include the uniform kernel which assigns equal weights within the bandwidth, and the triangular kernel, which assigns weights decreasing with the distance from the cutoff.

4.3 Asymptotic Theory

We consider an asymptotic framework where $n \to \infty$. Because all causal estimands and estimators are conditioned on $\boldsymbol{A}$, our asymptotic framework assumes a sequence of networks $\boldsymbol{A}_n$, preserving fundamental aspects of the network topology as in Ogburn et al. (2022). The analysis of the asymptotic properties of $\hat{\tau}_{d,g|d',g'}(h_n)$ requires a constraint on the asymptotic growth of the dependence in the data.

Assumption 6 (Local Dependence). *$n^{-1}\sum_i |\boldsymbol{N}_{i,n}|^3$ and $n^{-1}\sum_i \sum_{j\neq i}(\boldsymbol{W}_n^3)_{ij}$ are bounded.*

The quantity $n^{-1}\sum_i |\boldsymbol{N}_{i,n}|^3$ is the empirical third moment of the degree distribution of $\boldsymbol{W}_n$ whereas $n^{-1}\sum_{j\neq i}(\boldsymbol{W}_n^3)_{ij}$ is the average number of walks of length 3 emanating from unit i. Bounding these quantities ensures that most units have a sufficiently small degree in the dependency graph with respect to the sample size, limiting the amount of dependence in the data as n becomes large. Assumption 6 is analogous to Assumption 4 in Leung (2020), although here the dependency graphs are fixed.

Throughout this section, we maintain the assumption of homogeneous interference sets, boundaries, and outcome and score distributions across units. In Supplemental Appendix A, we relax these restrictions and analyze the estimator under heterogeneous settings.

Define $f_{d,g,d',g'}(0) = \int_{\bar{\mathcal{X}}_{i\mathcal{S}_i}(d,g\,|\,d',g')} f(x_i, \boldsymbol{x}_{\mathcal{S}_i}) d\mathcal{H}^{|\mathcal{S}_i|+1-\bar{s}}$. Additionally, let $\bar{\omega}_{d,g}(0)$ denote the integral over $\bar{\mathcal{X}}_{i\mathcal{S}_i}(d,g\,|\,d',g')$ of the conditional variance of $\mathbb{V}[\epsilon_{i,d,g}|(X_i, \boldsymbol{X}_{\mathcal{S}_i}) = (x_i, \boldsymbol{x}_{\mathcal{S}_i})]$ plus the squared approximation error, $[m_{d,g}(x_i, \boldsymbol{x}_{\mathcal{S}_i}) - \mathbb{E}[\,Y_i(d,g)\,|\,(X_i, \boldsymbol{X}_{\mathcal{S}_i}) \in \bar{\mathcal{X}}_{i\mathcal{S}_i}(d,g\,|\,d',g')\,]]^2$, weighted by $f(x_i, \boldsymbol{x}_{\mathcal{S}_i})$. Define $\bar{\omega}_{d',g'}(0)$ analogously but replacing (d,g) with (d',g'). Let $\bar{s}$ denote the common codimension of $\bar{\mathcal{X}}_{i\mathcal{S}_i}(d,g\,|\,d',g')$ across units.

Theorem 3. *Suppose Assumptions 1–6, and Assumptions S.3.1, S.3.2, and S.3.3 (see Supplementary Material S.3). If $nh_n^{\bar{s}} \to \infty$, $h_n \to 0$, and $h_n = O\big(n^{-1/(4+\bar{s})}\big)$, then*

$$\sqrt{nh_n^{\bar{s}}}\,\frac{\big(\hat{\tau}_{d,g|d',g'}(h_n) - \tau_{d,g|d',g'}\big(\bar{\mathcal{X}}_{i\mathcal{S}_i}(d,g\,|\,d',g')\big)\big) - h_n^2 B_{d,g,d'g'}(h_n)}{\sqrt{V_{d,g,d',g'}(h_n)}} \xrightarrow{d} \mathcal{N}(0,1),$$

where $B_{d,g,d'g'}(h_n) = B + o(1)$, and $V_{d,g,d',g'}(h_n) = V + o(1)$,

$$B = \Big(\frac{\mu^2_{d,g}(0) - \mu^2_{d',g'}(0)}{2!}\Big) e_1^\top (\Gamma^{\bar{s}})^{-1}\theta^{\bar{s}}, \quad V = \Big(\frac{\bar{\omega}_{d,g}(0) + \bar{\omega}_{d',g'}(0)}{f_{d,g,d',g'}(0)^2}\Big) e_1^\top (\Gamma^{\bar{s}})^{-1}\Psi^{\bar{s}}(\Gamma^{\bar{s}})^{-1}e_1.$$

The exact form of $\Gamma^{\bar{s}}$*,* $\theta^{\bar{s}}$ *and* $\Psi^{\bar{s}}$ *is given in Supplementary Material S.3.*

Proof. See Supplementary Material

Theorem 3 indicates that $\hat{\tau}_{d,g|d',g'}(h_n)$ is asymptotically normal with asymptotic bias $h_n^2 B$ and asymptotic variance $(nh_n^{\bar{s}})^{-1}V$.

Several considerations emerge from this result. First, the asymptotic bias depends on the second-order derivatives of the target outcome regression function, reflecting the linearization error; its contribution to the asymptotic distribution of $\hat{\tau}_{d,g|d',g'}(h_n)$ vanishes provided that $nh_n^{\bar{s}+4} \to 0$[9]. Second, the convergence rate of the asymptotic variance is governed by the dimension of the effective treatment boundary through the parameter $\bar{s}$, i.e., the number of score components $(x_i, \boldsymbol{x}_{\mathcal{S}_i})$ fixed at the cutoff in $\bar{\mathcal{X}}_{i\mathcal{S}_i}(d, g \mid d', g')$. This arises because the volume of the boundary neighborhoods $\mathcal{B}_{h_n}^{d,g}(\bar{\mathcal{X}}_{i\mathcal{S}_i}(d, g \mid d', g'))$ and $\mathcal{B}_{h_n}^{d',g'}(\bar{\mathcal{X}}_{i\mathcal{S}_i}(d, g \mid d', g'))$ is proportional to $h_n^{\bar{s}}$, as shown in the proof of Theorem 1. Consequently, the probability that an observation falls within such neighborhoods is proportional to $h_n^{\bar{s}}$, and thus, the estimator effectively uses approximately $nh_n^{\bar{s}}$ observations.

As a consequence, the convergence rate of $\hat{\tau}_{d,g|d',g'}(h_n)$ exhibits a curse of dimensionality driven by the parameter $\bar{s}$. Importantly, this curse does not depend on the full dimension of the multiscore space, i.e., $|\mathcal{S}_i| + 1$, but rather on $\bar{s}$, which captures the number of components of the score vector $(X_i, \boldsymbol{X}_{\mathcal{S}_i})$ that must simultaneously fall within a bandwidth h_n of the cutoff in order for an observation to contribute to the estimator.

To illustrate, consider an indirect effect comparing potential outcomes under zero versus all treated neighbors, for untreated units with two neighbors. The estimator assigns positive weight only to observations within $\mathcal{B}_{h_n}^{d,g}(\bar{\mathcal{X}}_{i\mathcal{S}_i}(d, g \mid d', g'))$ or $\mathcal{B}_{h_n}^{d',g'}(\bar{\mathcal{X}}_{i\mathcal{S}_i}(d, g \mid d', g')))$, that is, with $\tilde{X}_i \le h_n$ and under either effective treatment assignment. This condition requires that both neighbors' scores lie within the bandwidth—i.e., $||\boldsymbol{X}_{\mathcal{S}_i} - c|| < h_n$—and that $X_i - c < 0$. The effective treatment boundary in this case has dimension $|\mathcal{S}_i| + 1 - 2 = 1$, with $\bar{s} = 2$, and the convergence rate is $\sqrt{nh_n^6}$. When instead only one component must be near the cutoff (i.e., $\bar{s} = 1$), as in standard univariate RDDs, the estimator averages over approximately nh_n observations and

[9]With generic p-order distance-based local polynomial estimator this condition becomes $nh_n^{\bar{s}+2p+2} \to 0$.

achieves the standard univariate rate $\sqrt{nh_n^5}$ (Fan and Gijbels, 1996). This is the case for boundary direct effects $\tau_{1,g\,|\,0,g}\big(\bar{\mathcal{X}}_{i\mathcal{S}_i}(1,g\,|\,0,g)\big)$, which require only that X_i be near the cutoff, and $\boldsymbol{X}_{\mathcal{S}_i}$ is such that $e(\boldsymbol{X}_{\mathcal{S}_i}) = g$. Since these effects always satisfy $\bar{s} = 1$, their estimators retain the standard rate. The codimension can also be one for for some boundary indirect effects, e.g., $\tau_{0,1\,|\,0,0}\big(\bar{\mathcal{X}}_{i\mathcal{S}_i}(0,1\,|\,0,0)\big)$ with sum-of-treated exposure mapping, which compares untreated units with zero versus one treated neighbor. However, as seen before, boundary indirect effects $\tau_{d,g\,|\,d,g'}\big(\bar{\mathcal{X}}_{i\mathcal{S}_i}(d,g\,|\,d,g')\big)$ may involve higher $\bar{s}$, depending on the exposure mapping and the values g and g' that are being compared, and thus converge more slowly[10].

Finally, the asymptotic variance is unaffected by the data dependence due to the local nature of the estimator and the weak dependence by Assumption 6 (see also Jenish, 2012; Bartalotti and Brummet, 2017). The reason is that each observation within the boundary neighborhoods is approximately connected to at most $|\boldsymbol{N}_{i,n}|h_n$ other observations, so the average degree of the subgraph induced by proximity to the effective treatment boundary shrinks to zero as $h_n \to 0$ (see Lemma S.3.4). As a result, the sum of covariances in the estimator's asymptotic variance at most $O(nh_n^{\bar{s}+1})$ while the sum of the variances is $O(nh_n^{\bar{s}})$, meaning that dependence vanish asymptotically.

We also note that while $nh_n^{\bar{s}+1}$ is the rate of convergence of the sum of the covariances, the covariance rate of decay for two specific observations depends on the effect of interest and the clusterization of the network, which determine the extent of overlap of the arguments of the distance function. Specifically, for any two observations $\tilde{X}_i$ and $\tilde{X}_j$ are functions of $(X_i, \boldsymbol{X}_{\mathcal{S}_i})$ and $(X_j, \boldsymbol{X}_{\mathcal{S}_j})$ which may have common elements when units have overlapping interference sets. If the distance variables of two dependent observations depend on a disjoint set of scores, their covariance is $O(h_n^{2\bar{s}})$. In contrast, if their distance variables depend on the same subset of scores, their covariance is $O(h^{\bar{s}})$. If this is the case for a non-negligible fraction of observations, then the sum of the covariances is of the same order as the variances, and data dependence affects the asymptotic variance of the estimator (see also Section 4.4).

Remark 1. The bias properties of $\hat{\tau}_{d,g|d',g'}(h_n)$ hinge on Assumption S.3.1.c (see Appendix S.3), which imposes smoothness of $\mu_{d,g}(\tilde{x}_i)$ and $\mu_{d',g'}(\tilde{x}_i)$. While continuity

[10] Note that throughout we assume a common codimension $\bar{s}$ across units. Appendix A shows that under heterogeneous codimensions the estimator converges to a weighted average of boundary effects for units whose boundaries have the lowest codimension in the network.

of $m_{d,g}(x_i, \boldsymbol{x}_{\mathcal{S}_i})$ and $m_{d',g'}(x_i, \boldsymbol{x}_{\mathcal{S}_i})$ is sufficient for consistency of the estimator (see Lemma S.3.1-S.3.3), achieving the quadratic rate of bias decay, h_n^2, requires continuous differentiability of $\mu_{d,g}(\tilde{x}_i)$ and $\mu_{d',g'}(\tilde{x}_i)$. Verifying this condition may be challenging in practice due to the geometry of the effective treatment boundary. In Appendix S.3.6, we show that the assumption is readily satisfied for boundary direct effects if $m_{1,g}(x_i, \boldsymbol{x}_{\mathcal{S}_i})$, $m_{0,g}(x_i, \boldsymbol{x}_{\mathcal{S}_i})$, and $f(x_i, \boldsymbol{x}_{\mathcal{S}_i})$ are continuously differentiable.

Remark 2. Our estimator requires choosing a bandwidth h_n. Appendix B.1 derives the asymptotic MSE-optimal rate $h_n^{\text{opt}} \propto n^{-1/(\bar{s}+4)}$. Because this bandwidth does not satisfy $nh_n^{\bar{s}+4} \to 0$, we also consider a bias-corrected version, $\hat{\tau}^{bc}_{d,g|d',g'}(h_n, b_n)$ which subtracts from $\hat{\tau}_{d,g|d',g'}(h_n)$ an estimate of the leading bias using an auxiliary bandwidth b_n. We further derive confidence intervals robust to large bandwidth following Calonico et al. (2014) (see Supplemental Appendix B.1 for details).

4.4 Variance Estimation

The results of the previous sections suggest that the use of standard variance estimators assuming independent data (e.g. Calonico et al., 2014) might be appropriate when h_n is small. This irrelevance of data dependence is in sharp contrast with the parametric case, where dependence typically affects the asymptotic distribution of the estimators and must be accounted for to ensure valid inference. In our nonparametric setting, the asymptotic irrelevance of network dependence arises from $h_n \to 0$. However, in finite samples where the bandwidth h_n is not zero, the effect of network dependence may not vanish completely. Therefore, building on Leung (2020), we propose the following Eicker-Huber-White type variance estimator to account for such finite-sample dependence:

$$\hat{\mathcal{V}}_{d,g,d',g'}(h_n) = \frac{1}{n} e_1^T [\hat{V}_{d,g}(h_n) + \hat{V}_{d',g'}(h_n) - 2\hat{C}_{d',g',d,g}(h_n)] e_1 \tag{18}$$

where

$$\begin{aligned}
\hat{V}_{d,g}(h_n) &= \Gamma^{-1}_{d,g}(h_n)\hat{\bar{\Psi}}_{d,g}(h_n)\Gamma^{-1}_{d,g}(h_n), & \hat{\bar{\Psi}}_{d,g}(h_n) &= \mathcal{M}_{d,g}(h_n)^T \boldsymbol{W}_n \mathcal{M}_{d,g}(h_n)/n \\
\hat{V}_{d',g'}(h_n) &= \Gamma^{-1}_{d',g'}(h_n)\hat{\bar{\Psi}}_{d',g'}(h_n)\Gamma^{-1}_{d',g'}(h_n), & \hat{\bar{\Psi}}_{d',g'}(h_n) &= \mathcal{M}_{d',g'}(h_n)^T \boldsymbol{W}_n \mathcal{M}_{d',g'}(h_n)/n \\
\hat{C}_{d,g,d',g'}(h_n) &= \Gamma^{-1}_{d,g}(h_n)\hat{\bar{\Psi}}_{d,g,d',g'}(h_n)\Gamma^{-1}_{d',g'}(h_n) & \hat{\bar{\Psi}}_{d,g,d',g'}(h_n) &= \mathcal{M}_{d,g}(h_n)^T \boldsymbol{W}_n \mathcal{M}_{d',g'}(h_n)/n
\end{aligned} \tag{19}$$

In (19) $\boldsymbol{W}_n$ is the dependency graph, and $\mathcal{M}_{d',g'}(h_n)$ and $\mathcal{M}_{d',g'}(h_n)$ are $n \times 2$ matrices with i-th row given by the weighted linear expansion of $\tilde{X}_i/h_n$ times the regression residual $\hat{u}_i$. This estimator captures the covariance of observations within the bandwidth on each side of the cutoff, i.e., in region $\mathcal{X}_{i\mathcal{S}_i}(d,g)$ and $\mathcal{X}_{i\mathcal{S}_i}(d',g')$, as well as the covariance of observations across the cutoff.

There are two main justifications for this variance estimator. First, when a non-negligible fraction of connected units share the distance variable, $\hat{\tau}_{d,g|d',g'}(h_n)$ remains asymptotically normal, but its asymptotic variance includes the covariance of observations sharing the same distance measure, breaking the equivalence to the independent data case. (see Lemma S.3.7 and Theorem S.3.3 in Supplementary Material S.3). This situation may arise mechanically due to overlapping interference sets. For example, in Figure 2,, the minimum distance for observations in region $\mathcal{X}_{i\mathcal{S}_i}(0,0)$ is the perpendicular distance given by X_j. Thus, observations sharing the same neighbors will have the same distance measure. This differs from the no-interference multiscore RDD, where typically observations have distinct distance measures.

Second, the variance estimator in (18) consistently estimates $(nh_n^{\bar{s}})^{-1}V_{d,g,d',g'}(h_n)$ in Theorem 3, which can be seen as the variance arising from a "fixed-bandwidth" perspective, which treats $\hat{\tau}_{d,g|d',g'}(h_n)$ as locally parametric, holding the bandwidth fixed. Under such a perspective, each observation i within the bandwidth is approximately related to at most other $|\boldsymbol{N}_{i,n}|h_n$, where h_n is now constant. Therefore, contrary to the setting where $h_n \to 0$, the term involving the observations' covariances is now of the same order as the term involving the variances.[11] The estimator in (18) is consistent for the asymptotic variance $(nh_n^{\bar{s}})^{-1}V$ when $h_n \to 0$ (see Theorem S.3.2). Moreover, by indirectly estimating the asymptotic variance, it avoids estimating the unknown quantities $\bar{\omega}_{d,g}(0)$, $\bar{\omega}_{d',g'}(0)$ and $f_{d,g,d',g'}(0)$. Similar arguments favoring Eicker-Huber-White type variance estimators can be found, for instance, in Kim et al. (2017) in kernel-smoothing regression in time series. This type of variance estimator should also be used for bias-corrected estimators (see Subsection B.1), as the typical asymptotic regime used for the bias-corrected estimators, due to Calonico et al. (2014), allows one of the two bandwidths used for the construction of the estimator to be fixed.

[11]Specifically, the average degree of the subgraph within the bandwidth is asymptotically bounded, but does not converge to zero.

4.5 Estimation of Boundary Overall Direct and Indirect Effects

In this subsection, we summarize the estimation results for both the boundary overall direct and boundary overall indirect effects; full details are provided in Supplemental Appendix B.2 and C.2, respectively.

Theorem 2 show that the boundary overall direct effect $\tau_{1|0}$ s identified by $\lim_{x_i \downarrow c} \mathbb{E}[Y_i \mid X_i = x_i] - \lim_{x_i \uparrow c} \mathbb{E}[Y_i \mid X_i = x_i]$, precisely the quantity estimated in standard RDD using local polynomial regression (e.g., Hanh et al., 2001). This justifies the use of the conventional local polynomial RDD estimator to $\tau_{1|0}$. Importantly, we show that, under Assumptions 1–6, the estimator $\hat{\tau}_{1|0}(h_n)$ is consistent for $\tau_{1|0}$, meaning that even when interference is ignored, it retains a meaningful causal interpretation. Moreover, it is asymptotically normal and attains the no-interference RDD convergence rate. However, contrary to typical RDD applications, where observations are assumed to be i.i.d., the data may exhibit statistical dependence in our setting due to interference and network correlation, and, as shown in Section 4.4, accounting for data dependence can improve inference relative to conventional variance estimators in finite sample. For this reason, we also construct a network-robust variance estimator, analogous to Eq. (19). This variance estimator coincides with the standard heteroskedasticity-robust estimator (e.g., Calonico et al., 2014) when $\boldsymbol{W}$ is diagonal but diverges as data dependence increases.

In the Supplemental Appendix C.2, we show that the boundary overall indirect effect $\tau_{indirect}$ is identified by $\lim_{x_{\mathcal{S}_i}^{\min} \downarrow c} \mathbb{E}[Y_i \mid X_{\mathcal{S}_i}^{\min} = x_{\mathcal{S}_i}^{\min}] - \lim_{x_{\mathcal{S}_i}^{\min} \uparrow c} \mathbb{E}[Y_i \mid X_{\mathcal{S}_i}^{\min} = x_{\mathcal{S}_i}^{\min}]$, where $X_{\mathcal{S}_i}^{\min}$ denotes the score within i's interference set that is closest to the cutoff c, taking values $x_{\mathcal{S}_i}^{\min}$. Hence, we estimate the effect using a univariate local polynomial regression with $X_{\mathcal{S}_i}^{\min}$ as the forcing variable. Notably, this estimator attains the no-interference RDD rate of convergence, whereas estimators of boundary indirect effects typically converge more slowly, thus providing a practical alternative to estimating single boundary indirect effects.

5 Simulation Study

We report the results of a simulation study demonstrating the finite-sample properties of $\hat{\tau}_{1|0}(h_n)$ and $\hat{\tau}_{d,g|d',g'}(h_n)$, and their bias-corrected version $\hat{\tau}_{1|0}^{bc}(h_n, b_n)$ and

$\hat{\tau}^{bc}_{d,g|d',g'}(h_n, b_n)$. In this exercise, units are clustered in groups of size 3 ($\boldsymbol{A}$ is a block diagonal matrix). Interference occurs within clusters, so that $|S_i| = 2$ for each i. We use the sum-treated exposure mapping, common in the literature (see, e.g., Aronow and Samii, 2017), resulting in $G_i \in \{0, 1, 2\}$ and a partition of the multiscore space into six treatment regions. Outcomes are simulated from the model

$$Y_i = 0.5 + 1.5D_i + G_i + 0.5X_i + 4.3D_iX_i^2 - 1.5(1 - D_i)X_i^2 + 0.3\bar{\boldsymbol{X}}_{\mathcal{S}_i} + \epsilon_i \qquad (20)$$

where $\bar{\boldsymbol{X}}_{\mathcal{S}_i}$ is the average score within $\mathcal{S}_i$. Here, X_i is independently and identically distributed as a truncated normal with mean -0.3 and variance 1, and upper and lower bound -5 and 5, while the error terms are given by $\epsilon_i = D_i\big(2\frac{\sum_{j\in\mathcal{S}_i} u_j}{|\mathcal{S}_i|} + u_i\big) - 1.4(1 - D_i)\cdot \big(2\frac{\sum_{j\in\mathcal{S}_i} u_j}{|\mathcal{S}_i|} + u_i\big)$ with $u_i \overset{i.i.d.}{\sim} \mathcal{N}(0, 1)$, so that the correlation between the error terms of two neighbors depends on their treatment. Observations are then dependent only within each cluster with a block-diagonal dependency graph. In addition, Model (20) is non-linear in the individual score, which enables us to evaluate how the estimators differ with and without bias correction.

We simulate 1000 datasets with increasing sample size $n = \{750, 1500, 3000, 6000\}$ and increasing number of clusters $Z = \{250, 300, 1000, 2000\}$. For each, we estimate the boundary overall direct effect $\tau_{1|0}$ using the estimator in Eq.(B.3), the boundary direct effects $\tau_{10|00}(\mathcal{X}_{i\mathcal{S}_i}(10|00))$ and, the boundary indirect effects $\tau_{01|00}(\mathcal{X}_{i\mathcal{S}_i}(01|00))$ and $\tau_{02|00}(\mathcal{X}_{i\mathcal{S}_i}(02|00))$, using the estimator in Eq.(17) (Table 1). For the first two effects, the effective treatment boundaries has dimension $|S_i| + 1 - \bar{s}$ with $\bar{s} = 1$. In contrast, the effective treatment boundary for $\tau_{02|00}(\mathcal{X}_{i\mathcal{S}_i}(02|00))$ has $\bar{s} = 2$, implying a slower convergence rate for the corresponding estimator. We compute the standard error and confidence intervals using the variance estimator in Eq. (18). For comparison, we include the heteroskedasticity-robust plug-in residuals variance estimator without weights assuming i.i.d. data, and the cluster-robust variance estimator of Bartalotti (2019) accounting for dependence among observations on the same side of the cutoff, both implemented in `rdrobust` R package (Calonico et al., 2017). We estimate a different bandwidth for each sample size and effect following the plug-in procedure in Calonico et al. (2014). In addition, for sample size $n = 3000$, we estimate the same causal effects using the bias-corrected estimators defined in Eq. B.2 (Table 2).

Table 1 presents the results for the estimators without bias correction. Several considerations emerge from this simulation exercise. First, the estimators $\hat{\tau}_{1|0}(h_n)$ and

		Bias	S.D.	S.E.	S.E.$_{i.i.d.}$	S.E.$_{cl}$	C.R.	C.R.$_{i.i.d.}$	C.R.$_{cl}$	$\bar{N}_{d,g}$	$\bar{N}_{d',g'}$
n = 750	$\hat{\tau}_{1\|0}(h_n)$	-0.184	0.643	0.577	0.536	0.561	0.912	0.886	0.899	148.341	177.908
	$\hat{\tau}_{10\|00}(h_n)$	-0.189	0.939	0.812	0.780	0.823	0.902	0.890	0.906	57.658	69.806
	$\hat{\tau}_{01\|00}(h_n)$	-0.031	1.489	1.340	1.117	1.357	0.933	0.872	0.940	98.904	96.580
	$\hat{\tau}_{02\|00}(h_n)$	-0.064	4.294	2.982	2.932	3.060	0.855	0.847	0.862	22.952	34.422
n = 1500	$\hat{\tau}_{1\|0}(h_n)$	-0.156	0.446	0.423	0.395	0.411	0.918	0.891	0.907	279.640	330.839
	$\hat{\tau}_{10\|00}(h_n)$	-0.141	0.644	0.588	0.565	0.592	0.911	0.897	0.912	113.016	135.519
	$\hat{\tau}_{01\|00}(h_n)$	-0.030	1.052	0.943	0.781	0.949	0.928	0.851	0.928	203.788	198.410
	$\hat{\tau}_{02\|00}(h_n)$	0.146	2.840	2.259	2.187	2.285	0.920	0.912	0.921	48.221	72.686
n = 3000	$\hat{\tau}_{1\|0}(h_n)$	-0.137	0.337	0.314	0.295	0.306	0.909	0.883	0.896	512.603	596.299
	$\hat{\tau}_{10\|00}(h_n)$	-0.166	0.463	0.433	0.415	0.435	0.907	0.895	0.907	216.641	255.929
	$\hat{\tau}_{01\|00}(h_n)$	-0.042	0.737	0.669	0.549	0.671	0.935	0.864	0.935	418.464	404.431
	$\hat{\tau}_{02\|00}(h_n)$	-0.016	2.070	1.642	1.574	1.651	0.913	0.896	0.915	97.101	146.636
n = 6000	$\hat{\tau}_{1\|0}(h_n)$	-0.106	0.245	0.235	0.222	0.229	0.908	0.893	0.901	920.610	1051.498
	$\hat{\tau}_{10\|00}(h_n)$	-0.127	0.364	0.322	0.310	0.323	0.890	0.872	0.890	399.292	464.010
	$\hat{\tau}_{01\|00}(h_n)$	0.015	0.511	0.475	0.389	0.475	0.942	0.873	0.943	840.688	811.067
	$\hat{\tau}_{02\|00}(h_n)$	0.046	1.384	1.184	1.127	1.187	0.930	0.920	0.931	197.973	299.199

Table 1: Simulation results with groups of size three and one treated exposure mapping. One thousand replications. S.D. = empirical standard error. S.E. = estimated standard error. S.E.$_{i.i.d.}$ = estimated standard error with *i.i.d.* heteroskedasticity-robust HC0 plug-in residuals variance estimator. S.E.$_{cl}$ = estimated standard error with the cluster-robust variance estimator. C.R. = coverage rate. C.R.$_{i.i.d.}$ = coverage rate corresponding to the *i.i.d.* heteroskedasticity-robust HC0 plug-in residuals variance estimator. C.R.$_{cl}$ = coverage rate corresponding to the cluster-robust variance estimator. $N_{d,g}$ and $N_{d',g'}$ = effective sample size on each side of the treatment boundary.

$\hat{\tau}_{10|00}(h_n)$ exhibit some bias which decreases slightly with increasing sample size. In contrast, the estimator $\hat{\tau}_{01|00}(h_n)$ exhibit small bias. This discrepancy arises from the different degrees of non-linearity of the target outcome regression functions. In addition, the standard deviation of $\hat{\tau}_{01|00}(h_n)$ is consistently higher than that of $\hat{\tau}_{10|00}(h_n)$, due to clusterization at the distance level. As expected, $\hat{\tau}_{02|00}(h_n)$ has the highest variance among all estimators.

Second, our variance estimator generally provides more accurate estimates of the standard deviation than the *i.i.d.* estimator, with the magnitude of improvement depending on the degree of clustering induced by the treatment assignment. The improvement is substantial for $\hat{\tau}_{01|00}(h_n)$, due to the presence of a relevant average fraction of units with a common distance measure. The performance of the cluster-robust variance estimator is nearly identical to that of our variance estimator for $\hat{\tau}_{10|00}(h_n)$, $\hat{\tau}_{01|00}(h_n)$ and $\hat{\tau}_{02|00}(h_n)$. This is expected: under cluster dependence, these two estimators tend to coincide when the dependent observations are located on the same side of the zero-distance cutoff, as is the case here. In contrast, for $\hat{\tau}_{1|0}(h_n)$, our variance estimator outperforms the cluster-robust alternative, as it properly accounts for the covariance between units on opposite sides of the cutoff.

Lastly, the coverage of $\hat{\tau}_{02|00}(h_n)$ improves with larger sample sizes, while the coverage of $\hat{\tau}_{01|00}(h_n)$ approaches the nominal level in smaller samples, reflecting the slower convergence of $\hat{\tau}_{02|00}(h_n)$. Coverage also stabilizes for $\hat{\tau}_{1|0}(h_n)$ and $\hat{\tau}_{10|00}(h_n)$ in smaller samples due to their faster convergence. However, for these two estimators,

		Bias	S.D.	S.E.	S.E.$_{i.i.d.}$	S.E.$_{cl}$	C.R.	C.R.$_{i.i.d.}$	C.R.$_{cl}$	$\bar{N}_{d,g}$	$\bar{N}_{d',g'}$
n = 3000	$\hat{\tau}^{bc}_{1\|0}(h_n, b_n)$	0.007	0.349	0.338	0.320	0.331	0.940	0.926	0.934	512.878	596.780
	$\hat{\tau}^{bc}_{10\|00}(h_n, b_n)$	0.035	0.505	0.483	0.467	0.484	0.949	0.939	0.950	215.830	255.597
	$\hat{\tau}^{bc}_{01\|00}(h_n, b_n)$	0.005	0.845	0.788	0.651	0.791	0.938	0.875	0.938	417.212	404.337
	$\hat{\tau}^{bc}_{02\|00}(h_n, b_n)$	0.101	2.553	2.161	2.090	2.173	0.931	0.918	0.931	97.388	147.831

Table 2: Simulation results using bias correction with groups of size three and one treated exposure mapping. One thousand replications. S.D. = empirical standard error. S.E. = estimated standard error. S.E.$_{i.i.d.}$ = estimated standard error with *i.i.d.* heteroskedasticity-robust HC0 plug-in residuals variance estimator. S.E.$_{cl}$ = estimated standard error with the cluster-robust variance estimator. C.R. = coverage rate. C.R.$_{i.i.d.}$ = coverage rate corresponding to the *i.i.d.* heteroskedasticity-robust HC0 plug-in residuals variance estimator. C.R.$_{cl}$ = coverage rate corresponding to the cluster-robust variance estimator. $N_{d,g}$ and $N_{d',g'}$ = effective sample size on each side of the treatment boundary.

coverage settles below the nominal level because the selected bandwidths do not fully eliminate the leading bias in their distributions.

Table 2 presents the results for the bias-corrected estimators. The estimators for $\tau_{1|0}$ and $\tau_{10|00}(\bar{\mathcal{X}}_{i\mathcal{S}_i}(10|00))$ effectively remove the leading bias from the estimate. In addition, the estimated confidence intervals also provide better coverage of the true values across effects, reaching a rate close to the nominal level. Here, our standard error estimator and the i.i.d. estimator perform similarly, with the largest difference observed in the estimation of the standard error of $\hat{\tau}^{bc}_{01|00}(h_n, b_n)$ and $\hat{\tau}^{bc}_{02|00}(h_n, b_n)$.

Supplemental Appendix D presents two additional simulation studies: one with network data featuring varying degrees of overlap across interference sets, and one with grouped units and varying group sizes. In the network setting, we vary the likelihood that two units sharing a common neighbor are also directly connected, thereby inducing different levels of overlap across interference sets. Our estimators show low bias across scenarios, with variance increasing under a higher degree of overlap due to the increased proportion of observations sharing the distance variable. Our variance estimator outperforms the i.i.d. alternative, particularly when the overlap degree is high. In the group setting, our method yields less accurate inference for larger groups—and thus higher-dimensional multiscore spaces—because of sparse observations within effective treatment arms. Nevertheless, the boundary overall direct effect remains accurately estimated.

6 Empirical Illustration

The governmental program PROGRESA/Oportunidades, launched in 1997, targeted poverty in rural Mexico by providing subsidies to poor households, conditional on children's regular school attendance and health clinic visits. Among the 506 selected villages across seven rural states, 320 were randomly assigned to treatment and 186 to control. In treated villages, eligible households received subsidies based on a household poverty index. Several studies have leveraged the initial randomization to examine the spillover effects generated by the program on educational outcomes using linear-in-means models (e.g. Lalive and Cattaneo, 2009), and incorporating heterogeneous externalities (Arduini et al., 2020). Here, we do not leverage the village-level randomization and only analyze data from the 320 treated villages, where eligible households received subsidies according to a regression discountinuity design with the score being the household poverty index.

Our data comprises repeated observations for 24,000 households over three academic years (1997-1998, 1998-1999, and 1999-2000), with each academic year starting in August and ending in June. Baseline characteristics were collected in October 1997, while subsidies began in August 1998. The first wave of post-treatment data was collected in October 1998, and a second post-treatment survey was conducted in November 1999. We select children from treatment villages[12] who live with their mothers, for whom we have completed school enrollment data for 1997 and 1998, and who had completed grades 3 to 6 by October 1997, as in Lalive and Cattaneo (2009). However, we only include those children who were enrolled in school for the 1997-1998 academic year, as they are more likely to have interacted in the village school during that academic year.

For the interference sets, we consider clusters defined by village, grade completed in October 1997, and gender, as homophily in children's friendship networks is especially strong along these dimensions within villages (see, e.g., Shrum et al., 1988). For valid inference, it is necessary to assume stable friendship links among children over time. This assumption is supported by the program's timing, the absence of evidence for relocation across villages between 1997 and 1998, and the enrollment in school for the year 1997-1998 for all the children in our sample. Our final sample consists of 5,174 observations with unequally sized interference sets[13].

The score variable is the centered household poverty index, and the outcome is

[12] We focus exclusively on villages in regions 3 (Sierra Negra-Zongolica-Mazateca), 4 (Sierra Norte-Otomi Tepehua), and 5 (Sierra Gorda), where the cutoff values were nearly identical to avoid pooling observations with different cutoff values.

[13] To increase the sample size, in addition to the untreated children without treated peers in the treated villages, we also add to our sample children in control villages.

	Boundary	All observations N	Range	Treatment N	Range	Control N	Range
$\tau_{1\|0}$	$X_i = 0,\ X_j \in \mathbb{R}\ \forall j \in \mathcal{S}_i$	5174	[-542.50, 467.00]	3316	[0.00, 467.00]	1858	[-542.50, -0.10]
$\tau_{indirect}$	$X_i \in \mathbb{R},\ \exists j \in \mathcal{S}_i : X_j = 0$	4783	[-542.50, 379.50]	2789	[0.00, 379.50]	1994	[-542.50, -0.10]
$\tau_{10\|00}(\bar{\mathcal{X}}_{i\mathcal{S}_i}(10\|00))$	$X_i = 0,\ X_j < 0\ \forall j \in \mathcal{S}_i$	597	[-527.75, 365.50]	233	[0.00, 365.50]	364	[-527.75, -0.50]
$\tau_{11\|01}(\bar{\mathcal{X}}_{i\mathcal{S}_i}(11\|01))$	$X_i = 0,\ X_j \geq 0\ \forall j \in \mathcal{S}_i$	1303	[-542.50, 379.50]	957	[0.50, 379.50]	346	[-542.50, -0.50]
$\tau_{01\|00}(\bar{\mathcal{X}}_{i\mathcal{S}_i}(01\|00))$	$X_i < 0,\ X_j = 0\ \forall j \in \mathcal{S}_i$	710	[-700.72, 478.44]	346	[0.00, 478.44]	364	[-700.72, -0.50]
$\tau_{11\|10}(\bar{\mathcal{X}}_{i\mathcal{S}_i}(11\|10))$	$X_i \geq 0,\ X_j = 0\ \forall j \in \mathcal{S}_i$	1190	[-542.50, 575.94]	957	[0.50, 575.94]	233	[-542.50, -0.50]

Table 3: Boundaries and sample sizes for each effect for PROGRESA data. The range refers to the individual score variable in the first line and the minimum distance score in the remaining lines.

school enrollment in academic year 1998-1999. Note that PROGRESA is considered a sharp RDD, as the fraction of eligible households that do not receive the subsidies is negligible. Therefore, the treatment variables D_i should be considered the receipt of the subsidies, and the estimands should be interpreted as effects of the subsidies. We define the exposure mapping as the fraction of treated units in the interference set: $G_i = \frac{\sum_{j \in \mathcal{S}_i} D_j}{|\mathcal{S}_i|}$. Using our method we estimate (i) the direct effect of the cash transfer on school enrollment in the academic year 1998-1999 when having all treated peers ($G_i = 1$) and no treated peers ($G_i = 0$); (ii) the spillover effect of having all treated peers ($G_i = 1$) versus no treated peers ($G_i = 0$), both for treated and untreated units; and (iii) the boundary overall direct effect of receiving the cash transfer, and the boundary overall indirect effect of having an additional peer receiving the subsidies. We estimate these effects restricting to children with at most four neighbors (3,111 observations), as for larger groups the number of units with $G_i = 0$ is extremely small.

The associated effective treatment boundaries are described in Table 3, along with the range of the computed minimum distance measure and the number of observations on each effective treatment region. The boundary associated with the boundary direct effects is of dimension at most 4 with $\bar{s} = 1$, as discussed in Section 4, while that for the indirect effects also has dimension up to 4 but varying $\bar{s}_i$. Hence, the estimates for these latter effects apply only to units in the smallest groups (see Supplemental Appendix A), while the other estimated effects apply to all units.

Estimates are reported in Table 4. Bias-corrected estimates are very similar in magnitude but less precise, so they are omitted and provided in the replication files. Standard errors and confidence intervals are computed using the variance estimator described in Subsection 4.4. Our estimates indicate a positive boundary overall direct effect, suggesting a significant marginal impact of eligibility to PROGRESA on children's school enrollment. The boundary direct effect for children with ineligible

	Estimate	S.E.	C.I.	p-value	$N_{d,g}$	$N_{d',g'}$
$\hat{\tau}_{10\|00}(h_n)$	0.238	0.072	(0.097, 0.378)	0.001	202	129
$\hat{\tau}_{11\|01}(h_n)$	0.024	0.043	(-0.061, 0.109)	0.577	216	325
$\hat{\tau}_{01\|00}(h_n)$	0.077	0.098	(-0.115, 0.269)	0.433	170	158
$\hat{\tau}_{11\|10}(h_n)$	-0.046	0.043	(-0.131, 0.039)	0.286	158	353
$\hat{\tau}_{1\|0}(h_n)$	0.076	0.030	(0.017, 0.134)	0.011	741	1010
$\hat{\tau}_{indirect}(h_n)$	0.046	0.027	(-0.007, 0.100)	0.090	924	1079

Table 4: Estimates for PROGRESA data with conventional and robust confidence intervals, MSE-optimal bandwidths. S.E. = estimated standard errors, C.I. = Normal approximation confidence intervals. p-value = Normal approximation two-sided p-value. $N_{d,g}$, $N_{d',g'}$ = Effective sample sizes.

neighbors is also positive and significant, but the direct effect is small and non-significant for those with eligible neighbors. The boundary indirect effect estimates suggest a larger impact of having all eligible neighbors versus all ineligible neighbors for ineligible children than for eligible children. The estimate for $\tau_{indirect}$ is statistically significant at the 10% level, suggesting a (local) positive spillover effect of the program[14]. These results imply that the program directly increased school attendance among children with untreated peers and also generated a positive spillover effect for children with at least one peer at the eligibility cutoff. This, in turn, suggests that, thanks to spillover effects, the program is able to achieve a higher increase in school attendance. Policymakers wishing to improve the effectiveness of the program without increasing resources could then use a subsidy assignment strategy among eligible children stratified by clusters defined by village, grade, and gender. Note, however, that we focus on estimating individual-level estimands using RDD data from treated villages, and do not address village-level "overall effects" of assignment strategies (e.g., comparing village-level mean outcomes if all eligible households in a village were treated versus none). In principle, one could express such village-level effects as a combination of individual-level total and spillover effects, as in Hudgens and Halloran (2008). Establishing this link within our framework would require additional assumptions due to the local nature of our estimands. We view this as an important direction for future research.

The varying effect sizes may reflect local factors. A lower poverty index correlates with better living conditions and more educated parents (Lalive and Cattaneo, 2009). Children with non-poor friends, who are more likely to attend school, may

[14] The bias-corrected estimate is nearly identical (0.044 vs. 0.046) but less precise, removing 10% significance.

be more encouraged to attend school upon receiving a subsidy, explaining the larger estimate of $\hat{\tau}_{10|00}(h_n)$ compared to $\hat{\tau}_{11|01}(h_n)$. The estimators $\hat{\tau}_{01|00}(h_n)$ and $\hat{\tau}_{11|10}(h_n)$ estimate a spillover effect on ineligible (non-poor) and eligible (poor) children, respectively, whose friends have a poverty index near the cutoff. Non-poor families, facing less economic burden, may find it easier to send their children to school if their friends attend due to the subsidy. Conversely, children from low-income families might experience negative incentives if their beneficiary friends attend school more frequently, incentivizing poor children to seek employment over education (Attanasio et al., 2011).

Finally, our results may depend on the chosen exposure mapping. Here, we use the share of treated peers— also known as stratified interference, which is common in the literature on interference effect estimation (Sävje, 2023)— and is reasonable when spillovers are expected to increase with the number of treated peers. This choice is also related to prior analyses of PROGRESA using linear-in-means models (e.g., Arduini et al., 2020). However, alternative exposure mappings are possible and, when feasible, should be informed by domain knowledge (see also Section 7).

7 Conclusions

In this paper, we have provided an analytical framework for interference in the continuity-based approach to RDDs. Here, potential outcomes are influenced by the treatment of units within interference sets through an exposure mapping function. We have shown that the non-probabilistic nature of the individual treatment assignment results in a non-probabilistic assignment of the effective treatment, allowing us to interpret RDDs under interference as multiscore RDDs. In this context, the effective treatment depends on both individual scores and the scores of units in the interference set. We have characterized the resulting multiscore space in terms of effective treatment regions and boundaries and introduced novel causal estimands. We shown the identification such effects through continuity assumptions. An important finding is that the overall direct effect at the cutoff is identified as the difference in the right and left limit of the outcome conditional expectation at the cutoff point, which coincides with the identification strategy in the no-interference RDDs.

Our identification strategy relies on treatment unconfoundedness conditional on the individual score and the scores in the interference sets, a property resulting from the assignment rule. One might replace this general property with a stronger unconfoundedness assumption conditional on some summary statistics of the scores of the interference set instead of the complete vector. However, this assumption rests on the correct choice of such summary statistics. We leave the identification implications and the development of an estimator under such assumption to future work.

We have proposed a distance-based local polynomial estimator for estimating boundary effects and the standard RDD local polynomial estimator for estimating the boundary overall direct and indirect effects. We have considered these estimation strategies with and without bias correction and have derived their asymptotic properties under the assumption of local dependence. In addition, we have developed a variance estimator that accounts for network-induced dependence, providing more accurate inference than conventional estimators that assume i.i.d. data. A key result is that the convergence rate of our distance-based local polynomial estimators depends on the codimension of the effective treatment boundary, which reflects the number of individual and neighbor scores that must simultaneously lie at the cutoff. In particular, the conventional RDD rate is recovered when the codimension equals one. Our formal analysis generalizes beyond our interference framework and is of independent interest to the multivariate RDD literature. To our knowledge, this is also the first work to study local polynomial estimation with network-dependent data, thereby also indirectly contributing to the statistical literature on local polynomial estimation (Fan and Gijbels, 1996).

Our framework does have some limitations, which also present opportunities for future research. First, we assume a fixed, fully observed network. While this is plausible in a short time window—as in the PROGRESA application—networks may evolve or respond to treatment, leading to biased estimates of the causal effects. Extending the framework to jointly model stochastic network formation and outcomes would be valuable (e.g., Johnsson and Moon, 2021). Second, we assume a correctly specified exposure mapping, which is plausible when domain knowledge is available. In many cases, however, the true exposure mapping is unknown, and its misspecification may lead to misspecification of the multiscore space. Yet, if the chosen exposure mapping is a coarsening of the true one, the resulting estimand could still remain interpretable as a summary measure of interference effects (Vazquez-Bare, 2022). Moreover, Sävje (2023) argues that a misspecified exposure mapping can still support valid inference while helping researchers focus on relevant aspects of the applications at hand. In an RDD setting, we conjecture that a misspecified exposure mapping could lead to simplified effective treatment boundaries while still identifying causally interpretable quantities. For instance, the identification of the boundary overall direct effect can be considered as relying on a misspecified constant exposure mapping that disregards interference. Exploring these possibilities would be worthwhile.

In the case of non-compliance to treatment eligibility/assignment (fuzzy RDD), we have focused on intention-to-treat effects. In fuzzy contexts, different spillover effects are possible, including spillovers from treatment assignment to treatment receipt, from treatment receipt to outcomes, and directly from treatment assignment to outcomes. For instance, in a conditional cash transfer program such as PROGRESA, having eligible peers—regardless of the treatment receipt—may encourage school enrollment through increased awareness among households. While ITT effects capture the overall presence of such spillover effects, they cannot disentangle these different channels. In standard fuzzy RDDs, identifying the average effect of treatment receipt for compliers requires additional assumptions (Imbens and Lemieux, 2008). Under interference, non-compliance adds several complexities (Imai et al., 2021; DiTraglia et al., 2023). In addition, generalizing monotonicity assumptions from univariate to multivariate settings has proven challenging in RDDs (Choi and Lee, 2023). However, our formalization of interference might offer a foundation for exploring these complex scenarios.

We have shown that the convergence rate of the distance-based estimator deteriorates when the effective treatment boundary has low dimension relative to the multiscore space—as in the case of boundary indirect effects—since the data become sparse in neighborhoods of such boundaries. Furthermore, this method relies on a data transformation that might not be optimal because it groups all observations with the same distance from the boundary to the same point in the one-dimensional distance space, potentially increasing bias (Imbens and Wager, 2019). Existing literature on multiscore RDDs has predominantly concentrated on simpler scenarios featuring bivariate scores and two treatment regions. However, interference in large groups or networks may lead to boundaries with high and heterogeneous dimensions. Therefore, another direction for future research is developing alternative non-parametric estimation methods to handle this new setting effectively.

References

Angelucci, M. and De Giorgi, G. (2009). Indirect effects of an aid program: How do cash transfers affect ineligibles' consumption? *American Economic Review*, 99(1):486–508.

Arduini, T., Patacchini, E., and Rainone, E. (2020). Treatment effects with heterogeneous externalities. *Journal of Business & Economic Statistics*, 38(4):826–838.

Aronow, P. M., Basta, N. E., and Halloran, M. E. (2017). The regression discontinuity design under interference: A local randomization-based approach. *Observational Studies*, 3(2).

Aronow, P. M. and Samii, C. (2017). Estimating average causal effects under general interference, with application to a social network experiment. *The Annals of Applied Statistics*, 11(4):1912–1947.

Athey, S., Eckles, D., and Imbens, G. (2015). Exact p-values for network interference. *NBER Working Paper 21313*.

Attanasio, O., Sosa, L. C., Medina, C., Meghir, C., and Posso-Suárez, C. M. (2021). Long term effects of cash transfer programs in colombia. Working Paper 29056, National Bureau of Economic Research.

Attanasio, O. P., Meghir, C., and Santiago, A. (2011). Education choices in mexico: Using a structural model and a randomized experiment to evaluate progresa. *The Review of Economic Studies*, 79(1):37–66.

Auerbach, E., Cai, Y., and Rafi, A. (2024). Regression discontinuity design with spillovers. arXiv: 2404.06471.

Baird, S., Bohren, J. A., McIntosh, C., and Özler, B. (2018). Optimal design of experiments in the presence of interference. *The Review of Economics and Statistics*, 100(5):844–860.

Bartalotti, O. (2019). Regression discontinuity and heteroskedasticity robust standard errors: Evidence from a fixed-bandwidth approximation. *Journal of Econometric Methods*, 8(1):20160007.

Bartalotti, O. and Brummet, Q. (2017). Regression discontinuity designs with clustered data. In *Regression Discontinuity Designs*, volume 38, pages 383–420. Emerald Group Publishing Limited.

Basse, G. W., Feller, A., and Toulis, P. (2019). Randomization tests of causal effects under interference. *Biometrika*, 106(2):487–494.

Basta, N. E. and Halloran, M. E. (2019). Evaluating the effectiveness of vaccines using a regression discontinuity design. *American journal of epidemiology*, 188(6):987–990.

Battistin, E. and Rettore, E. (2002). Testing for programme effects in a regression discontinuity design with imperfect compliance. *Journal of the Royal Statistical Society: Series A (Statistics in Society)*, 165(1):39–57.

Battistin, E. and Rettore, E. (2008). Ineligibles and eligible non-participants as a double comparison group in regression-discontinuity designs. *Journal of Econometrics*, 142(2):715–30.

Borusyak, K. and Kolerman-Shemer, M. (2024). Regression discontinuity aggregation, with an application to the union effects on inequality.

Bowers, J., Fredrickson, M., and Panagopoulos, C. (2013). Reasoning about interference between units: a general framework. *Political Analysis*, 21(1):97–124.

Calonico, S., Cattaneo, M., Farrell, M. H., and Titiunik, R. (2017). rdrobust: Software for regression-discontinuity designs. *Stata Journal*, 17(2):372–404.

Calonico, S., Cattaneo, M. D., and Titiunik, R. (2014). Robust nonparametric confidence intervals for regression-discontinuity designs. *Econometrica*, 82(6):2295–2326.

Cattaneo, M. D., Titiunik, R., and Yu, R. R. (2025). Estimation and inference in boundary discontinuity designs.

Choi, J. and Lee, M. (2023). Complier and monotonicity for fuzzy multi-score regression discontinuity with partial effects. *Economics Letters*, 228(C):111169.

Cox, D. R. (1958). *Planning of Experiments*. New York: Wiley.

Crépon, B., Duflo, E., Gurgand, M., Rathelot, R., and Zamora, P. (2013). Do labor market policies have displacement effects? evidence from a clustered randomized experiment *. *The Quarterly Journal of Economics*, 128(2):531–580.

Dell, M. (2010). The persistent effects of peru's mining "mita". *Econometrica*, 78(6):1863–1903.

DiTraglia, F. J., García-Jimeno, C., O'Keeffe-O'Donovan, R., and Sánchez-Becerra, A. (2023). Identifying causal effects in experiments with spillovers and non-compliance. *Journal of Econometrics*, 235(2):1589–1624.

Díaz, J. D. and Zubizarreta, J. R. (2023). Complex discontinuity designs using covariates: Impact of school grade retention on later life outcomes in chile. *The Annals of Applied Statistics*, 17(1):67 – 88.

Fan, J. and Gijbels, I. (1996). *Local Polynomial Modelling and Its Applications*. Chapman and Hall, London.

Forastiere, L., Airoldi, E. M., and Mealli, F. (2021). Identification and estimation of treatment and interference effects in observational studies on networks. *Journal of the American Statistical Association*, 116(534):901–918.

Forastiere, L., Mealli, F., Wu, A., and Airoldi, E. M. (2022). Estimating causal effects under network interference with bayesian generalized propensity scores. *Journal of Machine Learning Research*, 23(289):1–61.

Halloran, M. E. and Struchiner, C. J. (1995). Causal inference in infectious diseases. *Epidemiology*, 6(2):142–151.

Hanh, J., Todd, P., and van der Klaauw, W. (2001). Identification and estimation of treatment effects with a regression-discontinuity design. *Econometrica*, 69(1):201–09.

Hernan, M. and Robins, J. (2023). *Causal Inference: What If*. CRC Press, 1st ed. edition.

Hudgens, M. G. and Halloran, M. E. (2008). Toward causal inference with interference. *Journal of the American Statistical Association*, 103(482):832–842.

Imai, K., Jiang, Z., and Malani, A. (2021). Causal inference with interference and noncompliance in two-stage randomized experiments. *Journal of the American Statistical Association*, 116(534):632–644.

Imbens, G. and Lemieux, T. (2008). Regression discontinuity designs: A guide to practice. *Journal of Econometrics*, 142(2):615–35.

Imbens, G. and Wager, S. (2019). Optimized regression discontinuity designs. *The Review of Economics and Statistics*, 101(2):264–278.

Imbens, G. and Zajonc, T. (2011). Regression discontinuity design with multiple forcing variables. Working Paper.

Jacob, B. A. and Lefgren, L. (2004). Remedial education and student achievement: A regression- discontinuity analysis. *Review of Economics and Statistics*, 86(1):226–44.

Jenish, N. (2012). Nonparametric spatial regression under near-epoch dependence. *Journal of Econometrics*, 167(1):224–239.

Johnsson, I. and Moon, H. R. (2021). Estimation of peer effects in endogenous social networks: Control function approach. *The Review of Economics and Statistics*, 103(2):328–345.

Keele, L. J. and Titiunik, R. (2015). Geographic boundaries as regression discontinuities. *Political Analysis*, 23(1):127–155.

Kim, M. S., Sun, Y., and Yang, J. (2017). A fixed-bandwidth view of the pre-asymptotic inference for kernel smoothing with time series data. *Journal of Econometrics*, 197(2):298–322.

Kojevnikov, D., Marmer, V., and Song, K. (2021). Limit theorems for network dependent random variables. *Journal of Econometrics*, 222(2):882–908.

Kolesár, M. and Rothe, C. (2018). Inference in regression discontinuity designs with a discrete running variable. *American Economic Review*, 108(8):2277–2304.

Lalive, R. and Cattaneo, M. A. (2009). Social interactions and schooling decisions. *The Review of Economics and Statistics*, 91(3):457–477.

Lee, D. S. (2008). Randomized experiments from non-random selection in u.s. house elections. *Journal of Econometrics*, 142(2):675–97.

Leung, M. (2020). Treatment and spillover effects under network interference. *The Review of Economics and Statistics*, 102(2):368–380.

Leung, M. P. and Loupos, P. (2023). Unconfoundedness with network interference. arXiv:2211.07823.

Liu, L. and Hudgens, M. (2014). Large sample randomization inference of causal effects in the presence of interference. *Journal of the American Statistical Association*, 109(505):288–301.

Liu, L., Hudgens, M. G., and Becker-Dreps, S. (2016). On inverse probability-weighted estimators in the presence of interference. *Biometrika*, 103(4).

Manski, C. F. (2013). Identification of treatment response with social interactions. *The Econometrics Journal*, 16(1):S1–S23.

Masry, E. and Fan, J. (1997). Local polynomial estimation of regression functions for mixing processes. *Scandinavian Journal of Statistics*, 24(2):165–179.

Matsudaira, J. D. (2008). Mandatory summer school and student achievement. *Journal of Econometrics*, 142(2):829–850.

McPherson, M., Smith-Lovin, L., and Cook, J. M. (2001). Birds of a feather: Homophily in social networks. *Annual Review of Sociology*, 27(1):415–444.

Ogburn, E. L., Sofrygin, O., Díaz, I., and van der Laan, M. J. (2022). Causal inference for social network data. *Journal of the American Statistical Association*, 119(545):597–611.

Papadogeorgou, G., Mealli, F., and CM, Z. (2019). Causal inference with interfering units for cluster and population level treatment allocation programs. *Biometrics*, 75(3):778–787.

Perez-Heydrich, C., Hudgens, M. G., Halloran, M. E., Clemens, J. D., Ali, M., and Emch, M. E. (2014). Assessing effects of cholera vaccination in the presence of interference. *Biometrics*, 70(3):731–744.

Qu, Z., Xiong, R., Liu, J., and Imbens, G. (2021). Semiparametric estimation of treatment effects in observational studies with heterogeneous partial interference. *arXiv preprint arXiv:2107.12420*.

Reardon, S. F. and Robinson, J. P. (2012). Regression discontinuity designs with multiple rating-score variables. *Journal of Research on Educational Effectiveness*, 5(1):83–104.

Ross, N. (2011). Fundamentals of Stein's method. *Probability Surveys*, 8:210–293.

Shrum, W., Cheek, N. H., and Hunter, S. M. (1988). Friendship in school: Gender and racial homophily. *Sociology of Education*, 61(4):227–239.

Sobel, M. E. (2006). What do randomized studies of housing mobility demonstrate? *Journal of the American Statistical Association*, 101(476):1398–1407.

Sofrygin, O. and van der Laan, M. (2017). Semi-parametric estimation and inference for the mean outcome of the single time-point intervention in a causally connected population. *Journal of Causal Inference*, 5(1):1–35.

Sävje, F. (2023). Causal inference with misspecified exposure mappings: separating definitions and assumptions. *Biometrika*, 111(1):1–15.

Tchetgen Tchetgen, E. J. and VanderWeele, T. J. (2012). On causal inference in the presence of interference. *Statistical Methods in Medical Research*, 21(1):55–75.

Trochim, W. (1984). *Research Design for Program Evaluation: The Regression-Discontinuity Approach*. Contemporary Evaluation Research Series. Sage Publications, Beverly Hills, Calif.

Vazquez-Bare, G. (2022). Identification and estimation of spillover effects in randomized experiments. *Journal of Econometrics*.

Viviano, D. (2024). Policy targeting under network interference. *The Review of Economic Studies*, 92:1257–1292.

Viviano, D., Lei, L., Imbens, G., Karrer, B., Schrijvers, O., and Shi, L. (2025). Causal clustering: design of cluster experiments under network interference.

Supplemental Appendix to "Regression Discontinuity Designs Under Interference"

Elena Dal Torrione[1], Tiziano Arduini[2], Laura Forastiere[1]

[1]Department of Biostatistics, Yale University
[2]Department of Economics and Finance, Tor Vergata University of Rome

A Heterogeneous Effects

We extend the analysis to scenarios where units can have heterogeneous cardinality of the interference sets and, thus, heterogeneous effective treatment boundaries, as well as heterogeneous outcome and score distributions. In general, both outcomes and score distributions can depend on network characteristics,such as the number of neighbors, and other fixed covariates, (e.g. Ogburn et al., 2022). In addition, the dimension of the multiscore space, and the geometry of the effective treatment boundaries may vary across units. When such heterogeneity arise, boundary causal effects must be defined as finite ample averages of the outcome expectations across the network nodes:

$$\tau_{d,g|d',g'}\big(\bar{\mathcal{X}}_{i\mathcal{S}_i}(d,g\,|\,d',g')\big) = \frac{1}{|V_g|}\sum_{i\in V_g}\tau_{i,d,g|d',g'}(\bar{\mathcal{X}}_{i\mathcal{S}_i}(d,g\,|\,d',g')) \tag{A.1}$$

where $\tau_{i,d,g|d',g'}(\bar{\mathcal{X}}_{i\mathcal{S}_i}(d,g\,|\,d',g')) = \mathbb{E}_i[Y_i(d,g) - Y_i(d',g')\,|(X_i,\boldsymbol{X}_{\mathcal{S}_i}) \in \bar{\mathcal{X}}_{i\mathcal{S}_i}(d,g\,|\,d',g')]$ is the $i-$specific boundary causal effect, and $V_g = \{i \in \mathcal{N} : g \in \mathcal{G}_i\}$ the set of units whose neighborhood treatment G_i can attain the value g, and for which then potential outcomes $Y_i(d,g)$ are well-defined. Here, the effective treatment boundary has potentially different dimension and codimension for each i, given by $|\mathcal{S}_i| + 1 - \bar{s}_i$ and $\bar{s}_i$.

Identification of boundary average causal effects is achieved under Assumptions 1-4 as

$$\tau_{d,g|d',g'}\big(\bar{\mathcal{X}}_{i\mathcal{S}_i}(d,g\,|\,d',g')\big) = \frac{1}{|V_g|}\sum_{i\in V_g}\lim_{\varepsilon\to 0}\mathbb{E}_i[Y_i\,|\,(X_i,\boldsymbol{X}_{\mathcal{S}_i})\in\mathcal{B}_\varepsilon^{d,g}(\bar{\mathcal{X}}_{i\mathcal{S}_i}(d,g\,|\,d',g'))] - \lim_{\varepsilon\to 0}\mathbb{E}_i[Y_i\,|\,(X_i,\boldsymbol{X}_{\mathcal{S}_i})\in\mathcal{B}_\varepsilon^{d',g'}(\bar{\mathcal{X}}_{i\mathcal{S}_i}(d,g\,|\,d',g'))]$$

by analogous arguments as in Theorem 1.

Under such heterogeneity, the estimator $\hat{\tau}_{d,g|d',g'}(h_n)$ defined in Section 4 is, in general, no longer consistent to (A.1). Instead, it converges to a weighted average of unit-specific boundary causal effects. Moreover, when the codimension of the effective treatment boundary $\bar{s}_i$ is heterogeneous, assuming that for n large enough $\inf_i \bar{s}_i = \bar{s}$, independent of n, only observations with $\bar{s}_i = \bar{s}$ contribute in the limit, because the number of observations within distance h_n of $\bar{\mathcal{X}}_{i\mathcal{S}_i}(d,g\,|\,d',g')_i$ scales as $nh_n^{\bar{s}_i}$. Hence, the contribution of higher-codimension observations ($\bar{s}_i > \bar{s}$) vanishes, and the estimator converges to a weighted average of boundary effects for units whose boundary has the lowest codimension in the network.

Formally, in Theorem S.5.1 we show that under similar assumptions to Theorem 3:

$$\hat{\tau}_{d,g|d',g'}(h_n) \xrightarrow{p} \frac{\sum_{i:\,\bar{s}_i=\bar{s}} \tau_{i,d,g|d',g'}(\bar{\mathcal{X}}_{i\mathcal{S}_i}(d,g\,|\,d',g'))\, f_{i,d,g,d',g'}(0)}{\sum_{i:\,\bar{s}_i=\bar{s}} f_{i,d,g,d',g'}(0)} \tag{A.2}$$

as $nh_n^{\bar{s}} \to \infty$ and $h_n \to 0$, where the summation is implicitly taken over units in the feasibility set V_g, and

$$f_{i,d,g,d',g'}(0) = \int_{\bar{\mathcal{X}}_{i\mathcal{S}_i}(d,g\,|\,d',g')} f_i(x_i,\boldsymbol{x}_{\mathcal{S}_i})\,d\mathcal{H}^{|\mathcal{S}_i|+1-\bar{s}}$$

The RHS of (A.2) corresponds to the weighted average of unit-specific boundary effects, with weights depending on the integrals of the score densities at the effective treatment boundary.

Depending on the source of heterogeneity, we distinguish two notable cases:

1. Homogeneous $|\mathcal{S}_i|$ and $\bar{\mathcal{X}}_{i\mathcal{S}_i}(d,g\,|\,d',g')$, and heterogeneous $\mathbb{E}_i[Y_i(d,g)|X_i = x_i, \boldsymbol{X}_{\mathcal{S}_i} = \boldsymbol{x}_{\mathcal{S}_i}]$ and $f_i(x_i,\boldsymbol{x}_{\mathcal{S}_i})$: the estimator converges to the weighted average in (A.2) but defined for the entire network. If, in addition, the score distributions are homogeneous, then $\hat{\tau}_{d,g|d',g'}(h_n)$ converges to the network average defined in (A.1).

2. Heterogeneous $|\mathcal{S}_i|$ and $\bar{\mathcal{X}}_{i\mathcal{S}_i}(d,g\,|\,d',g')$, and homogeneous $\mathbb{E}[Y_i(d,g) \mid X_i = x_i, \boldsymbol{X}_{\mathcal{S}_i} = \boldsymbol{x}_{\mathcal{S}_i}]$: when $\tau_{i,d,g|d',g'}(x_i, \boldsymbol{x}_{\mathcal{S}_i}) = \kappa$ is constant across all i, x_i, and $\boldsymbol{x}_{\mathcal{S}_i}$, the estimator converges to the network average in (A.1), equal to κ, regardless of the score density. This corresponds to a limiting case where causal effects are invariant to individual and neighborhood scores, and network characteristics, which we view as an unlikely scenario in practice.

Finally, we note that one method to recover the estimand (A.1) under heterogeneous $|\mathcal{S}_i|$ is to estimate boundary effects separately via distance-based local linear estimation for units with the same interference set cardinality, and then average the estimated effects across the sample units. However, this procedure may yield high variance, as it aggregates potentially noisy estimates.

B Additional Estimations Results

B.1 MSE-optimal Bandwidth, Bias Correction and Robust Confidence Intervals

As remarked in Section 4, the proposed estimator requires selecting a bandwidth h_n. The standard approach in RDDs for bandwidth selection minimizes the asymptotic Mean Squared Error (MSE) (Imbens and Kalyanaraman, 2012). In our setting, the MSE-optimal bandwidth is easily derived based on Theorem 3:

$$h_n^{opt} = \left(\frac{\bar{s}V}{4B^2}\right)^{\frac{1}{\bar{s}+4}} n^{-\frac{1}{\bar{s}+4}} \tag{B.1}$$

where

$$B = \Big(\frac{\mu^2_{d,g}(0) - \mu^2_{d',g'}(0)}{2!}\Big) e_1^\top (\Gamma^{\bar{s}})^{-1}\theta^{\bar{s}}, \quad V = \Big(\frac{\bar{\omega}_{d,g}(0) + \bar{\omega}_{d',g'}(0)}{f_{d,g,d',g'}(0)}\Big) e_1^\top (\Gamma^{\bar{s}})^{-1}\Psi^{\bar{s}}(\Gamma^{\bar{s}})^{-1}e_1.$$

The optimal bandwidth can be estimated using the plug-in selection procedure proposed by Calonico et al. (2014), which employs preliminary estimates of bias and variance with pilot bandwidths, or using plug-in estimators of the unknown quantities entering the asymptotic bias and variance (Imbens and Kalyanaraman, 2012).

In principle, as discussed in Section 4.3, the contribution of the asymptotic bias of our RDD estimator, shown in Theorem 3, would go to zero if the condition $nh_n^{\bar{s}+4} \to 0$

is met (Fan and Gijbels, 1996). However, the MSE-optimal bandwidth does not meet this requirement, analogously to no-interference RDDs (Calonico et al., 2014). In RDD applications, bias-corrected estimators are then commonly employed. The standard method proposed by Calonico et al. (2014) recenters the RDD estimator by subtracting an estimate of the leading bias and rescales it with a variance estimator that accounts for the additional variability introduced by the bias-correction term. This approach yields confidence intervals that are robust to large bandwidths. We also consider bias correction in our setting. Following Calonico et al. (2014), an estimator of the term $B_{d,g,d',g'}(h_n)$ in Theorem 3 can be obtained by using the local-quadratic estimators of the second derivatives $\frac{\mu^{(2)}_{d,g}(0)}{2!}$ and $\frac{\mu^{(2)}_{d',g'}(0)}{2!}$ with bandwidth b_n. Let us denote this estimator as $\hat{B}_{d,g,d',g'}(h_n, b_n)$. The bias-corrected estimator of $\tau_{d,g|d',g'}(0)$ is given by

$$\hat{\tau}^{bc}_{d,g|d',g'}(h_n, b_n) = \hat{\tau}_{d,g|d',g'}(h_n) - \hat{B}_{d,g,d',g'}(h_n, b_n) \tag{B.2}$$

The estimator $\hat{\tau}^{bc}_{d,g|d',g'}(h_n, b_n)$ is asymptotically normal with zero mean and asymptotic variance coincident with the independent data case under a similar asymptotic regime to Calonico et al. (2014), (Theorem S.3.4, Supplementary Material S.3). This is unsurprising given that $\hat{\tau}^{bc}_{d,g|d',g'}(h_n, b_n)$ differs from $\hat{\tau}_{d,g|d',g'}(h_n)$ by a term depending on local quadratic estimators, to which all previous considerations, *mutatis mutandis*, apply. Finally, the variance of $\hat{\tau}^{bc}_{d,g|d',g'}(h_n, b_n)$ can be estimated similarly as for $\hat{\tau}_{d,g|d',g'}(h_n)$, but with an extension to incorporate the additional variability induced by the bias correction term (see Supplementary Material S.3.7 for details).

B.2 Estimation of Boundary Overall Direct Effects

The boundary overall direct effect $\tau_{1|0}$ is identified as the difference between the right and left limit of the observed outcome regression functions conditional on the individual score X_i as X_i approaches the cutoff under continuity assumptions (Theorem 2). Letting $\tilde{\mu}(X_i) = \mathbb{E}[Y_i \mid X_i]$, Theorem 2 yields $\tau_{1|0} = \lim_{x_i \downarrow 0} \tilde{\mu}(x_i) - \lim_{x_i \uparrow 0} \tilde{\mu}(x_i)$, with $c = 0$. A natural choice is then to estimate the limits $\tilde{\mu}_1(0) = \lim\limits_{x_i \downarrow 0} \tilde{\mu}(x_i)$ and $\tilde{\mu}_0(0) = \lim\limits_{x_i \uparrow 0} \tilde{\mu}(x_i)$ by local linear regression using the individual score variable as the univariate regressor and without considering $\boldsymbol{X}_{\mathcal{S}_i}$, as in the standard no-interference

RDD. To do so, we solve

$$\hat{\beta}_1(h_n) = \arg\min_{b0,b1\in\mathbb{R}} \sum_i \mathbb{1}(X_i \geq 0)(Y_i - b_0 - b_1 X_i)^2 K_{h_n}(X_i),$$
$$\hat{\beta}_0(h_n) = \arg\min_{b_0,b_1\in\mathbb{R}} \sum_i \mathbb{1}(X_i < 0)(Y_i - b_0 - b_1 X_i)^2 K_{h_n}(X_i),$$

The final estimator of $\tau_{1|0}$ is given by

$$\hat{\tau}_{1|0}(h_n) = e_1^T \hat{\beta}_1(h_n) - e_1^T \hat{\beta}_0(h_n) \tag{B.3}$$

The following results establish consistency and asymptotic normality of $\hat{\tau}_{1|0}(h_n)$.

Theorem B.1. *Suppose Assumptions 1–6, and Assumptions S.3.1, S.3.2, and S.3.3 in Supplementary Material S.4 hold (with Assumption S.3.1.c replaced by Assumption S.4.4). If $nh_n \to \infty$, $h_n \to 0$, and $h_n = O(n^{-1/5})$, then*

$$\sqrt{nh_n}\frac{\big(\hat{\tau}_{1|0}(h_n) - \tau_{1|0}\big) - h_n^2 B_{1,0}(h_n)}{\sqrt{V(h_n)}} \xrightarrow{d} \mathcal{N}(0,1),$$

where

$$B_{1,0}(h_n) = \Big(\frac{\tilde{\mu}_1^{(2)}(0) - \tilde{\mu}_0^{(2)}(0)}{2}\Big) e_1^T(\Gamma^1)^{-1}\theta^1 + o(1), \quad V(h_n) = \frac{\bar{\omega}_1(0) + \bar{\omega}_0(0)}{f(0)^2} e_1^T(\Gamma^1)^{-1}\Psi^1(\Gamma^1)^{-1}e_1 + o(1)$$

The exact form of Γ^1, θ^1 and Ψ^1 is given in Supplementary Material S.3.

Proof. See Supplementary Material S.4.

The asymptotic distribution of $\hat{\tau}_{1|0}(h_n)$ matches that under independent data in no-interference RDDs, with a bias depending on the second-order derivatives of $\tilde{\mu}_1(x_i)$ and $\tilde{\mu}_0(x_i)$ at $x_i = 0$, and an asymptotic variance depending on $\bar{\omega}_1(0)$ and $\bar{\omega}_0(0)$, which are the right and left limits of the variance of Y_i conditional on $X_i = x_i$, and the marginal density $f(0) = f_{X_i}(0)$. Notably, this estimator achieves the nh_n^5 rate since the overall direct effects is defined on a subset of the multiscore space with codimension 1.

A variance estimator can be constructed analogously to the estimator in Eq. (19), replacing the distance measure with X_i and using the corresponding regression residuals. This estimator accounts for the dependence among observations on each side and across the cutoff using the dependency graph. The difference between this estimator and the typical RDD heteroskedasticity-robust variance estimator (e.g. Calonico et al., 2014) increases with the level of dependence in the data. These estimators coincide when $\boldsymbol{W}$ is diagonal (independent data).

Finally, a bias-corrected version of $\hat{\tau}_{1|0}(h_n)$, denoted by $\hat{\tau}^{bc}_{1|0}(h_n, b_n)$, can be obtained using local quadratic estimators of the second-order derivatives of $\tilde{\mu}(X_i)$, as described in Calonico et al. (2014).

C Additional Causal Estimands and Results

C.1 Boundary Point Average Causal Effects

In Section 3, we have introduced boundary average causal effects as our main estimands of interest. These effects can be rewritten as averages of point effects, defined as the difference of potential outcome expectation conditional on specific points of the effective treatment boundary. Formally, we define boundary point average effect as follows:

$$\tau_{d,g|d',g'}(x_i, \boldsymbol{x}_{\mathcal{S}_i}) = \mathbb{E}[\, Y_i(d,g) - Y_i(d',g') \,|\, (X_i, \boldsymbol{X}_{\mathcal{S}_i}) = (\bar{x}_i, \bar{\boldsymbol{x}}_{\mathcal{S}_i})\,] \tag{C.1}$$

with $d,\ d' \in \{0,1\},\ g,\ g' \in \mathcal{G}_i,\ (\bar{x}_i, \bar{\boldsymbol{x}}_{\mathcal{S}_i}) \in \bar{\mathcal{X}}_{i\mathcal{S}_i}(d,g \,|\, d',g')$, where the expectation is taken with respect to the distribution of potential outcomes conditional on the individual and neighborhood score, and the observed network under our model-based perspective. While boundary effects are informative about treatment effects on larger subpopulations than point effects, they aggregate over potentially heterogeneous individuals. Therefore, boundary point effects can be of interest to uncover individual treatment heterogeneity.

Boundary point effects can be identified by a similar strategy as in Theorem 1 for boundary effects, by taking the difference of the observed outcome expectations conditional on the neighborhood around specific points of decreasing radius. Specifically, let $\mathcal{B}_{\epsilon,d,g|d',g'}(\bar{x}_i, \bar{\boldsymbol{x}}_{\mathcal{S}_i})$ be a neighborhood of radius ε around $(\bar{x}_i, \bar{\boldsymbol{x}}_{\mathcal{S}_i})$, for $(\bar{x}_i, \bar{\boldsymbol{x}}_{\mathcal{S}_i}) \in \bar{\mathcal{X}}_{i\mathcal{S}_i}(d,g \,|\, d',g')$, containing all points within distance ε around $(\bar{x}_i, \bar{\boldsymbol{x}}_{\mathcal{S}_i})$.

Further let $\mathcal{B}^{d,g}_{\epsilon,d,g|d',g'}(\bar{x}_i, \bar{\boldsymbol{x}}_{\mathcal{S}_i}) = \mathcal{B}_{\epsilon,d,g|d',g'}(\bar{x}_i, \bar{\boldsymbol{x}}_{\mathcal{S}_i}) \cap \mathcal{X}_{i\mathcal{S}_i}(d,g)$ and $\mathcal{B}^{d',g'}_{\epsilon,d,g|d',g'}(\bar{x}_i, \bar{\boldsymbol{x}}_{\mathcal{S}_i})) = \mathcal{B}_{\epsilon,d,g|d',g'}(\bar{x}_i, \bar{\boldsymbol{x}}_{\mathcal{S}_i}) \cap \mathcal{X}_{i\mathcal{S}_i}(d',g')$. Then if assumptions 4.a and 4.b hold, as well as assumptions 1 and 2, it can be shown that boundary point effects are identified as:

$$\tau_{d,g|d',g'}(x_i, \boldsymbol{x}_{\mathcal{S}_i}) = \lim_{\varepsilon\to 0} \mathbb{E}[\, Y_i \,|\, (X_i, \boldsymbol{X}_{\mathcal{S}_i}) \in \mathcal{B}^{d,g}_{\epsilon,d,g|d',g'}(\bar{x}_i, \bar{\boldsymbol{x}}_{\mathcal{S}_i})\,] - \lim_{\varepsilon\to 0} \mathbb{E}[\, Y_i \,|\, (X_i, \boldsymbol{X}_{\mathcal{S}_i}) \in \mathcal{B}^{d',g'}_{\epsilon,d,g|d',g'}(\bar{x}_i, \bar{\boldsymbol{x}}_{\mathcal{S}_i})\,] \tag{C.2}$$

for all d, $d' \in \{0,1\}$, g, $g' \in \mathcal{G}_i$, and for all $(\bar{x}_i, \bar{\boldsymbol{x}}_{\mathcal{S}_i}) \in \bar{\mathcal{X}}_{i\mathcal{S}_i}(d, g \,|\, d', g')$.

Finally, estimation can be conducted by local polynomial regression using the distance from the point of interest as the one-dimensional forcing variable. We refer to Cattaneo et al. (2025) for the analysis of such point effects estimators in multivariate RDDs. The variance can be estimated using our network-robust variance estimator using the one-dimensional distance measure to the point of interest.

C.2 Overall Indirect Effect

In Section 2, we have defined the boundary overall indirect effect as

$$\tau_{indirect} = \sum_{d_i} \sum_{\boldsymbol{d}_{\mathcal{S}_i}} \sum_{\substack{\boldsymbol{d}'_{\mathcal{S}_i}: \\ d'_j \geq d_j \, \forall j \in \mathcal{S}_i, \\ \sum_{j\in\mathcal{S}_i} |d'_j - d_j| = 1}} \mathbb{E}[\, Y_i(d_i, g(\boldsymbol{d}'_{\mathcal{S}_i})) - Y_i(d_i, g(\boldsymbol{d}_{\mathcal{S}_i})) \,|\, (X_i, \boldsymbol{X}_{\mathcal{S}_i}) \in \ell\big((d_i, \boldsymbol{d}'_{\mathcal{S}_i}), (d_i, \boldsymbol{d}_{\mathcal{S}_i})\big)\,] \cdot \mathbb{P}(\, D_i = d_i, \boldsymbol{D}'_{\mathcal{S}_i} = \boldsymbol{d}'_{\mathcal{S}_i} \,|\, \exists j \in \mathcal{S}_i : X_j = c\,)$$

To clarify the interpretation of this estimand, consider the case of the *sum-of-treated* exposure mapping such that $G_i = \sum_{j\in\mathcal{S}_i} D_j$. Under this mapping, the estimand simplifies to

$$\tau_{indirect} = \sum_{\substack{d\in\{0,1\} \\ g\in\{0,\dots,|\mathcal{S}_i|-1\}}} \tau\big(\bar{\mathcal{X}}_{i\mathcal{S}_i}(d,\, g{+}1|d,\, g)\big) \cdot \mathbb{P}(\, (X_i, \boldsymbol{X}_{\mathcal{S}_i}) \in \bar{\mathcal{X}}_{i\mathcal{S}_i}(d,\, g{+}1|d,\, g) \,|\, \exists j \in \mathcal{S}_i : X_j = c\,) \tag{C.3}$$

which represents the weighted average of the boundary indirect effects $\tau\big(\bar{\mathcal{X}}_{i\mathcal{S}_i}(d, g+1 \,|\, d, g)\big)$—that is, the effect of increasing the neighborhood treatment level from g to $g+1$ for units lying on the corresponding effective treatment boundary—weighted by the probability of being at such boundary conditional on having at least one neighbor at the cutoff.

Under *one-treated* exposure mapping, the estimand becomes:

$$\tau_{indirect} = \sum_{d\in\{0,1\}} \tau\big(\bar{\mathcal{X}}_{i\mathcal{S}_i}(d,\, 1 \,|\, d,\, 0)\big) \cdot \mathbb{P}(\, (X_i, \boldsymbol{X}_{\mathcal{S}_i}) \in \bar{\mathcal{X}}_{i\mathcal{S}_i}(d,\, 1|d,\, 0) \,|\, \exists j \in \mathcal{S}_i : X_j = c\,), \tag{C.4}$$

i.e., the weighted average of the boundary indirect effects of having at least one treated neighbor versus none, for both treated and untreated units.

Let $X_{\mathcal{S}_i}^{min} = X_{j^*}$, where $j^* = \arg\min_{j \in \mathcal{S}_i} |X_j - c|$ denote the score of the neighbor closest to the cutoff. We denote its generic value by $x_{\mathcal{S}_i}^{\min}$. Geometrically, $|X_{\mathcal{S}_i}^{\min} - c|$ represents the orthogonal distance from the point $\boldsymbol{X}_{\mathcal{S}_i}$ to the subspace of $\mathcal{X}_{i\mathcal{S}_i}$ where at least one component of $\boldsymbol{x}_{\mathcal{S}_i}$ equals c.

The overall indirect effect is identified by

$$\lim_{x_{\mathcal{S}_i}^{min} \downarrow c} \mathbb{E}[\, Y_i \,|\, X_{\mathcal{S}_i}^{min} = x_{\mathcal{S}_i}^{min}\,] - \lim_{x_{\mathcal{S}_i}^{min} \uparrow c} \mathbb{E}[\, Y_i \,|\, X_{\mathcal{S}_i}^{min} = x_{\mathcal{S}_i}^{min}\,]$$

under Assumptions 1–4. This result follows easily from arguments analogous to those in Theorem 1 and Theorem 2, and is thus omitted. Based on this identification, $\tau_{indirect}$ can be estimated via univariate local linear regression using $X_{\mathcal{S}_i}^{min}$ as the one-dimensional regressor:

$$\hat{\tau}_{indirect}(h_n) = e_1^T \hat{\beta}_{1,indirect}(h_n) - e_1^T \hat{\beta}_{0,indirect}(h_n) \tag{C.5}$$

where

$$\hat{\beta}_{1,indirect}(h_n) = \underset{b0,b1 \in \mathbb{R}}{\arg\min} \sum_i \mathbb{1}(X_{\mathcal{S}_i}^{min} \geq 0)(Y_i - b_0 - b_1 X_{\mathcal{S}_i}^{min})^2 K_{h_n}(X_{\mathcal{S}_i}^{min}),$$
$$\hat{\beta}_{0,indirect}(h_n) = \underset{b0,b1 \in \mathbb{R}}{\arg\min} \sum_i \mathbb{1}(X_{\mathcal{S}_i}^{min} < 0)(Y_i - b_0 - b_1 X_{\mathcal{S}_i}^{min})^2 K_{h_n}(X_{\mathcal{S}_i}^{min}),$$

letting $c = 0$.

Let $\mu_{1,indirect}(x_{\mathcal{S}_i}^{min}) = \mathbb{E}[\, Y_i \,|\, X_{\mathcal{S}_i}^{min} = x_{\mathcal{S}_i}^{min}\,]$ for $x_{\mathcal{S}_i}^{min} \geq 0$, and $\mu_{0,indirect}(x_{\mathcal{S}_i}^{min}) = \mathbb{E}[\, Y_i \,|\, X_{\mathcal{S}_i}^{min} = x_{\mathcal{S}_i}^{min}\,]$ for $x_{\mathcal{S}_i}^{min} \leq 0$.

Theorem C.1. *Suppose Assumptions 1–6 hold. Further, suppose that Assumptions S.3.1, S.3.2, and S.3.3 in Supplementary Material S.4 hold, but replacing Assumption S.3.1.c with: $\mu_1(x_{\mathcal{S}_i}^{min})$ and $\mu_0(x_{\mathcal{S}_i}^{min})$ are 3-times continuously differentiable. If $nh_n \to \infty$, $h_n \to 0$, and $h_n = O(n^{-1/5})$, then*

$$\sqrt{nh_n} \frac{\big(\hat{\tau}_{indirect}(h_n) - \tau_{indirect}\big) - h_n^2 B_{indirect}(h_n)}{\sqrt{V_{indirect}(h_n)}} \xrightarrow{d} \mathcal{N}(0,1),$$

where $B_{indirect}(h_n) = O(1)$ and $V_{indirect}(h_n) = O(1)$.

Proof. The proof follows analogous arguments as those in Theorem 3 and B.1, and thus, is omitted for brevity.

Importantly, this estimator achieves the nh_n^5 rate. Specifically, $\hat{\tau}_{indirect}(h_n)$ averages observations in a neighborhood of the subset of $\mathcal{X}_{i\mathcal{S}_i}$ where at least one component of $\boldsymbol{X}_{\mathcal{S}_i}$ equals c. Since this subset is itself a boundary formed by a union of linear pieces, its properties follow from arguments analogous to those used for estimating boundary and overall direct effects. The codimension of this subset is one, implying an asymptotic variance of order $O\big((nh_n)^{-1}\big)$ and the usual RDD convergence rate. Thus, while estimators of boundary indirect effects $\tau_{d,g|d',g'}\big(\bar{\mathcal{X}}_{i\mathcal{S}_i}(d,g\,|\,d',g')\big)$ comparing specific values g and g' may converge more slowly, this aggregate measure attains the canonical fast rate of standard RDDs.

D Additional Simulation Results

D.1 Network Data

In this subsection, we present a simulation study to evaluate the finite-sample performance of $\hat{\tau}^{bc}_{1|0}(h_n, b_n)$ and $\hat{\tau}^{bc}_{d,g|d',g'}(h_n, b_n)$ under network interference with overlapping interference sets. Specifically, we consider scenarios where each unit's interference set coincides with its network neighborhood—that is, the set of nodes directly linked to it. The neighborhood treatment G_i is defined via the one-treated exposure mapping.

For sample sizes $n = \{750, 1500, 3000\}$, we simulate small-world networks (Watts and Strogatz, 1998) using the `sample_smallworld()` function from the R package `igraph`. Small-world networks are characterized by high clustering, meaning that two nodes sharing a neighbor tend to be connected. We fix the average node degree at 4 by setting the argument `nei = 2`, and vary the rewiring probability to generate networks with different levels of clustering, as measured by the global and average local clustering coefficients. The global clustering coefficient is defined as the ratio of the number of closed triplets (triangles) to the number of connected triplets in the network. The average local clustering coefficient averages the local clustering coefficients for each node, which is the ratio of the triangles connected to the node and the triples centered on the node.

This simulation design allows us to assess the performance of the proposed estimators in network settings and to investigate how network clustering affects performance—particularly through the induced clustering in the distance variable.

We consider two scenarios:

Scenario A: Rewiring probability $p = 0.15$, resulting in a global clustering coefficient of approximately 0.16 and an average local clustering coefficient of about 0.20.

Scenario B: Rewiring probability $p = 0.05$, resulting in a global clustering coefficient of approximately 0.35 and an average local clustering coefficient of about 0.37.

Outcomes are simulated from the model

$$Y_i = 0.5 + 1.5D_i + G_i + 0.5X_i + 4.3D_iX_i^2 - 1.5(1-D_i)X_i^2 + 0.3\bar{\boldsymbol{X}}_{\mathcal{S}_i} + \varepsilon_i \qquad \text{(D.1)}$$

where X_i is i.i.d. a truncated normal with mean -0.5 and variance 1, and upper and lower bound -5 and 5, while the error terms are given by $\varepsilon_i = D_i\big(2\frac{\sum_{j\in s_i} u_j}{|\mathcal{S}_i|} + u_i\big) - 1.4(1-D_i)\cdot\big(2\frac{\sum_{j\in s_i} u_j}{|\mathcal{S}_i|} + u_i\big)$ with $u_i \overset{i.i.d.}{\sim} \mathcal{N}(0,1)$. Observations are thus dependent up to second-order network neighbors (second-order dependence), and the boundary average effects are homogeneous across units.

Simulation results are reported in Tables D.1 (Scenario A) and D.2 (Scenario B). Each table reports the empirical bias, empirical standard deviation, estimated standard error (using both our proposed variance estimator and the standard i.i.d. estimator), and the associated confidence interval coverage rates. We also report the average effective sample sizes ($N_{d,g}$ and $N_{d',g'}$) and the proportion of units with unique score variables and minimum distance values (column "% Unique"). Values less than one in this column indicate overlapping distance variables among units.

According to the results, the proposed estimators are virtually unbiased across all sample sizes and scenarios. The standard deviation decreases substantially with sample size in both settings. Notably, $\hat{\tau}^{bc}_{1|0}(h_n, b_n)$ consistently has the lowest standard deviation, due to a larger average effective sample size. In contrast, $\hat{\tau}_{10|00}(h_n, b_n)$ exhibits the highest standard deviation, driven by a smaller fraction of units with $(D_i = 1, G_i = 0)$.

The estimator $\hat{\tau}_{01|00}(h_n, b_n)$ has a relatively large effective sample size but still exhibits high variance. This is explained by the clustering structure of the distance variable: in Scenario A, approximately 80% of units have unique distance values, while in Scenario B only 74% do. This increase in overlap leads to higher standard deviation in Scenario B.

Our proposed variance estimator performs well, approaching the empirical standard deviation in large samples. Coverage rates using this estimator converge to the nominal level. In comparison, the i.i.d. confidence intervals tend to undercover the true value, especially for smaller samples, although the coverage improves with larger sample sizes. For $\hat{\tau}_{01|00}(h_n, b_n)$, however, the coverage does not improve in large samples and it is substantially worse in Scenario B, with higher clustering in the network. Overall, our variance estimator appears more accurate than the one relying on the i.i.d. assumption, especially in Scenario B with higher clustering.

In conclusion, this simulation study demonstrates an overall good performance of the proposed distance-based estimators and the associated variance estimator. The study also highlights how increased clustering in the network can induce higher clustering in the distance variable. When this occurs, relying on the i.i.d. variance estimator leads to consistently poor coverage, whereas accounting for dependence significantly improves coverage.

Scenario A

		Bias	S.D.	S.E.	S.E.$_{i.i.d.}$	C.R.	C.R.$_{i.i.d.}$	$\bar{N}_{d,g}$	$\bar{N}_{d',g'}$	% Unique
n = 750	$\hat{\tau}^{bc}_{1\|0}(h_n, b_n)$	0.027	1.156	1.053	0.960	0.933	0.910	134.551	183.500	1.000
	$\hat{\tau}^{bc}_{10\|00}(h_n, b_n)$	0.027	2.539	2.060	2.054	0.880	0.877	30.739	41.192	1.000
	$\hat{\tau}^{bc}_{01\|00}(h_n, b_n)$	-0.027	2.313	1.974	1.893	0.902	0.900	113.716	76.904	0.795
n = 1500	$\hat{\tau}^{bc}_{1\|0}(h_n, b_n)$	0.047	0.787	0.756	0.680	0.944	0.906	263.448	357.809	1.000
	$\hat{\tau}^{bc}_{10\|00}(h_n, b_n)$	0.038	1.674	1.474	1.441	0.920	0.913	64.333	87.464	1.000
	$\hat{\tau}^{bc}_{01\|00}(h_n, b_n)$	-0.039	1.588	1.414	1.317	0.927	0.915	234.410	159.957	0.798
n = 3000	$\hat{\tau}^{bc}_{1\|0}(h_n, b_n)$	0.038	0.571	0.541	0.487	0.941	0.913	500.205	662.241	1.000
	$\hat{\tau}^{bc}_{10\|00}(h_n, b_n)$	0.032	1.149	1.050	1.024	0.934	0.929	129.772	175.393	1.000
	$\hat{\tau}^{bc}_{01\|00}(h_n, b_n)$	0.038	1.059	0.982	0.900	0.948	0.925	504.572	334.086	0.797

Table D.1: Simulation results using bias correction with small-world network and one treated exposure mapping with rewiring probability $p = 0.15$. One thousand replications. S.D. = empirical standard error. S.E. = estimated standard error. S.E.$_{i.i.d.}$ = estimated standard error with *i.i.d.* heteroskedasticity-robust HC0 plug-in residuals variance estimator. C.R. = coverage rate. C.R.$_{i.i.d.}$ = coverage rate corresponding to the *i.i.d.* heteroskedasticity-robust HC0 plug-in residuals variance estimator. $N_{d,g}$ and $N_{d',g'}$ = effective sample size on each side of the treatment boundary. % Unique = percentage of unique distance variables.

Scenario B

		Bias	S.D.	S.E.	S.E.$_{i.i.d.}$	C.R.	C.R.$_{i.i.d.}$	$\bar{N}_{d,g}$	$\bar{N}_{d',g'}$	% Unique
	$\hat{\tau}^{bc}_{1\|0}(h_n, b_n)$	-0.019	1.077	1.036	0.943	0.930	0.906	134.216	184.242	1.000
n = 750	$\hat{\tau}^{bc}_{10\|00}(h_n, b_n)$	0.036	2.461	2.005	1.992	0.901	0.904	29.272	39.542	1.000
	$\hat{\tau}^{bc}_{01\|00}(h_n, b_n)$	0.046	2.609	2.133	1.942	0.897	0.875	102.775	73.005	0.741
	$\hat{\tau}^{bc}_{1\|0}(h_n, b_n)$	-0.031	0.792	0.739	0.667	0.928	0.899	263.827	355.330	1.000
n = 1500	$\hat{\tau}^{bc}_{10\|00}(h_n, b_n)$	-0.103	1.627	1.427	1.399	0.903	0.897	61.228	83.298	1.000
	$\hat{\tau}^{bc}_{01\|00}(h_n, b_n)$	-0.070	1.722	1.531	1.355	0.922	0.888	213.644	149.110	0.741
	$\hat{\tau}^{bc}_{1\|0}(h_n, b_n)$	0.002	0.555	0.532	0.477	0.943	0.909	501.494	663.855	1.000
n = 3000	$\hat{\tau}^{bc}_{10\|00}(h_n, b_n)$	-0.028	1.068	1.015	0.985	0.941	0.934	123.655	168.285	1.000
	$\hat{\tau}^{bc}_{01\|00}(h_n, b_n)$	0.016	1.198	1.083	0.942	0.937	0.887	445.984	305.441	0.738

Table D.2: Simulation results using bias correction with small-world network and one treated exposure mapping with rewiring probability $p = 0.05$. One thousand replications. S.D. = empirical standard error. S.E. = estimated standard error. S.E.$_{i.i.d.}$ = estimated standard error with *i.i.d.* heteroskedasticity-robust HC0 plug-in residuals variance estimator. C.R. = coverage rate. C.R.$_{i.i.d.}$ = coverage rate corresponding to the *i.i.d.* heteroskedasticity-robust HC0 plug-in residuals variance estimator. $N_{d,g}$ and $N_{d',g'}$ = effective sample size on each side of the treatment boundary. % Unique = percentage of unique distance variables.

D.2 Varying Group Size

In this simulation study, we consider a scenario with equally sized groups. We keep the total sample size fixed at $n = 3000$ and vary the cluster size, denoted by M. Data are generated as Section 5, but using the one-treated exposure mapping.

The objective is to assess the performance of our proposed bias-corrected estimators in settings with larger group sizes, which correspond to higher-dimensional multiscore spaces and effective treatment boundaries than those considered in Section 5. The dimension of the multiscore space for each unit is, in fact, given by M. Under this data generating process, although the total sample size remains constant, the probability of observing certain neighborhood-treatment configurations (e.g., $G_i = 0$) decreases with M, reducing the effective sample size available for estimation near each boundary.

We simulate 1,000 datasets with group sizes $M \in \{3, 4, 5, 6\}$ and total sample size $n = 3000$, corresponding to $\{1000, 750, 600, 500\}$ groups, respectively.

We consider, for brevity, the estimators $\hat{\tau}^{bc}_{1|0}(h_n, b_n)$, $\hat{\tau}^{bc}_{10|00}(h_n, b_n)$, and $\hat{\tau}^{bc}_{01|00}(h_n, b_n)$,[1] and report the results in Table D.3. All estimators are approximately unbiased across different group sizes. The estimators $\hat{\tau}^{bc}_{10|00}(h_n, b_n)$ and $\hat{\tau}^{bc}_{01|00}(h_n, b_n)$ remain approximately unbiased for $M = \{3, 4, 5, 6\}$ but exhibit increasing standard

[1] The bandwidths h_n and b_n are computed using the plug-in procedure by Calonico et al. (2014).

deviations as the group size grows. The increase in the empirical standard deviation is more pronounced for $\hat{\tau}^{bc}_{01|00}(h_n, b_n)$, due to the high percentage of observations sharing the same distance measure, as indicated in column "% Unique." Our variance estimator for $\hat{\tau}^{bc}_{10|00}(h_n, b_n)$ and $\hat{\tau}^{bc}_{01|00}(h_n, b_n)$ is accurate for smaller group sizes ($M = \{3, 4\}$) but worsens in performance for larger groups, resulting in lower coverage rates. In contrast, the variance estimator for $\hat{\tau}^{bc}_{1|0}(h_n, b_n)$ remains relatively accurate across group sizes.

The high standard deviation of $\hat{\tau}^{bc}_{10|00}(h_n, b_n)$ and $\hat{\tau}^{bc}_{01|00}(h_n, b_n)$, together with the worsening performance of their variance estimators, arises from the reduced effective sample size. In our data generating process, larger groups lead to lower observed probabilities for some neighborhood treatment configurations. In particular, the observed probabilities $\Pr(G_i = 0)$ equal approximately $\{0.38, 0.23, 0.14, 0.09\}$ as group size increases.

To illustrate the impact of the effective sample size, we repeat the simulation focusing on $\hat{\tau}^{bc}_{01|00}(h_n, b_n)$ but choose the cutoff

$$c = -0.3 + \Phi^{-1}\big(0.35^{1/(M-1)}\big),$$

which ensures that the observed probability $\Pr(G_i = 0) \approx 0.35$ for each group size M. This adjustment keeps a larger effective sample size for estimation. As shown in Table D.4, this modification substantially reduces the estimator's standard error relative to Table D.3. Moreover, our variance estimator provides more accurate variance estimates and improved coverage, even in the presence of substantial clustering at the distance-measure level.

Overall, the results show that while our estimation method yields accurate inference when the effective sample size is sufficient, large groups may lead to sparse data within each effective treatment arm and thus less precise inference. Nevertheless, our results indicate that even if specific boundary effects cannot be precisely estimated due to limited observations, the boundary overall direct effect can still be estimated accurately when the total sample size is large, as in this setting.

		Bias	S.D.	S.E.	C.R.	$\bar{N}_{d,g}$	$\bar{N}_{d',g'}$	% Unique
M = 3	$\hat{\tau}^{bc}_{1\|0}(h_n, b_n)$	-0.013	0.651	0.639	0.950	603.549	723.666	1.000
	$\hat{\tau}^{bc}_{10\|00}(h_n, b_n)$	0.009	1.032	0.987	0.950	243.326	294.503	1.000
	$\hat{\tau}^{bc}_{01\|00}(h_n, b_n)$	0.039	1.402	1.280	0.929	481.672	411.999	0.637
M = 4	$\hat{\tau}^{bc}_{1\|0}(h_n, b_n)$	0.010	0.552	0.552	0.944	585.236	695.398	1.000
	$\hat{\tau}^{bc}_{10\|00}(h_n, b_n)$	0.036	1.104	1.069	0.946	150.242	181.642	1.000
	$\hat{\tau}^{bc}_{01\|00}(h_n, b_n)$	-0.065	1.638	1.568	0.931	393.081	271.343	0.455
M = 5	$\hat{\tau}^{bc}_{1\|0}(h_n, b_n)$	-0.026	0.509	0.504	0.958	575.230	681.489	1.000
	$\hat{\tau}^{bc}_{10\|00}(h_n, b_n)$	-0.034	1.324	1.221	0.928	92.785	111.590	1.000
	$\hat{\tau}^{bc}_{01\|00}(h_n, b_n)$	0.094	2.375	1.952	0.885	281.102	169.292	0.350
M = 6	$\hat{\tau}^{bc}_{1\|0}(h_n, b_n)$	-0.018	0.482	0.473	0.938	565.136	668.042	1.000
	$\hat{\tau}^{bc}_{10\|00}(h_n, b_n)$	-0.020	1.507	1.408	0.929	56.543	68.610	1.000
	$\hat{\tau}^{bc}_{01\|00}(h_n, b_n)$	-0.016	2.939	2.388	0.888	188.998	105.040	0.284

Table D.3: Simulation results over one thousand replications. S.D. = empirical standard error. S.E. = estimated standard error. C.R. = coverage rate. $N_{d,g}$ and $N_{d',g'}$ = effective sample size on each side of the treatment boundary.

		Bias	S.D.	S.E.	C.R.	$\bar{N}_{d,g}$	$\bar{N}_{d',g'}$	% Unique
M = 3	$\hat{\tau}^{bc}_{01\|00}(h_n, b_n)$	0.018	1.438	1.344	0.942	448.701	368.789	0.642
M = 4	$\hat{\tau}^{bc}_{01\|00}(h_n, b_n)$	0.041	1.382	1.280	0.942	526.895	436.620	0.439
M = 5	$\hat{\tau}^{bc}_{01\|00}(h_n, b_n)$	-0.015	1.327	1.252	0.941	562.791	474.355	0.330
M = 6	$\hat{\tau}^{bc}_{01\|00}(h_n, b_n)$	0.010	1.369	1.243	0.935	580.149	498.828	0.264

Table D.4: Simulation results over one thousand replications. S.D. = empirical standard error. S.E. = estimated standard error. C.R. = coverage rate. $N_{d,g}$ and $N_{d',g'}$ = effective sample size on each side of the treatment boundary.

References

Calonico, S., Cattaneo, M. D., and Titiunik, R. (2014). Robust nonparametric confidence intervals for regression-discontinuity designs. *Econometrica*, 82(6):2295–2326.

Cattaneo, M. D., Titiunik, R., and Yu, R. R. (2025). Estimation and inference in boundary discontinuity designs.

Fan, J. and Gijbels, I. (1996). *Local Polynomial Modelling and Its Applications*. Chapman and Hall, London.

Imbens, G. and Kalyanaraman, K. (2012). Optimal bandwidth choice for the regression discontinuity estimator. *The Review of Economic Studies*, 79(3):933–959.

Watts, D. J. and Strogatz, S. H. (1998). Collective dynamics of small-world networks. *Nature*, 393(6684):440–442.

Supplementary Material to "Regression Discontinuity Designs Under Interference"

Elena Dal Torrione[1], Tiziano Arduini[2], Laura Forastiere[1]

[1]Department of Biostatistics, Yale University
[2]Department of Economics and Finance, Tor Vergata University of Rome

S.1 Effective Treatment Boundary Derivation

We provide the derivation of the equality $\bar{\mathcal{X}}_{i\mathcal{S}_i}(d, g \,|\, d', g') = \bigcup_{\mathcal{D}_{i\mathcal{S}_i}(d,g)\times\mathcal{D}_{i\mathcal{S}_i}(d',g')} \ell(\boldsymbol{d}^{d,g}_{i\mathcal{S}_i}, \boldsymbol{d}^{d',g'}_{i\mathcal{S}_i})$ in Subsection 2.3. The derivation uses the fact that given the individual treatment rule in Eq. (1), each element $\boldsymbol{d}^{d,g}_{i\mathcal{S}_i} \in \mathcal{D}_{i\mathcal{S}_i}(d,g)$ can be mapped back to the set $\mathcal{X}_{i\mathcal{S}_i}(\boldsymbol{d}^{d,g}_{i\mathcal{S}_i}) = \{(x_i, \boldsymbol{x}_{\mathcal{S}_i}) \in \mathcal{X}_{i\mathcal{S}_i} : \forall z \in (\{i\} \cup \mathcal{S}_i),\ x_z \geq c \text{ if } d^{d,g}_z = 1,\ x_z < c \text{ if } d^{d,g}_z = 0\}$, and that each treatment region is the union of such sets over $\mathcal{D}_{i\mathcal{S}_i}(d,g)$, i.e.,

$$\mathcal{X}_{i\mathcal{S}_i}(d,g) = \bigcup_{\mathcal{D}_{i\mathcal{S}_i}(d,g)} \mathcal{X}_{i\mathcal{S}_i}(\boldsymbol{d}^{d,g}_{i\mathcal{S}_i})$$

Proof. Recall that the closure of a set is the union of its interior with its boundary. In addition, the closure of a union of sets is equal to the union of their closures. Therefore, denoting the closure of a set A as $Cl(A)$, we have

$$Cl\big(\mathcal{X}_{i\mathcal{S}_i}(d,g)\big) = \bigcup_{\mathcal{D}_{i\mathcal{S}_i}(d,g)} Cl\big(\mathcal{X}_{i\mathcal{S}_i}(\boldsymbol{d}^{d,g}_{i\mathcal{S}_i})\big)$$

where clearly $Cl\big(\mathcal{X}_{i\mathcal{S}_i}(\boldsymbol{d}^{d,g}_{i\mathcal{S}_i})\big) = \{(x_i, \boldsymbol{x}_{\mathcal{S}_i}) \in \mathcal{X}_{i\mathcal{S}_i} : \forall z \in (\{i\} \cup \mathcal{S}_i), x_z \geq c \text{ if } d^{d,g}_z = 1,\ x_z \leq c \text{ if } d^{d,g}_z = 0\}$.

Now by definition $\bar{\mathcal{X}}_{i\mathcal{S}_i}(d, g \,|\, d', g') = \bar{\mathcal{X}}_{i\mathcal{S}_i}(d,g) \cap \bar{\mathcal{X}}_{i\mathcal{S}_i}(d',g')$, where $\bar{\mathcal{X}}_{i\mathcal{S}_i}(d,g)$ and $\bar{\mathcal{X}}_{i\mathcal{S}_i}(d',g')$ denote the boundary of $\mathcal{X}_{i\mathcal{S}_i}(d,g)$ and $\mathcal{X}_{i\mathcal{S}_i}(d',g')$. Moreover, because $\mathcal{X}_{i\mathcal{S}_i}(d,g)$ and $\mathcal{X}_{i\mathcal{S}_i}(d',g')$ are disjoint, the intersection of their closure is equal to the intersection of their boundaries, $Cl\big(\mathcal{X}_{i\mathcal{S}_i}(d,g)\big) \cap Cl\big(\mathcal{X}_{i\mathcal{S}_i}(d',g')\big) = \bar{\mathcal{X}}_{i\mathcal{S}_i}(d,g) \cap \bar{\mathcal{X}}_{i\mathcal{S}_i}(d',g')$. Note that $Cl\big(\mathcal{X}_{i\mathcal{S}_i}(d,g)\big) \cap Cl\big(\mathcal{X}_{i\mathcal{S}_i}(d',g')\big)$ is equal to

$$\Big(\bigcup_{\mathcal{D}_{i\mathcal{S}_i}(d,g)} Cl\big(\mathcal{X}_{i\mathcal{S}_i}(\boldsymbol{d}^{d,g}_{i\mathcal{S}_i})\big)\Big) \bigcap \Big(\bigcup_{\mathcal{D}_{i\mathcal{S}_i}(d',g')} Cl\big(\mathcal{X}_{i\mathcal{S}_i}(\boldsymbol{d}^{d',g'}_{i\mathcal{S}_i})\big)\Big)$$

which in turn is equal to

$$\bigcup_{\mathcal{D}_{i\mathcal{S}_i}(d,g)\times\mathcal{D}_{i\mathcal{S}_i}(d',g')} \Big(Cl\big(\mathcal{X}_{i\mathcal{S}_i}(\boldsymbol{d}_{i\mathcal{S}_i}^{d,g})\big)\bigcap Cl\big(\mathcal{X}_{i\mathcal{S}_i}(\boldsymbol{d}_{i\mathcal{S}_i}^{d',g'})\big)\Big)$$

Finally, we note that the intersection $Cl(\mathcal{X}_{i\mathcal{S}_i}(\boldsymbol{d}_{i\mathcal{S}_i}^{d,g}))\cap Cl(\mathcal{X}_{i\mathcal{S}_i}(\boldsymbol{d}_{i\mathcal{S}_i}^{d',g'}))$ is equal to the set $\{(x_i,\boldsymbol{x}_{\mathcal{S}_i})\in\mathcal{X}_{i\mathcal{S}_i}:\forall z\in(\{i\}\cup\mathcal{S}_i),\ x_z\geq c \text{ if } d_z^{d,g}=d_z^{d',g'}=1,\ x_z\leq c \text{ if } d_z^{d,g}=d_z^{d',g'}=0,\ x_z=c \text{ if } d_z^{d,g}\neq d_z^{d',g'}\}$ which is the definition of $\ell(\boldsymbol{d}_{i\mathcal{S}_i}^{d,g},\boldsymbol{d}_{i\mathcal{S}_i}^{d',g'})$. $\square$

S.2 Proofs of Main Results in Section 3

Let us formally define the notion of $n-$rectifiable set. Let $\mathcal{H}^n$ denote the n-dimensional Hausdorff measure.

Definition 1 (n-rectifiable set (Simon, 1984))**.** *A set $M\subset\mathbb{R}^{n+k}$ is said to be countably n-rectifiable if*

$$M\subset M_0\cup\left(\cup_{j=1}^{\infty}F_j\left(\mathbb{R}^n\right)\right)$$

where $\mathcal{H}^n\left(M_0\right)=0$ and $F_j:\mathbb{R}^n\to\mathbb{R}^{n+k}$ are Lipschitz functions for $j=1,2,\ldots$.

An equivalent characterization is the following: a set M is countably n-rectifiable if and only if $M\subset\bigcup_{j=0}^{\infty}N_j$, where $\mathcal{H}^n(N_0)=0$ and each N_j, $j\geq 1$, is an n-dimensional embedded C^1 submanifold of $\mathbb{R}^{n+k}$ (Simon, 1984, Lemma 11.1).

As discussed in Section 2.3, the effective treatment boundary $\bar{\mathcal{X}}_{i\mathcal{S}_i}(d,g\,|\,d',g')$ is the union of finitely many linear pieces in the multiscore space $\mathcal{X}_{i\mathcal{S}_i}$. Therefore, $\bar{\mathcal{X}}_{i\mathcal{S}_i}(d,g\,|\,d',g')$ is $(|\mathcal{S}|_i+1-\bar{s}_i)-$rectifiable set, with dimension $|\mathcal{S}|_i+1-\bar{s}_i$, and codimension $\bar{s}_i$, where $\bar{s}_i$ is the minimum codimension across the linear pieces.

Thus, we can write the boundary average causal effect as

$$\tau_{d,g|d',g'}\big(\bar{\mathcal{X}}_{i\mathcal{S}_i}(d,g\,|\,d',g')\big)=\frac{\sum\limits_{\boldsymbol{d}_{i\mathcal{S}_i}^{d,g},\boldsymbol{d}_{i\mathcal{S}_i}^{d',g'}}\int\limits_{\ell(\boldsymbol{d}_{i\mathcal{S}_i}^{d,g},\boldsymbol{d}_{i\mathcal{S}_i}^{d',g'})}\tau_{d,g|d',g'}(x_i,\boldsymbol{x}_{\mathcal{S}_i})f(x_i,\boldsymbol{x}_{\mathcal{S}_i})d\mathcal{H}^{|\mathcal{S}_i|+1-\bar{s}_i}}{\sum\limits_{\boldsymbol{d}_{i\mathcal{S}_i}^{d,g},\boldsymbol{d}_{i\mathcal{S}_i}^{d',g'}}\int\limits_{\ell(\boldsymbol{d}_{i\mathcal{S}_i}^{d,g},\boldsymbol{d}_{i\mathcal{S}_i}^{d',g'})}f(x_i,\boldsymbol{x}_{\mathcal{S}_i})d\mathcal{H}^{|\mathcal{S}_i|+1-\bar{s}_i}} \tag{S.2.1}$$

where the summation ranges over all pairs $\boldsymbol{d}_{i\mathcal{S}_i}^{d,g},\boldsymbol{d}_{i\mathcal{S}_i}^{d',g'}$ in $\mathcal{D}_{i\mathcal{S}_i}(d,g)\times\mathcal{D}_{i\mathcal{S}_i}(d',g')$.

Note that integrals over pieces $\ell(\boldsymbol{d}_{i\mathcal{S}_i}^{d,g},\boldsymbol{d}_{i\mathcal{S}_i}^{d',g'})$ with codimension $s_{\ell(\boldsymbol{d}_{i\mathcal{S}_i}^{d,g},\boldsymbol{d}_{i\mathcal{S}_i}^{d',g'})}$ larger than $\bar{s}_i$ vanish since their $\mathcal{H}^{|\mathcal{S}_i|+1-\bar{s}_i}$-dimensional Hausdorff measure is zero. Hence, the expression above is equivalent to summing over only those pieces $\ell(\boldsymbol{d}^{d,g}_{i\mathcal{S}_i}, \boldsymbol{d}^{d',g'}_{i\mathcal{S}_i})$ with codimension $\bar{s}_i$.

For each $\ell(\boldsymbol{d}^{d,g}_{i\mathcal{S}_i}, \boldsymbol{d}^{d',g'}_{i\mathcal{S}_i})$, define the following index sets:

- $F_{\ell(\boldsymbol{d}^{d,g}_{i\mathcal{S}_i}, \boldsymbol{d}^{d',g'}_{i\mathcal{S}_i})}$: the set of indices $z \in (\mathcal{S}_i \cup \{i\})$ such that $x_z = c$ on $\ell(\boldsymbol{d}^{d,g}_{i\mathcal{S}_i}, \boldsymbol{d}^{d',g'}_{i\mathcal{S}_i})$ (i.e., the constrained components);

- $R_{\ell(\boldsymbol{d}^{d,g}_{i\mathcal{S}_i}, \boldsymbol{d}^{d',g'}_{i\mathcal{S}_i})}$: the complement set of indices where x_z is free to vary within some interval.

The codimension $s_{\ell(\boldsymbol{d}^{d,g}_{i\mathcal{S}_i}, \boldsymbol{d}^{d',g'}_{i\mathcal{S}_i})}$ equals the cardinality $|F_{\ell(\boldsymbol{d}^{d,g}_{i\mathcal{S}_i}, \boldsymbol{d}^{d',g'}_{i\mathcal{S}_i})}|$.

We henceforth drop the arguments $\boldsymbol{d}^{d,g}_{i\mathcal{S}_i}$ and $\boldsymbol{d}^{d',g'}_{i\mathcal{S}_i}$ and simply write ℓ_i for each piece. We also use $\sum_{\ell_i}$ and $\bigcup_{\ell_i}$ to denote summation and union over the relevant set of pieces $\ell(\boldsymbol{d}^{d,g}_{i\mathcal{S}_i}, \boldsymbol{d}^{d',g'}_{i\mathcal{S}_i})$ indexed by $\boldsymbol{d}^{d,g}_{i\mathcal{S}_i}$ and $\boldsymbol{d}^{d',g'}_{i\mathcal{S}_i}$.

We partition each $(x_i, \boldsymbol{x}_{\mathcal{S}_i})$ into $\boldsymbol{x}_{F_{\ell_i}}$, where each component is fixed at c on ℓ_i, and $\boldsymbol{x}_{R_{\ell_i}}$, which ranges over the domain

$$\mathcal{R}_{\ell_i} := \prod_{z \in R_{\ell_i}} I_z(\ell_i)$$

where $I_z(\ell_i) = [a, c]$, if $x_z \leq c$ on ℓ_i, and $I_z(\ell_i) = [c, b]$ if $x_z \geq c$ on ℓ_i.

The structure of each ℓ_i leads to the following simple parametrization of (S.2.1):

$$\frac{\sum\limits_{\ell_i \,:\, s_{\ell_i} = \bar{s}_i} \int\limits_{\mathcal{R}_{\ell_i}} \tau_{d,g|d',g'}(\boldsymbol{c}_{F_{\ell_i}}, \boldsymbol{x}_{R_{\ell_i}}) f(\boldsymbol{c}_{F_{\ell_i}}, \boldsymbol{x}_{R_{\ell_i}}) d\boldsymbol{x}_{R_{\ell_i}}}{\sum\limits_{\ell_i \,:\, s_{\ell_i} = \bar{s}_i} \int\limits_{\mathcal{R}_{\ell_i}} f(\boldsymbol{c}_{F_{\ell_i}}, \boldsymbol{x}_{R_{\ell_i}}) d\boldsymbol{x}_{R_{\ell_i}}} \tag{S.2.2}$$

Each integral is taken over the bounded rectangular domain corresponding to the "free" components of $(x_i, \boldsymbol{x}_{\mathcal{S}_i})$ for a given piece ℓ_i of dimension $|\mathcal{S}_i| + 1 - \bar{s}_i$.

Proof of Theorem 1. We start by proving convergence of

$$\mathbb{E}[\, Y_i(d, g) \,|\, (X_i, \boldsymbol{X}_{\mathcal{S}_i}) \in \mathcal{B}^{d,g}_{\varepsilon}(\bar{\mathcal{X}}_{i\mathcal{S}_i}(d, g \,|\, d', g'))\,]$$

Define the conditional mean function

$$m_{d,g}(x_i, \boldsymbol{x}_{\mathcal{S}_i}) = \mathbb{E}[\, Y_i(d, g) \,|\, (X_i, \boldsymbol{X}_{\mathcal{S}_i}) = (x_i, \boldsymbol{x}_{\mathcal{S}_i})\,]$$

The expectation $\mathbb{E}[Y_i(d,g) \,|\, (X_i, \boldsymbol{X}_{\mathcal{S}_i}) \in \bar{\mathcal{X}}_{i\mathcal{S}_i}(d,g \,|\, d',g')]$ can be written as

$$\frac{\sum\limits_{\ell_i : s_{\ell_i} = \bar{s}_i} \int\limits_{\mathcal{R}_{\ell_i}} m_{d,g}(\boldsymbol{c}_{F_{\ell_i}}, \boldsymbol{x}_{R_{\ell_i}}) f(\boldsymbol{c}_{F_{\ell_i}}, \boldsymbol{x}_{R_{\ell_i}}) d\boldsymbol{x}_{R_{\ell_i}}}{\sum\limits_{\ell_i : s_{\ell_i} = \bar{s}_i} \int\limits_{\mathcal{R}_{\ell_i}} f(\boldsymbol{c}_{F_{\ell_i}}, \boldsymbol{x}_{R_{\ell_i}}) d\boldsymbol{x}_{R_{\ell_i}}} \tag{S.2.3}$$

For a piece ℓ_i with constrained components F_{ℓ_i} fixed at $\boldsymbol{c}_{F_{\ell_i}}$ and free components R_{ℓ_i}, denote by $\mathcal{B}_\varepsilon^{d,g}(\ell_i)$ the ε-neighborhood around ℓ_i, restricted to the region

$$\mathcal{X}_{i\mathcal{S}_i}(\boldsymbol{d}_{i\mathcal{S}_i}^{d,g}) = \left\{(x_i, \boldsymbol{x}_{\mathcal{S}_i}) \in \mathcal{X}_{i\mathcal{S}_i} : \forall z \in (\{i\} \cup \mathcal{S}_i),\ x_z \geq c \text{ if } d_z^{d,g} = 1,\ x_z < c \text{ if } d_z^{d,g} = 0\right\}$$

Equivalently,

$$\mathcal{B}_\varepsilon^{d,g}(\ell_i) = \left\{(x_i, \boldsymbol{x}_{\mathcal{S}_i}) \in \mathcal{X}_{i\mathcal{S}_i} : \boldsymbol{x}_{F_{\ell_i}} \in N_\varepsilon^{d,g}(\boldsymbol{c}_{F_{\ell_i}}),\ \boldsymbol{x}_{R_{\ell_i}} \in \mathcal{R}_{\ell_i}\right\},$$

where

$$N_\varepsilon^{d,g}(\boldsymbol{c}_{F_{\ell_i}}) := \left\{\boldsymbol{x}_{F_{\ell_i}} : \|\boldsymbol{x}_{F_{\ell_i}} - \boldsymbol{c}_{F_{\ell_i}}\| \leq \varepsilon,\ x_z \geq c \text{ if } d_z^{d,g} = 1,\ x_z < c \text{ if } d_z^{d,g} = 0\right\}.$$

Geometrically, $N_\varepsilon^{d,g}(\boldsymbol{c}_{F_{\ell_i}})$ is the intersection of a s_{ℓ_i}-dimensional ball of radius ε centered at $\boldsymbol{c}_{F_{\ell_i}}$ with the orthant determined by the threshold c for each constrained coordinate. Hence its volume depends on ℓ_i only through the codimension s_{ℓ_i}. Denote

$$\text{Vol}(N_\varepsilon^{d,g}(\boldsymbol{c}_{F_{\ell_i}})) = V_\varepsilon^{s_{\ell_i}}, \qquad V_\varepsilon^{s_{\ell_i}} = \kappa_{s_{\ell_i}}\, \varepsilon^{s_{\ell_i}},$$

where $\kappa_{s_{\ell_i}} > 0$ is a constant depending only on the orthant fraction of the s_{ℓ_i}-dimensional ball.

Since the neighborhood $\mathcal{B}_\varepsilon^{d,g}(\bar{\mathcal{X}}_{i\mathcal{S}_i}(d,g \,|\, d',g'))$ is the union of $\mathcal{B}_\varepsilon^{d,g}(\ell_i)$, we can write $\mathbb{E}[Y_i(d,g) \,|\, (X_i, \boldsymbol{X}_{\mathcal{S}_i}) \in \mathcal{B}_\varepsilon^{d,g}(\bar{\mathcal{X}}_{i\mathcal{S}_i}(d,g \,|\, d',g'))]$ as

$$\frac{\sum\limits_{\ell_i} \int\limits_{\mathcal{R}_{\ell_i}} \int\limits_{N_\varepsilon^{d,g}(\boldsymbol{c}_{F_{\ell_i}})} m_{d,g}(\boldsymbol{x}_{F_{\ell_i}}, \boldsymbol{x}_{R_{\ell_i}}) f(\boldsymbol{x}_{F_{\ell_i}}, \boldsymbol{x}_{R_{\ell_i}}) d\boldsymbol{x}_{F_{\ell_i}} d\boldsymbol{x}_{R_{\ell_i}} + I_\varepsilon}{\sum\limits_{\ell_i} \int\limits_{\mathcal{R}_{\ell_i}} \int\limits_{N_\varepsilon^{d,g}(\boldsymbol{c}_{F_{\ell_i}})} f(\boldsymbol{x}_{F_{\ell_i}}, \boldsymbol{x}_{R_{\ell_i}}) d\boldsymbol{x}_{F_{\ell_i}} d\boldsymbol{x}_{R_{\ell_i}} + I'_\varepsilon} \tag{S.2.4}$$

and the terms I_ε and I'_ε include the integrals over the intersections of the neighborhoods $\mathcal{B}_\varepsilon^{d,g}(\ell_i)$.

We first establish the limit of the average integral

$$\frac{1}{V_\varepsilon^{s_{\ell_i}}} \int_{N_\varepsilon^{d,g}(\boldsymbol{c}_{F_{\ell_i}})} f(\boldsymbol{x}_{F_{\ell_i}}, \boldsymbol{x}_{R_{\ell_i}})\, d\boldsymbol{x}_{F_{\ell_i}}, \tag{S.2.5}$$

for fixed $\boldsymbol{x}_{R_{\ell_i}}$.

By Assumption 4.c, the density f is continuous. Hence, given $\boldsymbol{x}_{R_{\ell_i}}$ and any $\delta > 0$, there exists $r > 0$ such that whenever $\|\boldsymbol{x}_{F_{\ell_i}} - \boldsymbol{c}_{F_{\ell_i}}\| \leq r$,

$$\left| f(\boldsymbol{x}_{F_{\ell_i}}, \boldsymbol{x}_{R_{\ell_i}}) - f(\boldsymbol{c}_{F_{\ell_i}}, \boldsymbol{x}_{R_{\ell_i}}) \right| < \delta.$$

Therefore, for $\varepsilon < r$,

$$\begin{aligned}\frac{1}{V_\varepsilon^{s_{\ell_i}}} \left| \int_{N_\varepsilon^{d,g}(\boldsymbol{c}_{F_{\ell_i}})} \left(f(\boldsymbol{x}_{F_{\ell_i}}, \boldsymbol{x}_{R_{\ell_i}}) - f(\boldsymbol{c}_{F_{\ell_i}}, \boldsymbol{x}_{R_{\ell_i}}) \right) d\boldsymbol{x}_{F_{\ell_i}} \right| &\leq \frac{1}{V_\varepsilon^{s_{\ell_i}}} \int_{N_\varepsilon^{d,g}(\boldsymbol{c}_{F_{\ell_i}})} \left| f(\boldsymbol{x}_{F_{\ell_i}}, \boldsymbol{x}_{R_{\ell_i}}) - f(\boldsymbol{c}_{F_{\ell_i}}, \boldsymbol{x}_{R_{\ell_i}}) \right| d\boldsymbol{x}_{F_{\ell_i}} \\ &< \delta.\end{aligned}$$

Thus, (S.2.5) converges to $f(\boldsymbol{c}_{F_{\ell_i}}, \boldsymbol{x}_{R_{\ell_i}})$ as $\varepsilon \to 0$. Moreover,

$$\begin{aligned}\lim_{\varepsilon \to 0} \frac{1}{V_\varepsilon^{s_{\ell_i}}} \int\limits_{\mathcal{R}_{\ell_i}} \int\limits_{N_\varepsilon^{d,g}(\boldsymbol{c}_{F_{\ell_i}})} f(\boldsymbol{x}_{F_{\ell_i}}, \boldsymbol{x}_{R_{\ell_i}})\, d\boldsymbol{x}_{F_{\ell_i}}\, d\boldsymbol{x}_{R_{\ell_i}} &= \frac{1}{V_\varepsilon^{s_{\ell_i}}} \int\limits_{\mathcal{R}_{\ell_i}} \lim_{\varepsilon \to 0} \int\limits_{N_\varepsilon^{d,g}(\boldsymbol{c}_{F_{\ell_i}})} f(\boldsymbol{x}_{F_{\ell_i}}, \boldsymbol{x}_{R_{\ell_i}})\, d\boldsymbol{x}_{F_{\ell_i}}\, d\boldsymbol{x}_{R_{\ell_i}} \\ &= \int\limits_{\mathcal{R}_{\ell_i}} f(\boldsymbol{c}_{F_{\ell_i}}, \boldsymbol{x}_{R_{\ell_i}})\, d\boldsymbol{x}_{R_{\ell_i}},\end{aligned}$$

by the Dominated Convergence Theorem, since the score density is bounded by Assumption 4.d.

By the same argument, we also obtain convergence of

$$\frac{1}{V_\varepsilon^{s_{\ell_i}}} \int\limits_{\mathcal{R}_{\ell_i}} \int\limits_{N_\varepsilon^{d,g}(\boldsymbol{c}_{F_{\ell_i}})} m_{d,g}(\boldsymbol{x}_{F_{\ell_i}}, \boldsymbol{x}_{R_{\ell_i}}) f(\boldsymbol{x}_{F_{\ell_i}}, \boldsymbol{x}_{R_{\ell_i}})\, d\boldsymbol{x}_{F_{\ell_i}}\, d\boldsymbol{x}_{R_{\ell_i}}$$

to

$$\int_{\mathcal{R}_{\ell_i}} m_{d,g}(\boldsymbol{c}_{F_{\ell_i}}, \boldsymbol{x}_{R_{\ell_i}})\, f(\boldsymbol{c}_{F_{\ell_i}}, \boldsymbol{x}_{R_{\ell_i}})\, d\boldsymbol{x}_{R_{\ell_i}}.$$

because $m_{d,g}$ and f are continuous and bounded by Assumptions 4.b-4.c and 4.d.

Hence, each element of the numerator and denominator in (S.2.4) is of order $O(\varepsilon^{s_{\ell_i}})$, which implies that both summations are $O(\varepsilon^{\bar{s}_i})$. Moreover, since both the score density and the conditional mean of potential outcomes are bounded by Assumption 4.d, and the region of integration of I_ε and I'_ε has volume $O(\varepsilon^{\bar{s}_i+1})$, we obtain $|I_\varepsilon| \lesssim \varepsilon^{\bar{s}_i+1}$ and $|I'_\varepsilon| \lesssim \varepsilon^{\bar{s}_i+1}$. [1]

By dividing numerator and denominator of (S.2.4) by $V_\varepsilon^{\bar{s}_i} = \kappa_{\bar{s}_i}\varepsilon^{\bar{s}_i}$, we obtain

$$(\text{S.2.4}) \to \frac{\sum_{\ell_i} \int_{\mathcal{R}_{\ell_i}} m_{d,g}(\boldsymbol{c}_{F_{\ell_i}}, \boldsymbol{x}_{R_{\ell_i}}) f(\boldsymbol{c}_{F_{\ell_i}}, \boldsymbol{x}_{R_{\ell_i}})\, d\boldsymbol{x}_{R_{\ell_i}}}{\sum_{\ell_i} \int_{\mathcal{R}_{\ell_i}} f(\boldsymbol{c}_{F_{\ell_i}}, \boldsymbol{x}_{R_{\ell_i}})\, d\boldsymbol{x}_{R_{\ell_i}}},$$

where only terms with $s_{\ell_i} = \bar{s}_i$ contribute in the limit, since $\varepsilon^{s_{s_{\ell_i}} - \bar{s}_i} \to 0$ for $s_{s_{\ell_i}} > \bar{s}_i$. Hence,

$$(\text{S.2.4}) \to \mathbb{E}[\, Y_i(d,g) \,|\, (X_i, \boldsymbol{X}_{\mathcal{S}_i}) \in \bar{\mathcal{X}}_{i\mathcal{S}_i}(d, g \,|\, d', g')\,],$$

by the Dominated Convergence Theorem and Assumptions 4.b–4.c, 4.d. Analogously, one can show $\mathbb{E}[\, Y_i(d', g') \,|\, (X_i, \boldsymbol{X}_{\mathcal{S}_i}) \in \mathcal{B}_\varepsilon^{d',g'}(\bar{\mathcal{X}}_{i\mathcal{S}_i}(d, g \,|\, d', g'))\,]$ converges to $\mathbb{E}[\, Y_i(d', g') \,|\, (X_i, \boldsymbol{X}_{\mathcal{S}_i}) \in \bar{\mathcal{X}}_{i\mathcal{S}_i}(d, g \,|\, d', g')\,]$.

Therefore,

$$\begin{aligned}
\tau_{d,g|d',g'}\big(\bar{\mathcal{X}}_{i\mathcal{S}_i}(d, g \,|\, d', g')\big) &= \mathbb{E}[\, Y_i(d,g) - Y_i(d', g') \,|\, (X_i, \boldsymbol{X}_{\mathcal{S}_i}) \in \bar{\mathcal{X}}_{i\mathcal{S}_i}(d, g \,|\, d', g')\,] \\
&= \lim_{\varepsilon \to 0} \mathbb{E}[\, Y_i(d,g) \,|\, (X_i, \boldsymbol{X}_{\mathcal{S}_i}) \in \mathcal{B}_\varepsilon^{d,g}(\bar{\mathcal{X}}_{i\mathcal{S}_i}(d, g \,|\, d', g'))\,] \\
&\quad - \lim_{\varepsilon \to 0} \mathbb{E}[\, Y_i(d', g') \,|\, (X_i, \boldsymbol{X}_{\mathcal{S}_i}) \in \mathcal{B}_\varepsilon^{d',g'}(\bar{\mathcal{X}}_{i\mathcal{S}_i}(d, g \,|\, d', g'))\,] \\
&= \lim_{\varepsilon \to 0} \mathbb{E}[\, Y_i \,|\, (X_i, \boldsymbol{X}_{\mathcal{S}_i}) \in \mathcal{B}_\varepsilon^{d,g}(\bar{\mathcal{X}}_{i\mathcal{S}_i}(d, g \,|\, d', g'))\,] \\
&\quad - \lim_{\varepsilon \to 0} \mathbb{E}[\, Y_i \,|\, (X_i, \boldsymbol{X}_{\mathcal{S}_i}) \in \mathcal{B}_\varepsilon^{d',g'}(\bar{\mathcal{X}}_{i\mathcal{S}_i}(d, g \,|\, d', g'))\,],
\end{aligned}$$

where the last equality follows from Assumptions 1-2 and Property 3. □

Proof of Theorem 2. Let us define $\mathcal{X}_{\mathcal{S}_i} \subseteq \mathbb{R}^{|\mathcal{S}_i|}$ as the set of elements $\boldsymbol{x}_{\mathcal{S}_i}$. Further, for all $g \in \mathcal{G}_i$ define $\mathcal{X}_{\mathcal{S}_i}(g) = \{\boldsymbol{x}_{\mathcal{S}_i} \in \mathcal{X}_{\mathcal{S}_i} : e(\boldsymbol{x}_{\mathcal{S}_i}) = g\}$.

[1] To see this, note that each tubular neighborhood $\mathcal{B}_\varepsilon^{d,g}(\ell_i)$ is contained in a rectangular box $R_\epsilon^{d,g}(\ell_i) = \{(x_i, \boldsymbol{x}_{\mathcal{S}_i}) \in \mathcal{X}_{i\mathcal{S}_i} : \boldsymbol{x}_{R_{\ell_i}} \in \mathcal{R}_{\ell_i},\ |x_z - c| \leq \varepsilon \text{ for all } z \in F_{\ell_i}\}$, with volume $O(\varepsilon^{s_{\ell_i}})$. The intersection of tubes $\{\mathcal{B}_\varepsilon^{d,g}(\ell_i) : \ell_i \in \tilde{C}\}$ for any collection $\tilde{C}$ of pieces is then contained in the intersection of the corresponding boxes $\{R_\epsilon^{d,g}(\ell_i) : \ell_i \in \tilde{C}\}$. This set is described as follows: $x_z \in [a, c]$ if $z \in \cap_{\tilde{C}} W_{\ell_i}$, $x_z \in [c, b]$ if $z \in \cap_{\tilde{C}} P_{\ell_i}$, where W_{ℓ_i} and P_{ℓ_i} are index sets collecting the indices of the components varying in $[a, c]$ and $[c, b]$, respectively, in each ℓ_i, and $|x_z - c| \leq \varepsilon$ if $z \in \cap_{\tilde{C}} F_{\ell_i}$ or if z does not lie in all positive or all negative index sets. Hence, the intersection set is rectangular with volume $O(\varepsilon^{\bar{s}_i+1})$.

Note that $\bar{\mathcal{X}}_{is_i}(1, g \mid 0, g) = \{(x_i, \boldsymbol{x}_{s_i}) \in \mathcal{X}_{is_i} : x_i = c,\ \boldsymbol{x}_{s_i} \in \mathcal{X}_{s_i}(g)\}$ for all $g \in \mathcal{G}_i$. By Assumption 4.c we have that $\lim_{x_i \to c} f(x_i, \boldsymbol{x}_{s_i}) = f(c, \boldsymbol{x}_{s_i})$. Moreover,

$$\lim_{x_i \to c} \int\limits_{\mathcal{X}_{s_i}} f(x_i, \boldsymbol{x}_{s_i}) d\boldsymbol{x}_{s_i} = \int\limits_{\mathcal{X}_{s_i}} f(c, \boldsymbol{x}_{s_i}) d\boldsymbol{x}_{s_i}$$

by the Dominated Convergence Theorem following from Assumption 4.c and 4.d. Therefore, because $f(x_i) = \int_{\mathcal{X}_{s_i}} f(x_i, \boldsymbol{x}_{s_i}) d\boldsymbol{x}_{s_i}$ it follows that $\lim_{x_i \to c} f(x_i) = f(c)$.

We have

$$\begin{aligned}
\lim_{x_i \downarrow c} \mathbb{E}[\, Y_i \mid X_i = x_i \,] &= \lim_{x_i \downarrow c} \sum_{g \in \mathcal{G}_i} \int_{\mathcal{X}_{s_i}(g)} \mathbb{E}[\, Y_i \mid X_i = x_i, \boldsymbol{X}_{s_i} = \boldsymbol{x}_{s_i} \,] \cdot \frac{f(x_i, \boldsymbol{x}_{s_i})}{f(x_i)} d\boldsymbol{x}_{s_i} \\
&= \lim_{x_i \downarrow c} \sum_{g \in \mathcal{G}_i} \int_{\mathcal{X}_{s_i}(g)} \mathbb{E}[\, Y_i(1, g) \mid X_i = x_i, \boldsymbol{X}_{s_i} = \boldsymbol{x}_{s_i} \,] \cdot \frac{f(x_i, \boldsymbol{x}_{s_i})}{f(x_i)} d\boldsymbol{x}_{s_i} \\
&= \sum_{g \in \mathcal{G}_i} \int_{\mathcal{X}_{s_i}(g)} \mathbb{E}[\, Y_i(1, g) \mid X_i = c, \boldsymbol{X}_{s_i} = \boldsymbol{x}_{s_i} \,] \cdot \frac{f(c, \boldsymbol{x}_{s_i})}{f(c)} d\boldsymbol{x}_{s_i}
\end{aligned}$$

where the first equality come from the Law of Iterated expectations, the second equality from Assumptions 1-2, and the third equality follows from the Dominated Convergence Theorem, since $\frac{f(x_i, \boldsymbol{x}_{s_i})}{f(x_i)}$ is continuous, and $\mathbb{E}[\, Y_i(1, g) \mid X_i = x_i, \boldsymbol{X}_{s_i} = \boldsymbol{x}_{s_i} \,]$ is continuous and bounded by Assumption 4.b and 4.d.

Note that $\mathbb{P}(\, \boldsymbol{X}_{s_i} \in \mathcal{X}_{s_i}(g) \mid X_i = c \,) = \mathbb{P}(\, G_i = g \mid X_i = c \,) = \int\limits_{\mathcal{X}_{s_i}(g)} \frac{f(c, \boldsymbol{x}_{s_i})}{f(c)} d\boldsymbol{x}_{s_i}$, and

$$\int\limits_{\mathcal{X}_{s_i}(g)} \mathbb{E}[\, Y_i(1, g) \mid X_i = c, \boldsymbol{X}_{s_i} = \boldsymbol{x}_{s_i} \,] \cdot \frac{f(c, \boldsymbol{x}_{s_i})}{\int\limits_{\mathcal{X}_{s_i}(g)} f(c, \boldsymbol{x}_{s_i})} d\boldsymbol{x}_{s_i} = \mathbb{E}[\, Y_i(1, g) \mid (X_i, \boldsymbol{x}_{s_i}) \in \bar{\mathcal{X}}_{is_i}(1, g, |0, g) \,]$$

Hence, by multiplying and dividing each element of the summation in the last line of (S.2) by $\int\limits_{\mathcal{X}_{s_i}(g)} f(c, \boldsymbol{x}_{s_i}) d\boldsymbol{x}_{s_i}$, we obtain

$$\lim_{x_i \downarrow c} \mathbb{E}[\, Y_i \mid X_i = x_i \,] = \mathbb{E}[\, Y_i(1, g) \mid (X_i, \boldsymbol{x}_{s_i}) \in \bar{\mathcal{X}}_{is_i}(1, g, |0, g) \,] \cdot \mathbb{P}(\, G_i = g \mid X_i = c \,)$$

By analogous arguments

$$\lim_{x_i \uparrow c} \mathbb{E}[\, Y_i \mid X_i = x_i \,] = \sum_{g \in \mathcal{G}_i} \mathbb{E}[\, Y_i(0, g) \mid (X_i, \boldsymbol{x}_{s_i}) \in \bar{\mathcal{X}}_{is_i}(1, g, |0, g) \,] \cdot \mathbb{P}(\, G_i = g \mid X_i = c \,)$$

from which the conclusion follows. $\square$

S.3 Proofs of Main Results in Section 4

This section provides the asymptotic theory for $\hat{\tau}_{d,g|d',g'}(h_n)$. Recall the expression for the observed outcome

$$Y_i = \mu(\tilde{X}_{i,d,g,d',g'}) + u_{i,d,g,d',g'}, \quad i = 1, ..., n$$

with $\mu(\tilde{X}_{i,d,g,d',g'}) = \mathbb{E}[Y_i \,|\, \tilde{X}_{i,d,g,d',g'}, D_i, G_i]$, $u_{i,d,g,d',g'} = m(X_i, \boldsymbol{X}_{\mathcal{S}_i}) - \mu(\tilde{X}_{i,d,g,d',g'}) + \epsilon_i$, where $m(X_i, \boldsymbol{X}_{\mathcal{S}_i}) = \sum_{d,g} \mathbb{1}((X_i, \boldsymbol{X}_{\mathcal{S}_i}) \in \mathcal{X}_{i\mathcal{S}_i}(d,g)) \cdot m_{d,g}(X_i, \boldsymbol{X}_{\mathcal{S}_i})$, and $\epsilon_i = \sum_{d,g} \mathbb{1}((X_i, \boldsymbol{X}_{\mathcal{S}_i}) \in \mathcal{X}_{i\mathcal{S}_i}(d,g)) \cdot \epsilon_{i,d,g}$. We denote $\tilde{X}_{i,d,g,d',g'}$, and $u_{i,d,g,d',g'}$ by $\tilde{X}_i$ and u_i for convenience.

The outcome regression functions of interest are

$$\mu_{d,g}(\tilde{x}_i) = \mathbb{E}[Y_i \,|\, \tilde{X}_i = \tilde{x}_i, D_i = d, G_i = g], \quad \mu_{d',g'}(\tilde{x}_i) = \mathbb{E}[Y_i \,|\, \tilde{X}_i = \tilde{x}_i, D_i = d', G_i = g']$$

In what follows, results are stated for $\hat{\tau}_{d,g,d',g',p}(h_n)$, the distance-based $p-$order local polynomial estimator for $\tau_{d,g|d',g'}\big(\bar{\mathcal{X}}_{i\mathcal{S}_i}(d,g \,|\, d',g')\big)$. Here, we assume that all units have equally-sized interference sets $|\mathcal{S}_i|$ and common codimension $\bar{s}$. The data are identically, although non independently, distributed, so that $\mathbb{E}[Y_i(d,g) \,|\, (X_i, \boldsymbol{X}_{\mathcal{S}_i}) = (x_i, \boldsymbol{x}_{\mathcal{S}_i})]$ and $f(x_i, \boldsymbol{x}_{\mathcal{S}_i})$, and thus the boundary average causal effects, are homogeneous for all i. The case with heterogeneous interference sets and data distributions is treated in Section S.5.1.

S.3.1 Notation

Let $p, q \in \mathbb{Z}_+$. Define $\boldsymbol{r}_p(u) = [1, u, u^2, ..., u^p]$ and let $K_h^{\bar{s}}(u) = K(u/h)/h^{\bar{s}}$, where $K(\cdot)$ is a kernel function. The estimator $\hat{\tau}_{d,g,d',g',p}(h_n)$ is given by :

$$\begin{aligned}
\hat{\tau}_{d,g,d',g',p}(h_n) &= e_1^T \hat{\beta}_{d,g,p}(h_n) \; - e_1^T \hat{\beta}_{d',g',p}(h_n) \\
\hat{\beta}_{d,g,p}(h_n) &= \underset{\boldsymbol{b} \in \mathbb{R}^{p+1}}{\arg\min} \sum_i \mathbb{1}(D_i = d, G_i = g)(Y_i - \boldsymbol{r}_p(\tilde{X}_i)^T \boldsymbol{b})^2 \cdot K_{h_n^{\bar{s}}}(\tilde{X}_i) \\
\hat{\beta}_{d',g',p}(h_n) &= \underset{\boldsymbol{b} \in \mathbb{R}^{p+1}}{\arg\min} \sum_i \mathbb{1}(D_i = d', G_i = g')(Y_i - \boldsymbol{r}_p(\tilde{X}_i)^T \boldsymbol{b})^2 \cdot K_{h_n^{\bar{s}}}(\tilde{X}_i)
\end{aligned}$$

where h_n is a positive bandwidth and e_1 is the $(p+1)$-dimensional vector with the first entry equal to 1 and 0 elsewhere. We set $I_{i,d,g} = \mathbb{1}(D_i = d, G_i = g)$ and $I_{i,d',g'} =$

$\mathbb{1}(D_i = d', G_i = g')$, and $\boldsymbol{Y} = [Y_1, ..., Y_n]^T$. In addition, we define

$$\tilde{X}_p(h) = [\boldsymbol{r}_p(\tilde{X}_1/h), ..., \boldsymbol{r}_p(\tilde{X}_n/h)]^T,$$
$$W_{d,g}(h) = \text{diag}(I_{1,d,g} \cdot K_{h^{\bar{s}}}(\tilde{X}_1), ..., I_{n,d,g} \cdot K_{h^{\bar{s}}}(\tilde{X}_n)),$$
$$W_{d',g'}(h) = \text{diag}(I_{1,d',g'} \cdot K_{h^{\bar{s}}}(\tilde{X}_1), ..., I_{n,d',g'} \cdot K_{h^{\bar{s}}}(\tilde{X}_n)).$$

and the following sample quantities:

$$\Gamma_{d,g,p}(h) = \tilde{X}_p(h)^T W_{d,g}(h)\tilde{X}_p(h)/n, \qquad \Gamma_{d',g',p}(h) = \tilde{X}_p(h)^T W_{d',g'}(h)\tilde{X}_p(h)/n,$$
$$t_{d,g,p}(h) = \tilde{X}_p(h)^T W_{d,g}(h)\boldsymbol{Y}/n, \qquad t_{d',g',p}(h) = \tilde{X}_p(h)^T W_{d',g'}(h)\boldsymbol{Y}/n,$$
$$\theta_{d,g,p,q}(h) = \tilde{X}_p(h_n)^T W_{d,g}(h_n)S_q(h_n)/n, \qquad \theta_{d',g',p,q}(h_n) = \tilde{X}_p(h)^T W_{d',g'}(h_n)S_q(h_n)/n,$$

with $S_q(h) = [(\tilde{X}_1/h)^q, ..., (\tilde{X}_n/h)^q]$. Denote by $\bar{\Gamma}_{d,g,p}(h)$, $\bar{\Gamma}_{d',g',p}(h)$, $\bar{t}_{d,g,p}(h)$, $\bar{t}_{d',g',p}(h)$, $\bar{\theta}_{d,g,p,q}(h_n)$, $\bar{\theta}_{d',g',p,q}(h_n)$ their respective expectations. Let $H(h_n) = \text{diag}(1, h^{-1}, ..., h^{-p})$. Then:

$$\hat{\beta}_{d,g,p}(h_n) = H(h_n)\Gamma^{-1}_{d,g,p}(h_n)t_{d,g,p}(h_n), \quad \hat{\beta}_{d',g',p}(h_n) = H(h_n)\Gamma^{-1}_{d',g',p}(h_n)t_{d',g',p}(h_n)$$

Next, we define the population linear projection coefficients:

$$\beta_{d,g,p}(h_n) = H(h_n)\bar{\Gamma}^{-1}_{d,g,p}(h_n)\bar{t}_{d,g,p}(h_n), \quad \beta_{d',g',p}(h_n) = H(h_n)\bar{\Gamma}^{-1}_{d',g',p}(h_n)\bar{t}_{d',g',p}(h_n) \tag{S.3.1}$$

where

$$\beta_{d,g,p}(h_n) = \underset{\boldsymbol{b}\in\mathbb{R}^{p+1}}{\arg\min}\, \mathbb{E}\Big[\sum_i \mathbb{1}(D_i = d, G_i = g)(Y_i - \boldsymbol{r}_p(\tilde{X}_i)^T\boldsymbol{b})^2 \cdot K_{h_n^{\bar{s}}}(\tilde{X}_i)\Big]$$
$$\beta_{d',g',p}(h_n) = \underset{\boldsymbol{b}\in\mathbb{R}^{p+1}}{\arg\min}\, \mathbb{E}\Big[\sum_i \mathbb{1}(D_i = d', G_i = g')(Y_i - \boldsymbol{r}_p(\tilde{X}_i)^T\boldsymbol{b})^2 \cdot K_{h_n^{\bar{s}}}(\tilde{X}_i)\Big]$$

and introduce the following centered quantities:

$$t^*_{d,g,p}(h_n) = \tilde{X}_p(h_n)^T W_{d,g}(h_n)\boldsymbol{\nu}_{d,g}/n, \qquad t^*_{d',g',p}(h_n) = \tilde{X}_p(h_n)^T W_{d',g'}(h_n)\boldsymbol{\nu}_{d',g'}/n$$
$$\hat{\beta}^*_{d,g,p}(h_n) = H(h_n)\Gamma^{-1}_{d,g,p}(h_n)t^*_{d,g,p}(h_n), \qquad \hat{\beta}^*_{d',g',p}(h_n) = H(h_n)\Gamma^{-1}_{d',g',p}(h_n)t^*_{d',g',p}(h_n)$$
$$t^*_{d,g,d',g',p}(h_n) = t^*_{d,g,p}(h_n) - t^*_{d',g',p}(h_n),$$
$$\hat{\tau}^*_{d,g,d',g',p}(h_n) = e_1^T\hat{\beta}^*_{d,g,p}(h_n) - e_1^T\hat{\beta}^*_{d',g',p}(h_n). \tag{S.3.2}$$

with $\boldsymbol{\nu}_{d,g} = [\nu_{1,d,g}, ..., \nu_{n,d,g}]$ and $\boldsymbol{\nu}_{d',g'} = [\nu_{1,d',g'}, ..., \nu_{n,d',g'}]$ where for each i:

$$\nu_{i,\bullet} = Y_i - \boldsymbol{r}_p(\tilde{X}_i)^T \beta_{\bullet,p}(h_n), \quad \bullet \in \{(d,g),(d',g')\}$$

We denote the scaled variance and covariance of $t^*_{d,g,p}(h_n)$ and $t^*_{d',g',p}(h_n)$ by

$$\bar{\Psi}_{d,g,p}(h_n) = nh_n^{\bar{s}}\mathbb{V}[t^*_{d,g,p}(h_n)], \quad \bar{\Psi}_{d',g',p}(h_n) = nh_n^{\bar{s}}\mathbb{V}[t^*_{d',g',p}(h_n)],$$
$$\bar{\Psi}_{d,g,d',g',p}(h_n) = nh_n^{\bar{s}}\mathbb{C}[t^*_{d,g,p}(h_n), t^*_{d',g',p}(h_n)]$$

We further define the kernel-weighted subgraph for units with $(D_i = d, G_i = g)$, $\boldsymbol{W}^{d,g}(h_n)$ with entry $W^{d,g}_{ij}(h_n) = W_{ij} I_{i,d,g} I_{j,d,g} K\left(\frac{\tilde{X}_i}{h_n}\right) K\left(\frac{\tilde{X}_j}{h_n}\right)$. Let $\bar{\boldsymbol{D}}^{d,g}(h_n)$ denote the expected sum of its diagonal elements and let $\bar{\boldsymbol{N}}^{d,g}(h_n)$ be its expected average degree without the diagonal terms. Similarly, define $\boldsymbol{W}^{d',g'}(h_n)$, $\bar{\boldsymbol{D}}^{d',g'}(h_n)$ and $\bar{\boldsymbol{N}}^{d',g'}(h_n)$. Finally, let $\boldsymbol{W}^{d,g,d',g'}(h_n)$ with entry $W^{d,g,d',g'}_{ij}(h_n) = W_{ij} I_{i,d,g} I_{j,d',g'} K\left(\frac{\tilde{X}_i}{h_n}\right) K\left(\frac{\tilde{X}_j}{h_n}\right)$, and expected degree $\bar{\boldsymbol{N}}^{d,g,d',g'}(h_n)$.

Lastly, let N^s be the intersection of the s-dimensional unit ball centered at zero $\mathbf{0}_s$ with a generic orthant in $\mathbb{R}^s$ and let:

$$\Gamma^s_p = \int_{N^s} K(||\boldsymbol{u}_s||)\boldsymbol{r}_p(||\boldsymbol{u}_s||)\boldsymbol{r}_p(||\boldsymbol{u}_s||)^T d\boldsymbol{u}_s$$
$$\theta^s_{p,q} = \int_{N^s} K(||\boldsymbol{u}_s||)(||\boldsymbol{u}_s||)^q \boldsymbol{r}_p(||\boldsymbol{u}_s||) d\boldsymbol{u}_s$$
$$\Psi^s_p = \int_{N^s} K(||\boldsymbol{u}_s||)^2 \boldsymbol{r}_p(||\boldsymbol{u}_s||)\boldsymbol{r}_p(||\boldsymbol{u}_s||)^T d\boldsymbol{u}_s$$

For short, we will denote by $f_{d,g,d',g'}(0) = \int_{\bar{\mathcal{X}}_{i\mathcal{S}_i}(d,g\,|\,d',g')} f(x_i, \boldsymbol{x}_{\mathcal{S}_i}) d\mathcal{H}^{|\mathcal{S}_i|+1-\bar{s}}$.

Note. In the main text, we report our results for $p = 1$ and therefore drop the subscript p indexing the polynomial order to simplify notation (e.g., we write Γ^s instead of Γ^s_p and $\hat{\beta}_{d,g}(h_n)$ instead of $\hat{\beta}_{d,g,p}(h_n)$). In this appendix, we retain the full notation with p.

S.3.2 Assumptions

In addition to Assumptions 1-4, we make the following assumptions.

Assumption S.3.1. *For some positive κ the following holds for $(x_i, \boldsymbol{x}_{\mathcal{S}_i}) \in \mathcal{B}_\kappa(\bar{\mathcal{X}}_{i\mathcal{S}_i}(d,g\,|\,d',g'))$ for all i:*

a) $\mathbb{E}[\,Y_i^4\,|\,X_i = x_i, \boldsymbol{X}_{\mathcal{S}_i} = \boldsymbol{x}_{\mathcal{S}_i}\,]$ *is bounded.*

b) $\sigma_{\epsilon_{d,g}}(x_i, \boldsymbol{x}_{\mathcal{S}_i}) = \mathbb{V}[Y_i(d,g)|X_i = x_i, \boldsymbol{X}_{\mathcal{S}_i} = \boldsymbol{x}_{\mathcal{S}_i}]$ *and* $\sigma_{\epsilon_{d',g'}}(x_i, \boldsymbol{x}_{\mathcal{S}_i}) = \mathbb{V}[Y_i(d',g')|X_i = x_i, \boldsymbol{X}_{\mathcal{S}_i} = \boldsymbol{x}_{\mathcal{S}_i}]$ *are bounded away from zero and continuous. .*

c) $\mu_{d,g}(\tilde{x}_i)$ *and* $\mu_{d',g'}(\tilde{x}_i)$ *are S-times continuously differentiable with* $S \geq p+2$.

Assumption S.3.2. *For all* $i,\ j \in \boldsymbol{N}_i$, $|F_{\ell_i} \cup F_{\ell_j}| > \min\{\bar{s}_i, \bar{s}_j\} = \bar{s}$ *for any piece* ℓ_i, ℓ_j, *where* $\bar{s}_i$ *and* $\bar{s}_j$ *are the codimension of* $\bar{\mathcal{X}}_{i\mathcal{S}_i}(d,g\,|\,d',g')$ *and* $\bar{\mathcal{X}}_{j\mathcal{S}_j}(d,g|d',g')$.

Assumption S.3.3. *The kernel function* $K:\mathbb{R}\to\mathbb{R}$ *has support supp*$(K) = [-1,1]$, *is bounded and non-negative on* $[-1,1]$, *and is positive, symmetric and continuous on* $(-1,1)$.

S.3.3 Asymptotic Theory

In this section we establish the asymptotic distribution of our estimator. Recall that the boundary $\bar{\mathcal{X}}_{i\mathcal{S}_i}(d,g\,|\,d',g')$ is the union of pieces ℓ_i (Section 2, Appendix S.1), and that each neighborhood $\mathcal{B}^{d,g}_{\varepsilon}(\bar{\mathcal{X}}_{i\mathcal{S}_i}(d,g\,|\,d',g'))$ decomposes into tubular neighborhoods $\mathcal{B}^{d,g}_{\varepsilon}(\ell_i)$, with

$$\mathrm{Vol}(\mathcal{B}^{d,g}_{\varepsilon}(\ell_i)) = O(\varepsilon^{s_{\ell_i}}), \qquad \mathrm{Vol}(\mathcal{B}^{d,g}_{\varepsilon}(\bar{\mathcal{X}}_{i\mathcal{S}_i}(d,g\,|\,d',g'))) = O(\varepsilon^{\bar{s}_i}),$$

and analogously for $\mathcal{B}^{d',g'}_{\varepsilon}(\bar{\mathcal{X}}_{i\mathcal{S}_i}(d,g\,|\,d',g'))$ (see proof of Theorem 1).

We decompose $\hat{\beta}_{d,g,p}(h_n)$ as follows:

$$\begin{aligned}\hat{\beta}_{d,g,p}(h_n) =& \beta_{d,g,p}(h_n) + H(h_n)\Gamma^{-1}_{d,g,p}(h_n)\tilde{X}_p(h_n)W_{d,g}(h_n)\boldsymbol{\nu}_{d,g} \\ =& \beta_{d,g,p}(h_n) + \hat{\beta}^{*}_{d,g,p}(h_n)\end{aligned} \tag{S.3.3}$$

Under Assumption S.3.1.c a $(p+1)$-order Taylor expansion of $\mu_{d,g}(\tilde{X}_i)$ to the right of the cutoff yields

$$\beta_{d,g,p}(h_n) = \beta_{d,g,p}(0) + h_n^{p+1}\frac{\mu^{(p+1)}_{d,g}(0)}{(p+1)!}H(h_n)\bar{\Gamma}^{-1}_{d,g,p}(h_n)\bar{\theta}_{d,g,p,p+1}(h_n) + T_{d,g}(h_n)$$

where $\beta_{d,g,p}(0) = [\mu_{d,g}(0),\ \mu^{(1)}_{d,g}(0),\ ...,\ \mu^{(p)}_{d,g}(0)/p!]^T$ and

$$T_{d,g}(h_n) = H(h_n)\bar{\Gamma}^{-1}_{d,g,p}(h_n)\mathbb{E}\big[\tilde{X}_p(h_n)W_{d,g}(h_n)T_{d,g,p}/n\big], \quad T_{d,g,p} = [T_{d,g,1},\ldots,T_{d,g,n}]$$

with each Taylor reminder component satisfying $|T_{d,g,i}| \leq \sup_{\tilde{x}} |\mu_{d,g}^{(p+2)}(\tilde{x})| \cdot |\tilde{X}_i^{p+2}|/(p+2)!$. An analogous expansion holds for $\beta_{d',g',p}(h_n)$. Combining the two, we obtain

$$\begin{aligned}\hat{\tau}_{d,g,d',g',p}(h_n) =& \tau_{d,g|d',g'}\big(\bar{\mathcal{X}}_{i\mathcal{S}_i}(d,g\,|\,d',g')\big) + h_n^{p+1} B_{d,g,d',g',p,p+1}(h_n) + T_{d,g,d'g'}(h_n) \\ &+ \hat{\tau}^*_{d,g,d',g',p}(h_n)\end{aligned} \tag{S.3.4}$$

where $B_{d,g,d',g',p,p+1}(h_n) = \frac{\mu_{d,g}^{(p+1)}(0)}{(p+1)!} B_{d,g,p,p+1}(h_n) - \frac{\mu_{d',g'}^{(p+1)}(0)}{(p+1)!} B_{d',g',p,p+1}(h_n)$, with

$$B_{d,g,p,p+1}(h_n) = e_1^T \bar{\Gamma}^{-1}_{d,g,p}(h_n) \bar{\theta}_{d,g,p,p+1}(h_n), \quad B_{d',g',p,p+1}(h_n) = e_1^T \bar{\Gamma}^{-1}_{d',g',p}(h_n) \bar{\theta}_{d',g',p,p+1}(h_n),$$

and $T_{d,g,d'g'}(h_n) = e_1^T \big(T_{d,g}(h_n) - T_{d',g'}(h_n)\big)$.

The proof proceeds as follows. For effective treatment $\bullet \in \{(d,g),(d',g')\}$ Lemma S.3.1 establishes convergence in probability of $\Gamma_{\bullet,p}(h_n)$ to $\bar{\Gamma}_{\bullet,p}(h_n)$, and shows that $\bar{\Gamma}_{\bullet,p}(h_n)$ has deterministic limit $f_{d,g,d',g'}(0)\Gamma_p^{\bar{s}}$ as $h_n \to 0$. Lemma S.3.2 establishes convergence in probability of $t_{\bullet,p}(h_n)$ to $\bar{t}_{\bullet,p}(h_n)$, and that $\bar{t}_{\bullet,p}(h_n) \to \theta^{\bar{s}}_{p,0} \int_{\bar{\mathcal{X}}_{i\mathcal{S}_i}(d,g\,|\,d',g')} m_\bullet(x_i, \boldsymbol{x}_{\mathcal{S}_i}) f(x_i, \boldsymbol{x}_{\mathcal{S}_i})$. Lemma S.3.3 that $\theta_{\bullet,p,q}(h_n)$ converges in probability to $\bar{\theta}_{\bullet,p,q}(h_n)$, and that $\bar{\theta}_{\bullet,p,q}(h_n)$ converges to $f_{d,g,d',g'}(0)\theta^{\bar{s}}_{p,p+1}$. Combining Lemmas S.3.1 and S.3.3 implies that the bias term $B_{d,g,d',g',p,p+1}(h_n) \to (\Gamma_p^{\bar{s}})^{-1}\theta^{\bar{s}}_{p,q}$ as $h_n \to 0$. Lemma S.3.4 shows that the kernel-weighted dependency subgraphs has vanishing average degree, and Lemma S.3.5 derives the limiting variance of $t^*_{d,g,d',g',p}(h_n)$. Finally, Theorem S.3.1 establishes the asymptotic normality of the rescaled and recentered estimator $\hat{\tau}_{d,g,d',g',p}(h_n)$ using Stein's method and the dependency graph bounds of Leung (2020, Theorem A.4).

Lemma S.3.1 (Convergence of $\Gamma_{d,g,p}(h_n)$ and $\Gamma_{d',g',p}(h_n)$)**.** *Suppose Assumptions 1–3, 4.a, 4.c, 5–6 and S.3.3 hold. If $nh_n^{\bar{s}} \to \infty$ and $h_n < \kappa$ then*

$$\Gamma_{d,g,p}(h_n) = \bar{\Gamma}_{d,g,p}(h_n) + o_p(1), \quad \Gamma_{d',g',p}(h_n) = \bar{\Gamma}_{d',g',p}(h_n) + o_p(1)$$

. where $\bar{\Gamma}_{d,g,p}(h_n)$ and $\bar{\Gamma}_{d',g',p}(h_n)$ are bounded and bounded away from zero.

Moreover, if $h_n \to 0$

$$\bar{\Gamma}_{d,g}(h_n) = f_{d,g,d',g'}(0)\Gamma_p^{\bar{s}} + o(1), \qquad \bar{\Gamma}_{d',g'}(h_n) = f_{d,g,d',g'}(0)\Gamma_p^{\bar{s}} + o(1).$$

Proof. **Expectation of** $\Gamma_{d,g,p}(h_n)$. The generic element of $\Gamma_{d,g,p}(h_n)$ is

$$F_{d,g,k}(h_n) = \frac{1}{nh_n^{\bar{s}}} \sum_i I_{i,d,g}\, K\left(\frac{\tilde{X}_i}{h_n}\right) \left(\frac{\tilde{X}_i}{h_n}\right)^k, \quad k = 0, ..., 2p$$

We expand $\bar{\Gamma}_{d,g,p}(h_n) = \mathbb{E}[\Gamma_{d,g,p}(h_n)]$

$$\begin{aligned}
&= \frac{1}{h_n^{\bar{s}}} \int_{\mathcal{B}_{h_n}^{d,g}(\bar{\mathcal{X}}_{i\mathcal{S}_i}(d,g\,|\,d',g'))} K\left(\frac{\tilde{X}_i(x_i, \boldsymbol{x}_{\mathcal{S}_i})}{h_n}\right) r_p\left(\frac{\tilde{X}_i(x_i, \boldsymbol{x}_{\mathcal{S}_i})}{h_n}\right) r_p\left(\frac{\tilde{X}_i(x_i, \boldsymbol{x}_{\mathcal{S}_i})}{h_n}\right)^T f(x_i, \boldsymbol{x}_{\mathcal{S}_i})\, d(x_i, \boldsymbol{x}_{\mathcal{S}_i}) \\
&= \frac{1}{h_n^{\bar{s}}} \sum_{\ell_i} \int_{\mathcal{B}_{h_n}^{d,g}(\ell_i)} K\left(\frac{\tilde{X}_i(x_i, \boldsymbol{x}_{\mathcal{S}_i})}{h_n}\right) r_p\left(\frac{\tilde{X}_i(x_i, \boldsymbol{x}_{\mathcal{S}_i})}{h_n}\right) r_p\left(\frac{\tilde{X}_i(x_i, \boldsymbol{x}_{\mathcal{S}_i})}{h_n}\right)^T f(x_i, \boldsymbol{x}_{\mathcal{S}_i})\, d(x_i, \boldsymbol{x}_{\mathcal{S}_i}) + \frac{1}{h_n^{\bar{s}}} I_{ih_n} \\
&= \frac{1}{h_n^{\bar{s}}} \sum_{\ell_i} \int_{\mathcal{R}_{\ell_i}} \int_{N_{h_n}^{d,g}(\mathbf{0}_{F_{\ell_i}})} K\left(\frac{\|\boldsymbol{x}_{F_{\ell_i}}\|}{h_n}\right) r_p\left(\frac{\|\boldsymbol{x}_{F_{\ell_i}}\|}{h_n}\right) r_p\left(\frac{\|\boldsymbol{x}_{F_{\ell_i}}\|}{h_n}\right)^T f(\boldsymbol{x}_{F_{\ell_i}}, \boldsymbol{x}_{R_{\ell_i}})\, d\boldsymbol{x}_{F_{\ell_i}}\, d\boldsymbol{x}_{R_{\ell_i}} + \frac{1}{h_n^{\bar{s}}} I_{ih_n} \\
&= \sum_{\ell_i} h_n^{s_{\ell_i} - \bar{s}} \int_{\mathcal{R}_{\ell_i}} \int_{N^{s_{\ell_i}}} K(\|\boldsymbol{u}\|) r_p(\|\boldsymbol{u}\|) r_p(\|\boldsymbol{u}\|)^T f(h_n \boldsymbol{u}, \boldsymbol{x}_{R_{\ell_i}})\, d\boldsymbol{u}\, d\boldsymbol{x}_{R_{\ell_i}} + \frac{1}{h_n^{\bar{s}}} I_{ih_n}
\end{aligned}$$

where the second equality comes from decomposing $\mathcal{B}_{h_n}^{d,g}(\bar{\mathcal{X}}_{i\mathcal{S}_i}(d,g\,|\,d',g'))$ as the union of $\mathcal{B}_{h_n}^{d,g}(\ell_i)$, with I_{ih_n} collecting overlap terms; the third equality follows from $\mathcal{B}_{\varepsilon}^{d,g}(\ell_i) = \mathcal{R}_{\ell_i} \times N^{s_{\ell_i}}$ and $\tilde{X}_i = \|\boldsymbol{X}_{F_{\ell_i}}\|$ on $\mathcal{B}_{h_n}^{d,g}(\ell_i)$; the last equality follows by the change of variables $\boldsymbol{x}_{F_{\ell_i}} = h_n \boldsymbol{u}$, which maps $N_{h_n}^{d,g}(\mathbf{0}_{F_{\ell_i}})$ to the normalized domain $N^{s_{\ell_i}}$.

Hence, $\bar{\Gamma}_{d,g,p}(h_n)$ is bounded and bounded away from zero by Assumptions 4.a, 4.c and S.3.3.

Variance concentration We now show that the variance of $F_{k,d,g}(h_n)$ converges to zero:

$$\begin{aligned}
\mathbb{V}[F_{k,d,g}(h_n)] = &\frac{1}{n^2 h_n^{2\bar{s}}} \sum_i \mathbb{V}\left[I_{i,d,g} K\left(\frac{\tilde{X}_i}{h_n}\right) \left(\frac{\tilde{X}_i}{h_n}\right)^k\right] \\
&+ \frac{1}{n^2 h_n^{2\bar{s}}} \sum_i \sum_{j \in \boldsymbol{N}_i \setminus \{i\}} \mathbb{C}\left[I_{i,d,g} K\left(\frac{\tilde{X}_i}{h_n}\right) \left(\frac{\tilde{X}_i}{h_n}\right)^k, I_{j,d,g} K\left(\frac{\tilde{X}_i}{h_n}\right) \left(\frac{\tilde{X}_i}{h_n}\right)^k\right].
\end{aligned}$$

Expanding,

$$\begin{aligned}\mathbb{V}[F_{k,d,g}(h_n)] = &\frac{1}{n^2 h_n^{2\bar{s}}}\sum_i \mathbb{E}\left[I_{i,d,g}K\left(\frac{\tilde{X}_i}{h_n}\right)^2\left(\frac{\tilde{X}_i}{h_n}\right)^{2k}\right] \\ &+ \frac{1}{n^2 h_n^{2\bar{s}}}\sum_i \sum_{j\in \boldsymbol{N}_i\setminus\{i\}} \mathbb{E}\left[I_{i,d,g}K\left(\frac{\tilde{X}_i}{h_n}\right)\left(\frac{\tilde{X}_i}{h_n}\right)^k I_{j,d,g}K\left(\frac{\tilde{X}_i}{h_n}\right)\left(\frac{\tilde{X}_i}{h_n}\right)^k\right] \\ &- \frac{1}{n^2 h_n^{2\bar{s}}}\sum_i \mathbb{E}\left[I_{i,d,g}K\left(\frac{\tilde{X}_i}{h_n}\right)\left(\frac{\tilde{X}_i}{h_n}\right)^k\right]^2 \\ &- \frac{1}{n^2 h_n^{2\bar{s}}}\sum_i \sum_{j\in \boldsymbol{N}_i\setminus\{i\}} \mathbb{E}\left[I_{i,d,g}K\left(\frac{\tilde{X}_i}{h_n}\right)\left(\frac{\tilde{X}_i}{h_n}\right)^k\right]\mathbb{E}\left[I_{j,d,g}K\left(\frac{\tilde{X}_k}{h_n}\right)\left(\frac{\tilde{X}_j}{h_n}\right)^k\right].\end{aligned}$$

The first term is $O((nh_n^{\bar{s}})^{-1}) = o(1)$, by the same arguments used in computing the expectation. The second term is also $O((nh_n^{\bar{s}})^{-1})$: by the arithmetic–geometric inequality it is bounded by

$$\frac{1}{nh_n^{2\bar{s}}}\max_i \mathbb{E}\left[I_{i,d,g}K\left(\frac{\tilde{X}_i}{h_n}\right)\left(\frac{\tilde{X}_i}{h_n}\right)^k\right]\cdot\frac{1}{n}\sum_i |\boldsymbol{N}_i| = O((nh_n^{\bar{s}})^{-1}),$$

since $\frac{1}{n}\sum_i |\boldsymbol{N}_i| = O(1)$ by Assumption 6. The last two terms are $O(n^{-1})$ by Assumption 6, since each expectation term is $O(h_n^{\bar{s}})$. Hence, the component-wise variance of $\Gamma_{d,g,p}(h_n)$ converges to zero, which yields the first conclusion.

Limiting expectation computation We show the limit of $\bar{\Gamma}_{d,g,p}(h_n)$ for $h_n \to 0$ by the following decomposition

$$\bar{\Gamma}_{d,g,p}(h_n) = \sum_{\ell_i : s_{\ell_i}=\bar{s}} \int_{\mathcal{R}_{\ell_i}} \int_{N^{\bar{s}}} K(\|\boldsymbol{u}\|) r_p(\|\boldsymbol{u}\|) r_p(\|\boldsymbol{u}\|)^T f(\boldsymbol{u}h_n, \boldsymbol{x}_{R_{\ell_i}})\, d\boldsymbol{u}\, d\boldsymbol{x}_{R_{\ell_i}} + \frac{1}{nh_n^{\bar{s}}} I_{ih_n} + I(s_{\ell_i} > \bar{s})$$

with

$$I(s_{\ell_i} > \bar{s}) = \sum_{\ell_i : s_{\ell_i} > \bar{s}} h_n^{s_{\ell_i}-\bar{s}} \int_{\mathcal{R}_{\ell_i}} \int_{N^{s_{\ell_i}}} K(\|\boldsymbol{u}\|) r_p(\|\boldsymbol{u}\|) r_p(\|\boldsymbol{u}\|)^T f(\boldsymbol{u}h_n, \boldsymbol{x}_{R_{\ell_i}})\, d\boldsymbol{u}\, d\boldsymbol{x}_{R_{\ell_i}}$$

Both $I(s_{\ell_i} > \bar{s})$ and the overlap terms are $O(h_n)$ (I_{ih_n} are $O(h_n^{\bar{s}+1})$, as shown in Theorem

1). Moreover, by Assumption 4.c and the Dominated Convergence theorem we have

$$\sum_{\ell_i : s_{\ell_i} = \bar{s}} \int_{\mathcal{R}_{\ell_i}} \int_{N^{\bar{s}}} K(\|\boldsymbol{u}\|) r_p(\|\boldsymbol{u}\|) r_p(\|\boldsymbol{u}\|)^T f(\boldsymbol{u} h_n, \boldsymbol{x}_{R_{\ell_i}}) \, d\boldsymbol{u} \, d\boldsymbol{x}_{R_{\ell_i}} = f_{d,g,d',g'}(0) \Gamma_p^{\bar{s}} + o(1)$$

Hence, $\bar{\Gamma}_{d,g,p}(h_n) = f_{d,g,d',g'}(0) \cdot \Gamma_p^{\bar{s}} + o(1)$. The conclusions for $\Gamma_{d',g',p}(h_n)$ follows by analogous arguments. □

Lemma S.3.2 (Convergence of $t_{d,g,p}(h_n)$ and $t_{d',g',p}(h_n)$)**.** *Suppose Assumptions 1–6, S.3.1.b and S.3.3 hold. If* $nh_n^{\bar{s}} \to \infty$ *and* $h_n < \kappa$ *then*

$$t_{d,g,p}(h_n) = \bar{t}_{d,g,p}(h_n) + o_p(1), \quad t_{d',g',p}(h_n) = \bar{t}_{d',g',p}(h_n) + o_p(1)$$

where $\bar{t}_{d,g,p}(h_n)$ *and* $\bar{t}_{d',g',p}(h_n)$ *are bounded.*

Moreover, if $h_n \to 0$

$$\bar{t}_{d,g,p}(h_n) = \theta_{p,0}^{\bar{s}} \int\limits_{\bar{\mathcal{X}}_{is_i}(d,g \,|\, d',g')} m_{d,g}(x_i, \boldsymbol{x}_{\mathcal{S}_i}) f(x_i, \boldsymbol{x}_{\mathcal{S}_i}) + o(1), \qquad \bar{t}_{d',g',p}(h_n) = \theta_{p,0}^{\bar{s}} \int\limits_{\bar{\mathcal{X}}_{is_i}(d,g \,|\, d',g')} m_{d',g'}(x_i, \boldsymbol{x}_{\mathcal{S}_i}) f(x_i, \boldsymbol{x}_{\mathcal{S}_i}) + o(1).$$

Proof. Since the procedure is analogous to Lemma S.3.1 we only sketch the proof.

We first compute the limiting expectation of $t_{d,g,p}(h_n)$:

$$\begin{aligned}\mathbb{E}[t_{d,g,p}(h_n)] =& \sum_{\ell_i} h_n^{s_{\ell_i} - \bar{s}} \int_{\mathcal{R}_{\ell_i}} \int_{N^{s_{\ell_i}}} K(\|\boldsymbol{u}\|) r_p(\|\boldsymbol{u}\|) m_{d,g}(h_n \boldsymbol{u}, \boldsymbol{x}_{R_{\ell_i}}) f(h_n \boldsymbol{u}, \boldsymbol{x}_{R_{\ell_i}}) \, d\boldsymbol{u} \, d\boldsymbol{x}_{R_{\ell_i}} + \frac{1}{h_n^{\bar{s}}} I_{ih_n} \\ =& \theta_{p,0}^{\bar{s}} \int_{\bar{\mathcal{X}}_{is_i}(d,g \,|\, d',g')} m_{d,g}(x_i, \boldsymbol{x}_{\mathcal{S}_i}) f(x_i, \boldsymbol{x}_{\mathcal{S}_i}) + o(1)\end{aligned}$$

by Assumption 4.b, 4.c and S.3.3 and the Dominated Convergence Theorem. Similarly, one obtains the limiting expectation for $t_{d',g',p}(h_n)$.

Convergence to zero of the component-wise variance of $t_{d,g,p}(h_n)$ and $t_{d',g',p}(h_n)$ can also be shown similarly to Lemma S.3.1 using boundedness of the conditional variance (Assumption S.3.1.b). □

Lemma S.3.3 (Convergence of $\theta_{d,g,p,q}(h_n)$ and $\theta_{d',g',p,q}(h_n)$)**.** *Suppose Assumptions 1–3, 4.a, 4.c, 5–6 and S.3.3 hold. If* $nh_n^{\bar{s}} \to \infty$ *and* $h_n < \kappa$ *then*

$$\theta_{d,g,p,q}(h_n) = \bar{\theta}_{d,g,p,q}(h_n) + o_p(1), \quad \theta_{d',g',p,q}(h_n) = \bar{\theta}_{d',g',p,q}(h_n) + o_p(1)$$

. where $\bar{\theta}_{d,g,p,q}(h_n)$ *and* $\bar{\theta}_{d',g',p,q}(h_n)$ *are bounded and bounded away from zero.*

Moreover, if $h_n \to 0$

$$\bar{\theta}_{d,g,p,q}(h_n) = f_{d,g,d',g'}(0)\theta^{\bar{s}}_{p,q} + o(1), \qquad \bar{\theta}_{d',g',p,q}(h_n) = f_{d,g,d',g'}(0)\theta^{\bar{s}}_{p,q} + o(1).$$

Proof. Since the procedure is again analogous to Lemma S.3.1 we only sketch the proof. We first compute the limiting expectation of $\theta_{d,g,p,q}(h_n)$ by a similar decomposition as in Lemma S.3.1:

$$\bar{\theta}_{d,g,p,q}(h_n) = \sum_{\ell_i : s_{\ell_i} = \bar{s}} \int_{\mathcal{R}_{\ell_i}} \int_{N^{\bar{s}}} K(\|\boldsymbol{u}\|) r_p(\|\boldsymbol{u}\|) \|\boldsymbol{u}\|^q f(\boldsymbol{u}h_n, \boldsymbol{x}_{R_{\ell_i}})\, d\boldsymbol{u}\, d\boldsymbol{x}_{R_{\ell_i}} + \frac{1}{nh_n^{\bar{s}}} I_{ih_n} + I(s_{\ell_i} > \bar{s})$$

where $I(s_{\ell_i} > \bar{s})$ collects the sum of the integral terms over the pieces $\ell_i : s_{\ell_i} > \bar{s}$, and I_{ih_n} contains the overlap terms. Hence, since $I(s_{\ell_i} > \bar{s})$ and I_{ih_n} are $O(h_n)$, Assumption 4.c and the Dominated Convergence theorem yield

$$\sum_{\ell_i : s_{\ell_i} = \bar{s}} \int_{\mathcal{R}_{\ell_i}} \int_{N^{\bar{s}}} K(\|\boldsymbol{u}\|) r_p(\|\boldsymbol{u}\|) \|\boldsymbol{u}\|^q f(\boldsymbol{u}h_n, \boldsymbol{x}_{R_{\ell_i}})\, d\boldsymbol{u}\, d\boldsymbol{x}_{R_{\ell_i}} = f_{d,g,d',g'}(0)\theta^{\bar{s}}_{p,q} + o(1)$$

Hence, $\bar{\theta}_{d,g,p,q}(h_n) = f_{d,g,d',g'}(0)\theta^{\bar{s}}_{p,q} + o(1)$. Similarly, one obtains the limiting expectation of $\theta_{d',g',p,q}(h_n)$. Convergence to zero of the component-wise variance of $\theta_{d,g,p,q}(h_n)$ and $\theta_{d,g',p,q}(h_n)$ is shown analogously to Lemma S.3.1. □

Lemma S.3.4. *Suppose Assumptions 1–3, 4.a, 4.c, 5–6, S.3.2, and S.3.3 hold. If $nh_n^{\bar{s}} \to \infty$ and $h_n < \kappa$, then for each $\bullet \in \{(d,g),(d',g')\}$,*

$$\frac{1}{nh_n^{\bar{s}}} \sum_{i=1}^{n} \sum_{j \in \boldsymbol{N}_i} W^{\bullet}_{ij}(h_n) \; = \; \bar{\boldsymbol{D}}^{\bullet}(h_n) + \bar{\boldsymbol{N}}^{\bullet}(h_n) + o_p(1).$$

where $\bar{\boldsymbol{D}}^{\bullet}(h_n)$ is bounded and bounded away from zero and $\bar{\boldsymbol{N}}^{\bullet}(h_n)$ is bounded. Moreover, if $h_n \to 0$,

$$\bar{\boldsymbol{D}}^{\bullet}(h_n) = f_{d,g,d',g'}(0) \int_{N^{\bar{s}}} K(\|\boldsymbol{u}\|)^2\, d\boldsymbol{u} + o(1), \qquad \bar{\boldsymbol{N}}^{\bullet}(h_n) = o(1),$$

and for the cross-side case $\bullet = (d,g;d',g')$,

$$\bar{\boldsymbol{D}}^{d,g;d',g'}(h_n) = 0, \qquad \bar{\boldsymbol{N}}^{d,g;d',g'}(h_n) = o(1).$$

Proof. **Expectation calculation.** We start with $\boldsymbol{W}^{d,g}(h_n)$.

$$\frac{1}{nh_n^{\bar{s}}}\sum_i \mathbb{E}\left[\sum_{j\in \boldsymbol{N}_i} W_{ij}^{d,g}(h_n)\right] = \underbrace{\frac{1}{nh_n^{\bar{s}}}\sum_i \mathbb{E}\left[I_{i,d,g}K\left(\frac{\tilde{X}_i}{h_n}\right)^2\right]}_{\bar{\boldsymbol{D}}^{d,g}(h_n)} + \underbrace{\frac{1}{nh_n^{\bar{s}}}\sum_i \sum_{j\in \boldsymbol{N}_i\setminus\{i\}} \mathbb{E}\left[I_{i,d,g}I_{j,d,g}K\left(\frac{\tilde{X}_i}{h_n}\right)K\left(\frac{\tilde{X}_j}{h_n}\right)\right]}_{\bar{\boldsymbol{N}}^{d,g}(h_n)} \tag{S.3.5}$$

where $\bar{\boldsymbol{D}}^{d,g}(h_n)$ is bounded away from zero and bounded by Assumption 4.c and S.3.3, and $\bar{\boldsymbol{N}}^{d,g}(h_n)$ is bounded by Assumption 6 and S.3.3.

Variance bound. We now show concentration of variance of $\frac{1}{nh_n^{\bar{s}}}\sum_i \sum_{j\in \boldsymbol{N}_i} W_{ij}^{d,g}(h_n)$. Expanding the second moment:

$$\begin{aligned}\mathbb{E}\left[\left(\frac{1}{nh_n^{\bar{s}}}\sum_i \sum_{j\in \boldsymbol{N}_i} W_{ij}^{d,g}(h_n)\right)^2\right] &= \frac{1}{n^2h_n^{2\bar{s}}}\sum_{i\neq j}\sum_{k\in \boldsymbol{N}_i}\sum_{l\in \boldsymbol{N}_j}\mathbb{E}\left[K\left(\frac{\tilde{X}_i}{h_n}\right)K\left(\frac{\tilde{X}_j}{h_n}\right)K\left(\frac{\tilde{X}_k}{h_n}\right)K\left(\frac{\tilde{X}_l}{h_n}\right)\right]\\ &+ \frac{1}{n^2h_n^{2\bar{s}}}\sum_i \sum_{j\in \boldsymbol{N}_i}\mathbb{E}\left[K\left(\frac{\tilde{X}_i}{h_n}\right)^2K\left(\frac{\tilde{X}_j}{h_n}\right)^2\right]\\ &+ \frac{1}{n^2h_n^{2\bar{s}}}\sum_i \sum_{j\in \boldsymbol{N}_i}\sum_{k\in \boldsymbol{N}_i\setminus\{j\}}\mathbb{E}\left[K\left(\frac{\tilde{X}_i}{h_n}\right)^2K\left(\frac{\tilde{X}_j}{h_n}\right)K\left(\frac{\tilde{X}_k}{h_n}\right)\right]\end{aligned} \tag{S.3.6}$$

The last two terms in (S.3.6) can be bounded by

$$\frac{1}{n^2h_n^{2\bar{s}}}\max_i \mathbb{E}\left[K\left(\frac{\tilde{X}_i}{h_n}\right)^4\right]\sum_i \left(|\boldsymbol{N}_{i,n}| + |\boldsymbol{N}_{i,n}|^2\right),$$

which is $O((nh_n^{\bar{s}})^{-1})$ by Assumption 6 and since $\mathbb{E}\left[K\left(\frac{\tilde{X}_i}{h_n}\right)^4\right] = O(h_n^{\bar{s}})$.

The first term is bounded by

$$\mathbb{E}\Big[\Big(\frac{1}{nh_n^{\bar{s}}}\sum_i\sum_{j\in\boldsymbol{N}_i}W_{ij}^{d,g}(h_n)\Big)\Big]^2+\frac{1}{n^2h_n^{2\bar{s}}}\sum_i\sum_{j\in\boldsymbol{N}_i}\sum_{k\in\boldsymbol{N}_i\cup\boldsymbol{N}_j}\sum_{l\in\boldsymbol{N}_i\cup\boldsymbol{N}_j\cup\boldsymbol{N}_k}\mathbb{E}\left[K\left(\frac{\tilde{X}_i}{h_n}\right)K\left(\frac{\tilde{X}_j}{h_n}\right)K\left(\frac{\tilde{X}_k}{h_n}\right)K\left(\frac{\tilde{X}_l}{h_n}\right)\right]$$
$$-\mathbb{E}\left[K\left(\frac{\tilde{X}_i}{h_n}\right)K\left(\frac{\tilde{X}_k}{h_n}\right)\right]\mathbb{E}\left[K\left(\frac{\tilde{X}_j}{h_n}\right)K\left(\frac{\tilde{X}_l}{h_n}\right)\right] \tag{S.3.7}$$

By the arithmetic-geometric mean inequality, (S.3.7) is bounded by

$$\mathbb{E}\Big[\Big(\frac{1}{nh_n^{\bar{s}}}\sum_i\sum_{j\in\boldsymbol{N}_i}W_{ij}^{d,g}(h_n)\Big)\Big]^2+\frac{1}{n^2h_n^{2\bar{s}}}\max_i\mathbb{E}\left[K\left(\frac{\tilde{X}_i}{h_n}\right)^4\right]\sum_i\sum_{j\in\boldsymbol{N}_i}\sum_{k\in\boldsymbol{N}_i\cup\boldsymbol{N}_j}|\boldsymbol{N}_i\cup\boldsymbol{N}_j|+|\boldsymbol{N}_k|$$
$$\leq\mathbb{E}\Big[\Big(\frac{1}{nh_n^{\bar{s}}}\sum_i\sum_{j\in\boldsymbol{N}_i}W_{ij}^{d,g}(h_n)\Big)\Big]^2+\frac{1}{nh_n^{2\bar{s}}}\max_i\mathbb{E}\left[K\left(\frac{\tilde{X}_i}{h_n}\right)^4\right]\frac{\sum_i|\boldsymbol{N}_i|^3+3\sum_{i,j}(\boldsymbol{W}^3)_{ij}}{n}$$

where the second summand is $O((nh_n^{\bar{s}})^{-1})$ by Assumption 6. Hence, because

$$\mathbb{V}\Big[\frac{1}{nh_n^{\bar{s}}}\sum_i\sum_{j\in\boldsymbol{N}_i}W_{ij}^{d,g}(h_n)\Big]=\mathbb{E}\Big[\Big(\frac{1}{nh_n}\sum_i\sum_{j\in\boldsymbol{N}_i}W_{ij}^{d,g}(h_n)\Big)^2\Big]-\mathbb{E}\Big[\frac{1}{nh_n}\sum_i\sum_{j\in\boldsymbol{N}_i}W_{ij}^{d,g}(h_n)\Big]^2$$

we obtain

$$\mathbb{V}\Big[\frac{1}{nh_n^{\bar{s}}}\sum_i\sum_{j\in\boldsymbol{N}_i}W_{ij}^{d,g}(h_n)\Big]\leq\frac{1}{n^2h_n^{2\bar{s}}}\max_i\mathbb{E}\left[K\left(\frac{\tilde{X}_i}{h_n}\right)^4\right]\Big(\sum_i(|\boldsymbol{N}_{i,n}|+|\boldsymbol{N}_{i,n}|^2)+\sum_i|\boldsymbol{N}_{i,n}|^3+3\sum_{i,j}(\boldsymbol{W}_n^3)_{ij}\Big)$$
$$=O((nh_n^{\bar{s}})^{-1})\to 0$$

Diagonal limiting contribution. We now establish limit of (S.3.5) as $h_n\to 0$. The first summand limit in (S.3.5) is established using analgous arguments as in Lemma S.3.1, yielding

$$\bar{\boldsymbol{D}}^{d,g}(h_n)=f_{d,g,d',g'}(0)\int_{N^{\bar{s}}}K(\|\boldsymbol{u}\|)^2\,d\boldsymbol{u}+o(1).$$

Average degree limiting contribution. Consider

$$\mathbb{E}\left[I_{i,d,g}I_{j,d,g}K\left(\frac{\tilde{X}_i}{h_n}\right)K\left(\frac{\tilde{X}_j}{h_n}\right)\right],\qquad i\neq j.$$

The domain of integration of this expectation is the intersection of the two neighborhoods

$$\mathcal{B}_{h_n}^{d,g}(\bar{\mathcal{X}}_{i\mathcal{S}_i}(d,g\,|\,d',g')) \cap \mathcal{B}_{h_n}^{d,g}(\mathcal{X}_{j\mathcal{S}_j}(d,g|d',g')) = \bigcup_{\ell_i,\ell_j} \left(\mathcal{B}_{h_n}^{d,g}(\ell_i) \cap \mathcal{B}_{h_n}^{d,g}(\ell_j)\right).$$

Moreover, the functions $\tilde{X}_i = \tilde{X}_i(X_i, \boldsymbol{X}_{\mathcal{S}_i})$ and $\tilde{X}_j = \tilde{X}_j(X_j, \boldsymbol{X}_{\mathcal{S}_j})$ may have common arguments if the index sets $\tilde{\mathcal{S}}_i = (\mathcal{S}_i \cup \{i\})$ and $\tilde{\mathcal{S}}_j = (\mathcal{S}_j \cup \{j\})$ overlap. Let $\boldsymbol{X}_{\tilde{\mathcal{S}}_i \cup \tilde{\mathcal{S}}_j}$ be the random vector collecting the scores of units in $\tilde{\mathcal{S}}_i \cup \tilde{\mathcal{S}}_j$.

We can bound

$$\mathbb{E}\left[\left|I_{i,d,g}I_{j,d,g}K\left(\frac{\tilde{X}_i}{h_n}\right)K\left(\frac{\tilde{X}_j}{h_n}\right)\right|\right] \leq \sum_{\ell_i,\ell_j}\int_{\mathcal{B}_{h_n}^{d,g}(\ell_i)\cap\mathcal{B}_{h_n}^{d,g}(\ell_j)} \left|K\left(\tfrac{\tilde{X}_i}{h_n}\right)K\left(\tfrac{\tilde{X}_j}{h_n}\right)\right| f(\boldsymbol{x}_{\tilde{\mathcal{S}}_i\cup\tilde{\mathcal{S}}_j})\, d\boldsymbol{x}_{\tilde{\mathcal{S}}_i\cup\tilde{\mathcal{S}}_j}.$$

where $f(\boldsymbol{x}_{\tilde{\mathcal{S}}_i\cup\tilde{\mathcal{S}}_j})$ is the joint density of $\boldsymbol{X}_{\tilde{\mathcal{S}}_i\cup\tilde{\mathcal{S}}_j}$. Thus the intersection domain $\mathcal{B}_{h_n}^{d,g}(\ell_i) \cap \mathcal{B}_{h_n}^{d,g}(\ell_j)$ is contained in a hyper-rectangle of the form

$$\prod_{z\in F_{\ell_i}\cup F_{\ell_j}} I_z(\ell_i) \;\times\; \prod_{z\in R_{\ell_i}\cup R_{\ell_j}} I_z(\ell_i,h_n),$$

where the interval $I_z(\ell_i) = O(1)$ and the interval $I_z(\ell_i, h_n) = O(h_n)$.

The total volume of this rectangular set is $O(h_n^{|F_{\ell_i}\cup F_{\ell_j}|})$. Therefore, we obtain the uniform bound

$$\mathbb{E}\left[\left|I_{i,d,g}I_{j,d,g}K\left(\frac{\tilde{X}_i}{h_n}\right)K\left(\frac{\tilde{X}_j}{h_n}\right)\right|\right] \leq C\sum_{\ell_i,\ell_j} h_n^{|F_{\ell_i}\cup F_{\ell_j}|} = O(h_n^{\bar{s}+1}).$$

since $|F_{\ell_i} \cup F_{\ell_j}| \geq \bar{s}+1$ by Assumption S.3.2. Hence, the second term in (S.3.5) is

$$\bar{\boldsymbol{N}}^{d,g}(h_n) = O(h_n),$$

using the fact that $\frac{1}{n}\sum_i |\boldsymbol{N}_i| = O(1)$ by Assumption 6.

The proof for the convergence of $\frac{1}{nh_n^{\bar{s}}}\sum_i\sum_{j\in\boldsymbol{N}_i} W_{ij}^{d',g'}(h_n)$ and $\frac{1}{nh_n^{\bar{s}}}\sum_i\sum_{j\in\boldsymbol{N}_i} W_{ij}^{d,g,d',g'}(h_n)$ can be shown analogously. □

Lemma S.3.5 (Variance of $t^*_{d,g,d',g'}(h_n)$)**.** *Suppose Assumptions 1–6, S.3.1.b, S.3.2, and S.3.3 hold. If $h_n < \kappa$,*

$$nh_n^{\bar{s}}\mathbb{V}[t^*_{d,g,d',g'}(h_n)] = \bar{\Psi}_{d,g,p}(h_n) + \bar{\Psi}_{d',g',p}(h_n) - \bar{\Psi}_{d,g,d',g',p}(h_n),$$

is bounded and bounded away from zero. Moreover, if $nh_n^{\bar{s}} \to \infty$ *and* $h_n \to 0$

$$\bar{\Psi}_{d,g,p}(h_n) + \bar{\Psi}_{d',g',p}(h_n) - \bar{\Psi}_{d,g,d',g',p}(h_n) = (\bar{\omega}_{d,g}(0) + \bar{\omega}_{d',g'}(0))\Psi_p^{\bar{s}} + o(1).$$

where for $\bullet \in \{(d,g),(d',g')\}$ *where*

$$\bar{\omega}_\bullet(0) = \int_{\bar{\mathcal{X}}_{is_i}(d,g\,|\,d',g')} \Big(\sigma_\bullet(x_i,\boldsymbol{x}_{\mathcal{S}_i}) + \Big(m_\bullet(x_i,\boldsymbol{x}_{\mathcal{S}_i}) - \frac{\int_{\bar{\mathcal{X}}_{is_i}(d,g\,|\,d',g')} m_\bullet(x_i,\boldsymbol{x}_{\mathcal{S}_i}) f(x_i,\boldsymbol{x}_{\mathcal{S}_i})}{\int_{\bar{\mathcal{X}}_{is_i}(d,g\,|\,d',g')} f(x_i,\boldsymbol{x}_{\mathcal{S}_i})}\Big)^2\Big) f(x_i,\boldsymbol{x}_{\mathcal{S}_i}) d(x_i,\boldsymbol{x}_{\mathcal{S}_i})$$

Proof. We start from

$$\mathbb{V}[t^*_{d,g,d',g'}(h_n)] = \mathbb{V}[t^*_{d,g,p}(h_n)] + \mathbb{V}[t^*_{d',g',p}(h_n)] - \mathbb{C}[t^*_{d,g,p}(h_n), t^*_{d',g',p}(h_n)].$$

We establish the result for $\mathbb{V}[t^*_{d,g,p}(h_n)]$; the arguments for $\mathbb{V}[t^*_{d',g',p}(h_n)]$ and $\mathbb{C}[t^*_{d,g,p}(h_n), t^*_{d',g',p}(h_n))$ are analogous.

Decomposition of the variance Expanding the variance yields

$$\begin{aligned} nh_n^{\bar{s}}\mathbb{V}[t^*_{d,g,p}(h_n)] = &\underbrace{\frac{1}{nh_n^{\bar{s}}}\sum_i \mathbb{E}\big[I_{i,d,g} K\left(\frac{\tilde{X}_i}{h_n}\right)^2 r_p\left(\frac{\tilde{X}_i}{h_n}\right) r_p\left(\frac{\tilde{X}_i}{h_n}\right)^T \nu^2_{i,d,g}\big]}_{T_1} \\ &+ \underbrace{\frac{1}{nh_n^{\bar{s}}}\sum_i \sum_{j\in \boldsymbol{N}_i\setminus\{i\}} \mathbb{E}\big[I_{i,d,g} I_{j,d,g}\, K\left(\frac{\tilde{X}_i}{h_n}\right) K\left(\frac{\tilde{X}_j}{h_n}\right) r_p\left(\frac{\tilde{X}_i}{h_n}\right) r_p(\frac{\tilde{X}_j}{h_n})^T \nu_{i,d,g}\nu_{j,d,'g'}\big]}_{T_2}. \end{aligned} \tag{S.3.8}$$

Both terms are bounded and bounded away from zero under Assumptions 4.c and S.3.3. Moreover, by Assumption S.3.1.b $|T_2| \le C\,\bar{\boldsymbol{N}}^{d,g}(h_n)$ for some constant $C > 0$, and $\bar{\boldsymbol{N}}^{d,g}(h_n) = o(1)$ by Lemma S.3.4.

Limit of T_1**.** Expanding $\nu^2_{i,d,g}$ gives

$$\begin{aligned} T_1 =& h_n^{-\bar{s}} \int_{\mathcal{B}^{d,g}_{h_n}(\bar{\mathcal{X}}_{is_i}(d,g\,|\,d',g'))} K\left(\frac{\tilde{X}_i(x_i,\boldsymbol{x}_{\mathcal{S}_i})}{h_n}\right)^2 r_p\left(\frac{\tilde{X}_i(x_i,\boldsymbol{x}_{\mathcal{S}_i})}{h_n}\right) r_p\left(\frac{\tilde{X}_i(x_i,\boldsymbol{x}_{\mathcal{S}_i})}{h_n}\right)^T \big[\sigma_{d,g}(x_i,\boldsymbol{x}_{\mathcal{S}_i}) + m_{d,g}(x_i,\boldsymbol{x}_{\mathcal{S}_i})^2 \\ &+ \quad (r_p(\tilde{X}(x_i,\boldsymbol{x}_{\mathcal{S}_i}))^T\beta_{d,g,p}(h_n))^2 - 2\, m_{d,g}(x_i,\boldsymbol{x}_{\mathcal{S}_i})\, r_p(\tilde{X}(x_i,\boldsymbol{x}_{\mathcal{S}_i}))^T\beta_{d,g,p}(h_n)\big]\, f(x_i,\boldsymbol{x}_{\mathcal{S}_i})\, d(x_i,\boldsymbol{x}_{\mathcal{S}_i}). \end{aligned}$$

Using the boundary neighborhood decomposition and change of variable $\boldsymbol{u} = \boldsymbol{x}_{F_{\ell_i}}/h_n$, we obtain

$$T_1 = \sum_{h_i} h_n^{s_{\ell_i}-\bar{s}} \int_{\mathcal{R}_{\ell_i}} \int_{N^{s_{\ell_i}}} K(\|\boldsymbol{u}\|)^2 r_p(\|\boldsymbol{u}\|) r_p(\|\boldsymbol{u}\|)^T \big[m_{d,g}(\boldsymbol{u}h_n, \boldsymbol{x}_{R_{\ell_i}})^2 + \sigma_{d,g}(\boldsymbol{u}h_n, \boldsymbol{x}_{R_{\ell_i}})$$
$$+ (r_p(\|\boldsymbol{u}\|h_n)^T \beta_{d,g,p}(h_n))^2 - 2\, m_{d,g}(\boldsymbol{u}h_n, \boldsymbol{x}_{R_{\ell_i}})\, r_p(\|\boldsymbol{u}\|h_n)^T \beta_{d,g,p}(h_n) \big] f(\boldsymbol{u}h_n, \boldsymbol{x}_{R_{\ell_i}})\, d\boldsymbol{u}\, d\boldsymbol{x}_{R_{\ell_i}}.$$

As $h_n \to 0$

$$r_p(\|\boldsymbol{u}\|h_n)\beta_{d,g,p}(h_n) \;\to\; \frac{\int_{\bar{\mathcal{X}}_{is_i}(d,g\,|\,d',g')} m_{d,g}(x_i, \boldsymbol{x}_{\mathcal{S}_i}) f(x_i, \boldsymbol{x}_{\mathcal{S}_i})}{\int_{\bar{\mathcal{X}}_{is_i}(d,g\,|\,d',g')} f(x_i, \boldsymbol{x}_{\mathcal{S}_i})},$$

since $r_p(\|\boldsymbol{u}\|h_n)^T \beta_{d,g,p}(h_n) = r_p(\|\boldsymbol{u}\|)\bar{\Gamma}_{d,g}(h_n)\bar{t}_{d,g,p}(h_n)$ and

$$\bar{\Gamma}_{d,g}(h_n)\bar{t}_{d,g,p}(h_n) = (\Gamma_p^{\bar{s}})^{-1}\theta_{p,0}^{\bar{s}} \frac{\int_{\bar{\mathcal{X}}_{is_i}(d,g\,|\,d',g')} m_{d,g}(x_i, \boldsymbol{x}_{\mathcal{S}_i}) f(x_i, \boldsymbol{x}_{\mathcal{S}_i})}{\int_{\bar{\mathcal{X}}_{is_i}(d,g\,|\,d',g')} f(x_i, \boldsymbol{x}_{\mathcal{S}_i})} + o(1)$$

by Lemma S.3.1 and S.3.2, and $(\Gamma_p^{\bar{s}})^{-1}\theta_{p,0}^{\bar{s}} = e_1$, where e_1 is the p-dimensional unit vector with first entry equal to 1 and all others equal to 0.
Then by continuity of $m_{d,g}(\cdot)$, $f(\cdot)$, $\sigma_{d,g}(\cdot)$, (Assumptions 4.c-4.b and S.3.1.b), and by the Dominated Convergence Theorem, $T_1 = \bar{\omega}_{d,g}(0)\Psi_p^{\bar{s}} + o(1)$.

By the same arguments we obtain

$$nh_n^{\bar{s}}\mathbb{V}[t^*_{d',g',p}(h_n)] = \bar{\omega}_{d',g'}(0)\Psi_p^{\bar{s}} + o(1), \qquad nh_n^{\bar{s}}\mathbb{C}[t^*_{d,g,p}(h_n), t^*_{d',g',p}(h_n)] = o(1).$$

Combining the above yields the conclusion. □

Theorem S.3.1. *Suppose Assumptions 1–6, S.3.1, S.3.2, and S.3.3 hold. If* $nh_n^{\bar{s}} \to \infty$, $h_n \to 0$, *and* $h_n = O\big(n^{-1/(2p+2+\bar{s})}\big)$, *then*

$$\sqrt{nh_n^{\bar{s}}}\, \frac{(\hat{\tau}_{d,g,d',g',p}(h_n) - \tau_{d,g|d',g'}\big(\bar{\mathcal{X}}_{is_i}(d,g\,|\,d',g')\big)) - h_n^{p+1}B_{d,g,d',g',p,p+1}(h_n)}{\sqrt{V_{d,g,d',g',p}(h_n)}} \xrightarrow{d} \mathcal{N}(0,1),$$

where $B_{d,g,d',g',p,p+1}(h_n) = B_{d,g,d',g',p,p+1} + o(1)$ *and* $V_{d,g,d',g'p}(h_n) = V_{d,g,d',g',p} + o(1)$,

$$B_{d,g,d',g',p,p+1} = \Big(\frac{\mu_{d,g}^{p+1}(0) - \mu_{d',g'}^{p+1}(0)}{(p+1)!}\Big) e_1^\top (\Gamma_p^{\bar{s}})^{-1}\theta_{p,p+1}^{\bar{s}}, \quad V_{d,g,d',g',p} = \frac{\bar{\omega}_{d,g}(0) + \bar{\omega}_{d',g'}(0)}{f_{d,g,d',g'}(0)^2} e_1^\top (\Gamma_p^{\bar{s}})^{-1}\Psi_p^{\bar{s}}(\Gamma_p^{\bar{s}})^{-1}e_1.$$

Proof of Theorem S.3.1. Define

$$Z_{i,d,g,p}(h_n) = e_1^T \bar{\Gamma}^{-1}_{d,g,p}(h_n) \, \tfrac{1}{nh_n^{\bar{s}}} \, I_{i,d,g} K\left(\frac{\tilde{X}_i}{h_n}\right) r_p\left(\frac{\tilde{X}_i}{h_n}\right) \nu_{i,d,g},$$
$$Z_{i,d',g',p}(h_n) = e_1^T \bar{\Gamma}^{-1}_{d',g',p}(h_n) \, \tfrac{1}{nh_n^{\bar{s}}} \, I_{i,d',g'} K\left(\frac{\tilde{X}_i}{h_n}\right) r_p\left(\frac{\tilde{X}_i}{h_n}\right) \nu_{i,d',g'},$$

and set $Z_{i,d,g,d',g',p}(h_n) = Z_{i,d,g,p}(h_n) - Z_{i,d',g',p}(h_n)$. Then

$$\sum_i Z_{i,d,g,d',g',p}(h_n) = e_1^T \bar{\Gamma}^{-1}_{d,gp,}(h_n) t^*_{d,g,p}(h_n) - e_1^T \bar{\Gamma}^{-1}_{d',g'p,}(h_n) t^*_{d',g',p}(h_n)$$

Variance. Denote $nh_n^{\bar{s}} \, \mathbb{V}\Big[\sum_i Z_{i,d,g,d',g',p}(h_n)\Big] = V_{d,g,d',g',p}(h_n)$. By Lemmas S.3.1 and S.3.5,

$$V_{d,g,d',g',p}(h_n) = \tfrac{\bar{\omega}_{d,g}(0)+\bar{\omega}_{d',g'}(0)}{f_{d,g,d',g'}(0)} \, (\Gamma_p^{\bar{s}})^{-1} \Psi_p^{\bar{s}} (\Gamma_p^{\bar{s}})^{-1} + o(1).$$

CLT via dependency graph. By Assumption 5, the collection $\{Z_{i,d,g,d',g',p}(h_n)\}_i$ admits dependency graph $\boldsymbol{W}_n$. Let $\tilde{\sigma}_n^2 = V_{d,g,d',g',p}(h_n)/nh_n^{\bar{s}}$, the variance of $Z_{i,d,g,d',g',p}(h_n)$, and set $\xi_n = \sum_i Z_{i,d,g,d',g',p}(h_n)/\tilde{\sigma}_n$. Applying the Wasserstein bound of Leung (2020, Theorem A.4),

$$\Delta(\xi_n, \mathcal{N}(0,1)) \leq \tfrac{1}{\tilde{\sigma}_n^3} \max_i \mathbb{E}[|Z_{i,d,g,d',g',p}(h_n)|^3] \sum_i |\boldsymbol{N}_i|^2 + \tfrac{1}{\tilde{\sigma}_n^2} \Big(\tfrac{4}{\pi} \max_i \mathbb{E}[Z_{i,d,g,d',g',p}(h_n)^4]\Big)^{1/2} \Big(4 \sum_i |\boldsymbol{N}_i|^3 + 3 \sum_{i,j} (\boldsymbol{W}^3)_{ij}\Big)^{1/2}. \tag{S.3.9}$$

Moment bounds. Using the c_r-inequality,

$$\mathbb{E}[|Z_i|^3] \leq 4(\mathbb{E}[|Z_{i,d,g,p}(h_n)|^3] + \mathbb{E}[|Z_{i,d',g',p}(h_n)|^3]) = O(n^{-3} h_n^{-2\bar{s}}),$$

and similarly,

$$\mathbb{E}[Z_i^4] \leq 8(\mathbb{E}[Z_{i,d,g,p}(h_n)^4] + \mathbb{E}[Z_{i,d',g',p}(h_n)^4]) = O(n^{-4} h_n^{-3\bar{s}}).$$

using boundedness of the third and fourth conditional moment of the outcome (Assumption S.3.1.a), Assumptions 4.b and the fact that the domain of integration has volume proportional to $h_n^{\bar{s}}$, as shown, for example, in Lemma S.3.1.

Rate of convergence. Plugging these bounds into (S.3.9) and using Assumption 6, we obtain

$$\Delta(\xi_n, \mathcal{N}(0,1)) = O((nh_n^{\bar{s}})^{-1/2}) = o(1).$$

Hence $\xi_n \xrightarrow{d} \mathcal{N}(0,1)$.

Conclusion. By Lemma S.3.1, $\sqrt{nh_n^{\bar{s}}} \cdot \frac{\hat{\tau}^*_{d,g,d',g',p}(h_n)}{\sqrt{V_{d,g,d',g',p}(h_n)}} = \xi_n + o_p(1)$, so $\hat{\tau}^*_{d,g,d',g',p}(h_n)$ (rescaled) has the same asymptotic distribution as ξ_n. Moreover, by Lemmas S.3.1 and S.3.3, $h_n^{p+1} B_{d,g,d',g',p,p+1}(h_n) = O(h_n^{p+1})$ and $T_{d,g,d'g'}(h_n) = O(h_n^{p+2})$ since the term $\mathbb{E}\big|\tilde{X}_p(h_n) W_{d,g}(h_n) T_{d,g,p}/n\big| \leq h_n^{p+2} \frac{\sup_{\tilde{x}} |\mu_{d,g}^{(p+2)}(\tilde{x})|}{(p+2)!} \bar{\theta}_{d,g,p,p+2}(h_n)$, and analogously for the term $\mathbb{E}\big|\tilde{X}_p(h_n) W_{d',g'}(h_n) T_{d',g',p}/n\big|$. Then Eq.(S.3.4) and $h_n = O(n^{-1/(2p+2+\bar{s})})$ yield the conclusion. □

Proof of Theorem 3. The result follows from Theorem S.3.1 by setting $p = 1$ and, for notational simplicity, writing $B = B_{d,g,d',g',1,2}$ and $V = V_{d,g,d',g',1}$. □

S.3.4 Variance Estimation

Define

$$\begin{aligned}
\hat{\Psi}_{d,g,p}(h_n) &= \mathcal{M}_{d,g,p}(h_n) \boldsymbol{W} \mathcal{M}_{d,g,p}(h_n)^T/n, \\
\hat{\Psi}_{d',g',p}(h_n) &= \mathcal{M}_{d',g',p}(h_n) \boldsymbol{W} \mathcal{M}_{d',g',p}(h_n)^T/n, \qquad \text{(S.3.10)} \\
\hat{\Psi}_{d,g,d',g',p}(h_n) &= \mathcal{M}_{d,g,p}(h_n) \boldsymbol{W} \mathcal{M}_{d',g',p}(h_n)^T/n,
\end{aligned}$$

where $\boldsymbol{W}$ is the dependency graph and

$$\mathcal{M}_{d,g,p}(h_n)^T = \Big[I_{1,d,g} K\left(\frac{\tilde{X}_1}{h_n}\right) r_p\left(\frac{\tilde{X}_1}{h_n}\right) \hat{u}_{1,d,g} \;\; \cdots \;\; I_{n,d,g} K\left(\frac{\tilde{X}_n}{h_n}\right) r_p\left(\frac{\tilde{X}_n}{h_n}\right) \hat{u}_{n,d,g}\Big],$$

$$\mathcal{M}_{d',g',p}(h_n)^T = \Big[I_{1,d',g'} K\left(\frac{\tilde{X}_1}{h_n}\right) r_p\left(\frac{\tilde{X}_1}{h_n}\right) \hat{u}_{1,d',g'} \;\; \cdots \;\; I_{n,d',g'} K\left(\frac{\tilde{X}_n}{h_n}\right) r_p\left(\frac{\tilde{X}_n}{h_n}\right) \hat{u}_{n,d',g'}\Big],$$

with $\hat{u}_{i,d,g}$ and $\hat{u}_{i,d',g'}$ denoting the regression residuals.

Let

$$\mathcal{V}_{d,g,d',g',p}(h_n) = \frac{V_{d,g,d',g'}(h_n)}{nh_n^{\bar{s}}}$$

where $V_{d,g,d',g',p}(h_n)$ is defined in Theorem S.3.1. $\mathcal{V}_{d,g,d',g',p}(h_n)$ can be seen as the "fixed-bandwidth" asymptotic variance of $\hat{\tau}_{d,g,d',g',p}(h_n)$.

An estimator of $\mathcal{V}_{d,g,d',g',p}(h_n)$ is

$$\hat{\mathcal{V}}_{d,g,d',g',p}(h_n) = \frac{1}{n} e_1^T \left[\hat{V}_{d,g,p}(h_n) + \hat{V}_{d',g',p}(h_n) - 2\,\hat{V}_{d,g,d',g',p}(h_n)\right] e_1, \tag{S.3.11}$$

where

$$\begin{aligned}
\hat{V}_{d,g,p}(h_n) &= \Gamma_{d,g,p}(h_n)^{-1}\,\hat{\Psi}_{d,g}(h_n)\,\Gamma_{d,g,p}(h_n)^{-1},\\
\hat{V}_{d',g',p}(h_n) &= \Gamma_{d',g',p}(h_n)^{-1}\,\hat{\Psi}_{d',g'}(h_n)\,\Gamma_{d',g',p}(h_n)^{-1},\\
\hat{V}_{d,g,d',g',p}(h_n) &= \Gamma_{d,g,p}(h_n)^{-1}\,\hat{\Psi}_{d,g,d',g'}(h_n)\,\Gamma_{d',g',p}(h_n)^{-1}.
\end{aligned}$$

We show that this estimator is consistent for $\mathcal{V}_{d,g,d',g',p}(h_n)$. Convergence of this estimator to h the asymptotic variance $(nh_n^{\bar{s}})^{-1}V_{d,g,d',g',p}$ follows since $V_{d,g,d',g',p}(h_n) = V_{d,g,d',g',p} + o(1)$ for $h_n \to 0$ by Lemma S.3.1 and S.3.5.

Lemma S.3.6. *Suppose Assumptions 1–6, S.3.1, S.3.2, and S.3.3 hold. If $nh_n^{\bar{s}} \to \infty$,*

$$\begin{aligned}
\hat{\Psi}_{d,g,p}(h_n) &= \bar{\Psi}_{d,g,p}(h_n) + o_p(1)\\
\hat{\Psi}_{d',g',p}(h_n) &= \bar{\Psi}_{d',g',p}(h_n) + o_p(1)\\
\hat{\Psi}_{d,g,d',g',p}(h_n) &= \bar{\Psi}_{d,g,d',g',p}(h_n) + o_p(1)
\end{aligned}$$

where $\bar{\Psi}_{d,g,p}(h_n) = \bar{\omega}_{d,g}(0)\Psi_p^{\bar{s}} + o(1)$, $\bar{\Psi}_{d',g',p}(h_n) = \bar{\omega}_{d',g'}(0)\Psi_p^{\bar{s}} + o(1)$, and $\hat{\Psi}_{d,g,d',g',p}(h_n) = o(1)$ if $h_n \to 0$.

Proof. The generic element of $\hat{\Psi}_{d,g,p}(h_n)$ is

$$\frac{1}{nh_n^{\bar{s}}}\sum_i \sum_{j\in \boldsymbol{N}_i} \hat{u}_{i,d,g}\hat{u}_{j,d,g}\, I_{i,d,g}I_{j,d,g}K\left(\frac{\tilde{X}_i}{h_n}\right)K\left(\frac{\tilde{X}_j}{h_n}\right)\left(\frac{\tilde{X}_i}{h_n}\right)^l\left(\frac{\tilde{X}_j}{h_n}\right)^v, \qquad l,v = 0,\dots,p. \tag{S.3.12}$$

We prove the claim for $l, v = 0$. The proof for the other elements is analogous. We have

$$\hat{u}_{i,d,g} = (\beta_{d,g,p}(h_n) - \hat{\beta}_{d,g,p}(h_n))^T r_p(\tilde{X}_i) + \nu_{i,d,g}, \quad i = 1, ..., n$$

Expanding the product $\hat{u}_{i,d,g}\hat{u}_{j,d,g}$, expression (S.3.12) becomes

$$
\begin{aligned}
\text{(S.3.12)} = \frac{1}{nh_n^{\bar{s}}} \sum_i \sum_{j \in \boldsymbol{N}_i} \Big[& \\
& (\beta_{d,g,p}(h_n) - \hat{\beta}_{d,g,p}(h_n))^T r_p(\tilde{X}_i)(\beta_{d,g,p}(h_n) - \hat{\beta}_{d,g,p}(h_n))^T r_p(\tilde{X}_j) && \text{(I)} \\
& + \nu_{j,d,g}(\beta_{d,g,p}(h_n) - \hat{\beta}_{d,g,p}(h_n))^T r_p(\tilde{X}_i) && \text{(II)} \\
& + \nu_{i,d,g}(\beta_{d,g,p}(h_n) - \hat{\beta}_{d,g,p}(h_n))^T r_p(\tilde{X}_j) && \text{(III)} \\
& + \nu_{i,d,g}\nu_{j,d,g}\Big] I_{i,d,g} I_{j,d,g} K\left(\frac{\tilde{X}_i}{h_n}\right) K\left(\frac{\tilde{X}_j}{h_n}\right). && \text{(IV)}
\end{aligned}
$$

Leading term (IV). For (IX), we have $\mathbb{E}[(IX)] = e_1 \mathbb{V}[t^*_{d,g,p}(h_n)]e_1 = e_1^T \bar{\Psi}_{d,g,p}(h_n)e_1$ by Lemma S.3.5. Moreover, using the same bounding arguments as in Lemma S.3.4,

$$
\begin{aligned}
\mathbb{V}\Big[(IX)\Big] &\leq \frac{1}{n^2 h_n^{2\bar{s}}} \max_i \mathbb{E}\left[\nu_{i,d,g}^4 K\left(\frac{\tilde{X}_i}{h_n}\right)^4\right] \Big(\sum_i (|\boldsymbol{N}_{i,n}| + |\boldsymbol{N}_{i,n}|^2) + \sum_i |\boldsymbol{N}_{i,n}|^3 + 3\sum_{i,j} (\boldsymbol{W}_n^3)_{ij}\Big) \\
&= O((nh_n^{\bar{s}})^{-1}) \to 0
\end{aligned}
$$

since $\mathbb{E}\left[\nu_{i,d,g}^4 K\left(\frac{\tilde{X}_i}{h_n}\right)^4\right]$ is bounded by Assumption S.3.1.a, 4.b, 4.c and S.3.3. Hence

$$(IX) = e_1^T \bar{\Psi}_{d,g,p}(h_n)e_1 + o_p(1).$$

where $e_1^T \bar{\Psi}_{d,g,p}(h_n)e_1 = \bar{\omega}_{d,g}(0)e_1^T \Psi_p^{\bar{s}} e_1 + o(1)$ if $h_n \to 0$ by Lemma S.3.5.

Remaining terms (I)-(III) Define

$$M(h_n) = \left[\frac{1}{nh_n^{\bar{s}}} \sum_i \sum_{j \in \boldsymbol{N}_i} r_p\left(\frac{\tilde{X}_i}{h_n}\right) r_p\left(\frac{\tilde{X}_j}{h_n}\right)^T I_{i,d,g} I_{j,d,g} K\left(\frac{\tilde{X}_i}{h_n}\right) K\left(\frac{\tilde{X}_j}{h_n}\right)\right]$$

Term (I) is equal to

$$(I) = \big[H^{-1}(h_n)(\beta_{d,g,p}(h_n) - \hat{\beta}_{d,g,p}(h_n))\big]^T M(h_n)\big[H^{-1}(h_n)(\beta_{d,g,p}(h_n) - \hat{\beta}_{d,g,p}(h_n))\big]$$

The term $M(h_n)$ is $O_p(1)$, since for some $C > 0$ it is bounded by $C \cdot \frac{1}{nh_n^{\bar{s}}} \sum_i \sum_{j \in \boldsymbol{N}_i} W_{ij}^{d,g}(h_n)$ which is $O_p(1)$ by Lemma S.3.4. Furthermore, $H^{-1}(h_n)(\beta_{d,g,p}(h_n) - \hat{\beta}_{d,g,p}(h_n)) = o_p(1)$ by Lemma S.3.1 and S.3.2 as $nh_n^{\bar{s}} \to \infty$. Thus, (I) $= o_p(1)$. Convergence in probability to zero of $(II) - (III)$ can be proved similarly by factorizing $H^{-1}(h_n)(\beta_{d,g,p}(h_n) - \hat{\beta}_{d,g,p}(h_n))$, yielding the conclusion. The proofs for $\hat{\Psi}_{d',g',p}(h_n)$ and $\hat{\Psi}_{d,g,d',g',p}(h_n)$ are analogous. $\square$

Theorem S.3.2. *Suppose Assumptions 1–6, S.3.1, S.3.2, and S.3.3 hold. If* $nh_n^{\bar{s}} \to \infty$ *and* $h_n \to 0$

$$nh_n^{\bar{s}} \hat{\mathcal{V}}_{d,g,d',g',p}(h_n) \xrightarrow{p} V_{d,g,d',g',p}(h_n)$$

where $V_{d,g,d',g',p}(h_n) = V_{d,g,d',g',p} + o(1)$ *if* $h_n \to 0$*.*

Proof. The proof follows from Lemma S.3.1 and S.3.6. $\square$

S.3.5 Common Distance Variable

We consider the case where a non negligible fraction of connected units can share the same distance variable. Define $\boldsymbol{K}_i \subseteq (\boldsymbol{N}_i \setminus \{i\})$ as the set of indices such that for $j \in \boldsymbol{K}_{i,n}$, $|F_{\ell_i} \cup F_{\ell_j}| = \min\{\bar{s}_i, \bar{s}_j\}$ for some pieces ℓ_i, ℓ_j, forming $\bar{\mathcal{X}}_{is_i}(d, g \,|\, d', g')$ and $\bar{\mathcal{X}}_{js_j}(d, g|d', g')$.

Lemma S.3.7. *Suppose Assumptions 1–6, S.3.1.b, and S.3.3 hold. If* $nh_n^{\bar{s}} \to \infty$ *and* $h_n \to 0$

$$nh_n^{\bar{s}} \mathbb{V}[t^*_{d,g,d',g'}(h_n)] = (\bar{\omega}_{d,g}(0) + \bar{\omega}_{d',g'}(0))\Psi_p^{\bar{s}} + R_n + o(1)$$

where $R_n = O(1)$ *collects the covariance contribution from* i, j*, with* $j \in \boldsymbol{K}_i$*.*

Proof. Consider $\mathbb{V}[t^*_{d,g,p}(h_n)]$. As in Lemma S.3.5, we can write

$$\begin{aligned} nh_n^{\bar{s}} \mathbb{V}[t^*_{d,g,p}(h_n)] = & \underbrace{\frac{1}{nh_n^{\bar{s}}} \sum_i \mathbb{E}\Big[I_{i,d,g} K\left(\frac{\tilde{X}_i}{h_n}\right)^2 r_p\left(\frac{\tilde{X}_i}{h_n}\right) r_p\left(\frac{\tilde{X}_i}{h_n}\right)^T u_i^2 \Big]}_{T_1} \\ & + \underbrace{\frac{1}{nh_n^{\bar{s}}} \sum_i \sum_{j \in \boldsymbol{N}_i \setminus \{i\}} \mathbb{E}\Big[I_{i,d,g} I_{j,d,g} K\left(\frac{\tilde{X}_i}{h_n}\right) K\left(\frac{\tilde{X}_j}{h_n}\right) r_p\left(\frac{\tilde{X}_i}{h_n}\right) r_p\left(\frac{\tilde{X}_j}{h_n}\right)^T u_i u_j \Big]}_{T_2}. \end{aligned} \tag{S.3.13}$$

The first term T_1 is exactly as in Lemma S.3.5, giving

$$T_1 \;=\; \bar{\omega}_{d,g}(0) \int_{N^{\bar{s}}} K(\|\boldsymbol{u}\|)^2 r_p(\boldsymbol{u}) r_p(\boldsymbol{u})^T \, d\boldsymbol{u} + o(1).$$

For T_2, decompose neighbors $j \in \boldsymbol{N}_i$ into those in $\boldsymbol{K}_i$ and the remainder:

$$T_2 = \frac{1}{nh_n^{\bar{s}}} \sum_i \sum_{j \in \boldsymbol{K}_i} \mathbb{E}[\cdots] \; + \; \frac{1}{nh_n^{\bar{s}}} \sum_i \sum_{j \in \boldsymbol{N}_i \setminus (\{i\} \cup \boldsymbol{K}_i)} \mathbb{E}[\cdots]. \tag{S.3.14}$$

The second sum is $o(1)$ by the same arguments as in Lemma S.3.5, since for such pairs with $|F_{\ell_i} \cup F_{\ell_j}| \geq \bar{s} + 1$ for all ℓ_i, ℓ_j.

For $j \in \boldsymbol{K}_i$, for some ℓ_i, ℓ_j $|F_{\ell_i} \cup F_{\ell_j}| = \bar{s}$. Thus

$$\mathbb{E}[\cdots] \; = \; O(h_n^{\bar{s}}), \qquad \frac{1}{nh_n^{\bar{s}}} \sum_i \sum_{j \in \boldsymbol{K}_i} \mathbb{E}[\cdots] \; = \; R_{d,g,n},$$

since all terms in $\mathbb{E}[\cdots]$ are uniformly bounded. Moreover, $R_{d,g,n}$ is $O(1)$ because $\frac{1}{n} \sum_i |\boldsymbol{K}_i| \leq \frac{1}{n} \sum_i |\boldsymbol{N}_i| = O(1)$. Hence

$$nh_n^{\bar{s}} \mathbb{V}[t^*_{d,g,p}(h_n)] \; = \; \bar{\omega}_{d,g}(0) \Psi_p^{\bar{s}} \; + \; R_{d,g,n} \; + \; o(1).$$

Analogous arguments yield $nh_n^{\bar{s}} \mathbb{V}[t^*_{d',g',p}(h_n)] \; = \; \bar{\omega}_{d',g'}(0) \Psi_p^{\bar{s}} \; + \; R_{d',g',n} \; + \; o(1)$ and $nh_n^{\bar{s}} \mathbb{C}[t^*_{d,g,p}(h_n), t^*_{d',g',p}(h_n)] = R_{d,g,d',g',n} + o(1)$ with each $R_{\cdot,n} = O(1)$. Assume $R_n \to R_p$. Letting $R_n = R_{n,d,g} + R_{n,d,g} - 2R_{n,d,g,d',g'}$ yields the conclusion. $\square$

Theorem S.3.3. *Suppose Assumptions 1–6, S.3.1, S.3.2, and S.3.3 hold. If* $nh_n^{\bar{s}} \to \infty$, $h_n \to 0$, *and* $h_n = O\big(n^{-1/(2p+2+\bar{s})}\big)$, *then*

$$\sqrt{nh_n^{\bar{s}}} \, \frac{\left(\hat{\tau}_{d,g,d',g',p}(h_n) - \tau_{d,g|d',g'}\big(\bar{\mathcal{X}}_{i\mathcal{S}_i}(d,g \,|\, d',g')\big)\right) - h_n^{p+1} B_{d,g,d',g',p,p+1}(h_n)}{\sqrt{V_{d,g,d',g',p}(h_n)}} \xrightarrow{d} \mathcal{N}(0,1),$$

where $B_{d,g,d',g',p,p+1}(h_n)$ *is as in Theorem S.3.1 and*

$$V_p(h_n) = \frac{\bar{\omega}_{d,g}(0) + \bar{\omega}_{d',g'}(0)}{f_{d,g,d',g'}(0)} e_1^T (\Gamma_p^{\bar{s}})^{-1} (\Psi_p^{\bar{s}} + R_p^{\bar{s}}) (\Gamma_p^{\bar{s}})^{-1} e_1 + o(1).$$

Proof. The proof follows from analogous arguments as Theorem S.3.1 and using Lemma S.3.1, S.3.3 and S.3.7. $\square$

S.3.6 Differentiability of $\mu_{d,g}(\tilde{x}_i)$ and $\mu_{d',g'}(\tilde{x}_i)$

The bias properties of $\hat{\tau}_{d,g,d',g',p}(h_n)$ hinge on Assumption S.3.1.c, which imposes smoothness of $\mu_{d,g}(\tilde{x}_i)$ and $\mu_{d',g'}(\tilde{x}_i)$. Continuity of $m_{d,g}(x_i, \boldsymbol{x}_{\mathcal{S}_i})$ and $m_{d',g'}(x_i, \boldsymbol{x}_{\mathcal{S}_i})$

(or a stronger version continuity condition when causal effects are heterogeneous) is sufficient for consistency of the estimator, i.e. convergence to the estimand (see Theorem S.5.1). However, obtaining the quadratic rate of bias decay, h_n^{2+2p}, requires differentiability of $\mu_{d,g}(\tilde{x}_i)$ and $\mu_{d',g'}(\tilde{x}_i)$. Verifying this condition can be challenging. Here, we illustrate a simple case where this assumption is satisfied–namely, in the estimation of boundary direct effects.

Consider

$$\mu_{1,g}(\tilde{x}_i) = \mathbb{E}\Big[Y_i(1,g) \;\Big|\; \tilde{X}_i = \tilde{x}_i,\ D_i = 1,\ G_i = g\Big].$$

For direct boundary effects, the Euclidean distance to the effective treatment boundary is $\tilde{X}_i = |X_i|$, so we may parametrize

$$\mu_{1,g}(\epsilon) = \frac{\int_{\mathcal{X}_{s_i}(g)} m_{1,g}(\epsilon, \boldsymbol{x}_{\mathcal{S}_i})\, f(\epsilon, \boldsymbol{x}_{\mathcal{S}_i})\, d\boldsymbol{x}_{\mathcal{S}_i}}{\int_{\mathcal{X}_{s_i}(g)} f(\epsilon, \boldsymbol{x}_{\mathcal{S}_i})\, d\boldsymbol{x}_{\mathcal{S}_i}}.$$

where $\mathcal{X}_{s_i}(g)$ is the set of $_{s_i}$ where $e(\boldsymbol{x}_{\mathcal{S}_i}) = g$. Assume that, in a neighborhood $\mathcal{B}_\kappa(\mathcal{X}_{i\mathcal{S}_i}(1, g, |0, g))$ of $\mathcal{X}_{i\mathcal{S}_i}(1, g, |0, g)$, both f and $m_{d,g}$ are s-times continuously differentiable in ϵ for all d, g. For $0 \leq k \leq s$, the map $(\epsilon, \boldsymbol{x}_{\mathcal{S}_i}) \mapsto \partial_\epsilon^k m_{d,g}(\epsilon, \boldsymbol{x}_{\mathcal{S}_i})$ is continuous and bounded on $\mathcal{B}_\kappa(\mathcal{X}_{i\mathcal{S}_i}(1, g, |0, g))$. Therefore, by differentiating under the integral sign we obtain for $\epsilon < \kappa$

$$\partial_\epsilon^k \int_{\mathcal{X}_{s_i}(g)} m_{1,g}(\epsilon, \boldsymbol{x}_{\mathcal{S}_i}) f(\epsilon, \boldsymbol{x}_{\mathcal{S}_i})\, d\boldsymbol{x}_{\mathcal{S}_i} = \int_{\mathcal{X}_{s_i}(g)} \partial_\epsilon^k m_{1,g}(\epsilon, \boldsymbol{x}_{\mathcal{S}_i}) f(\epsilon, \boldsymbol{x}_{\mathcal{S}_i})\, d\boldsymbol{x}_{\mathcal{S}_i},$$

which is continuous as $\epsilon \to 0$ by the Dominated Convergence Theorem. Similarly,

$$\partial_\epsilon^k \int_{\mathcal{X}_{s_i}(g)} f(\epsilon, \boldsymbol{x}_{\mathcal{S}_i})\, d\boldsymbol{x}_{\mathcal{S}_i} = \int_{\mathcal{X}_{s_i}(g)} \partial_\epsilon^k f(\epsilon, \boldsymbol{x}_{\mathcal{S}_i})\, d\boldsymbol{x}_{\mathcal{S}_i}$$

Hence, $\mu_{1,g}(\epsilon)$ is $s-$times continuously differentiable being the ratio of two continuously differentiable functions. Analogously, $\mu_{0,g}(\epsilon)$ is also s-times continuously differentiable.

S.3.7 Bias Correction

In this section, we establish the asymptotic normality of the bias-corrected estimator $\hat{\tau}^{bc}_{d,g|d',g',p,p+1}(h_n, b_n)$ of $\tau_{d,g|d',g'}\big(\bar{\mathcal{X}}_{i\mathcal{S}_i}(d, g \,|\, d', g')\big)$

$$\hat{\tau}^{bc}_{d,g|d',g',p,p+1}(h_n, b_n) = \hat{\tau}_{d,g,d',g',p}(h_n) - \hat{B}_{d,g,d',g',p,p+1}(h_n, b_n),$$

where $\hat{B}_{d,g,d',g',p,p+1}(h_n, b_n)$ is equal to

$$h_n^{p+1} e_{p+1}^T \big[\hat{\beta}_{d',g',p+1}(b_n)\hat{B}_{d',g',p,p+1}(h_n) - \hat{\beta}_{d,g,p+1}(b_n)\hat{B}_{d,g,p,p+1}(h_n)\big],$$

$\hat{\beta}_{d,g,p+1}(b_n)$ and $\hat{\beta}_{d',g',p+1}(b_n)$ are the $(p+1)$-order local polynomial estimators with bandwidth b_n, e_{p+1} is the $p+2$ -dimensional vector with the $p+2$-th entry equal to 1 and all other zeros, and $\hat{B}_{\bullet,p,p+1}(h_n) = e_1^T \Gamma^{-1}_{\bullet,p}(h_n)\theta_{\bullet,p,p+1}(h_n)$ (see Subsection S.3.1 for the related definitions).

Since most passages are similar to the derivations for the asymptotic normality of $\hat{\tau}_{d,g|d',g'}(h_n)$ without bias correction, we only sketch the proof.

We consider the centered estimators.

$$\hat{\tau}^{bc*}_{d,g|d',g',p,p+1}(h_n, b_n) = \hat{\tau}^*_{d,g,d',g',p}(h_n) - \hat{B}^*_{d,g,d',g',p,p+1}(h_n, b_n)$$

where $\hat{\tau}^*_{d,g,d',g',p}(h_n)$ is defined in Subsection S.3.1, and $\hat{B}^*_{d,g,d',g',p,p+1}(h_n, b_n)$ uses the centered versions of $\hat{\beta}_{d,g,p+1}(b_n)$ and $\hat{\beta}_{d',g',p+1}(b_n)$, obtained by replacing Y_i in their expressions with

$$\nu_{i,\bullet,p+1}(b_n) = Y_i - \mathbf{r}_{p+1}(\tilde{X}_i)^T \beta_{\bullet,p+1}(b_n), \quad \bullet \in \{(d,g),(d'g')\}$$

with $\beta_{\bullet,p+1}(b) = \underset{\boldsymbol{b}\in\mathbb{R}^{p+2}}{\arg\min}\,\mathbb{E}\Big[\sum_i I_{i,\bullet}(Y_i - \boldsymbol{r}_{p+1}(\tilde{X}_i)^T\boldsymbol{b})^2 \cdot K_{b^{\bar{s}}}(\tilde{X}_i)\Big]$.

Under Assumption S.3.1.c, if $\max\{h_n, b_n\} < \kappa$, a Taylor expansion yields

$$\begin{aligned}\hat{\tau}^{bc}_{d,g|d',g',p,p+1}(h_n, b_n) =& \tau_{d,g|d',g'}\big(\bar{\mathcal{X}}_{i\mathcal{S}_i}(d, g \,|\, d', g')\big) + h_n^{p+1} B_{d,g,d',g',p,p+1}(h_n) + T_{d,g,d'g'}(h_n) \\ &- h_n^{p+1}\hat{B}_{d,g,d',g',p,p+1}(h_n) - h_n^{p+1} b_n B^{bc}_{d,g,d',g',p,p+1}(h_n, b_n) + T^{bc}_{d,g,d',g'}(h_n, b_n) \\ &+ \hat{\tau}^{bc*}_{d,g|d',g',p,p+1}(h_n, b_n)\end{aligned} \tag{S.3.15}$$

where $B_{d,g,d',g',p,p+1}(h_n)$ and $T_{d,g,d'g'}(h_n)$ are defined in Subsection S.3.3,

$\hat{B}_{d,g,d',g',p,p+1}(h_n) = \frac{\mu^{(p+1)}_{d,g}(0)}{(p+1)!}\hat{B}_{d,g,p,p+1}(h_n) - \frac{\mu^{(p+1)}_{d',g'}(0)}{(p+1)!}\hat{B}_{d',g',p,p+1}(h_n)$, with $\hat{B}_{\bullet,p,p+1}(h_n) = e_1^T\Gamma^{-1}_{d,g,p}(h_n)\theta_{d,g,p,p+1}(h_n)$, and $B^{bc}_{d,g,d',g',p,p+1}(h_n,b_n)$ is equal to

$$\frac{\mu^{(p+2)}_{d,g}(0)}{(p+2)!}\hat{B}_{d,g,p+1,p+2}(b_n)\frac{B_{d,g,p,p+1}(h_n)}{(p+1)!} - \frac{\mu^{(p+2)}_{d',g'}(0)}{(p+2)!}\hat{B}_{d',g',p+1,p+2}(b_n)\frac{B_{d',g',p,p+1}(h_n)}{(p+1)!}$$

with $\hat{B}_{\bullet,p+1,p+2}(h_n) = e_1^T\Gamma^{-1}_{\bullet,p+1}(h_n)\theta_{\bullet,p+1,p+2}(h_n)$, and $B_{\bullet,p,p+1}(h_n) = e_1^T\bar{\Gamma}^{-1}_{\bullet,p+1}(h_n)\bar{\theta}_{\bullet,p,p+1}(h_n)$.

We denote the variance and covariance of $t^*_{d,g,p+1}(b_n)$ and $t^*_{d',g',p+1}(b_n)$, multiplied by $nb_n^{\bar{s}}$, by $\bar{\Psi}_{d,g,p+1}(b_n)$, $\bar{\Psi}_{d',g',p+1}(b_n)$ and $\bar{\Psi}_{d,g,d',g',p+1}(b_n)$, and we let

$$\bar{\Psi}_{d,g,p,p+1}(h_n,b_n) = \frac{n(h_nb_n)^{\bar{s}}}{m_n^{\bar{s}}}\mathbb{C}[t^*_{d,g,p}(h_n), t^*_{d,g,p+1}(b_n)]$$
$$\bar{\Psi}_{d',g',p,p+1}(h_n,b_n) = \frac{n(h_nb_n)^{\bar{s}}}{m_n^{\bar{s}}}\mathbb{C}[t^*_{d',g',r}(h_n), t^*_{d',g',p+1}(b_n)]$$
$$\bar{\Psi}_{d,g,d',g',p,p+1}(h_n,b_n) = \frac{n(h_nb_n)^{\bar{s}}}{m_n^{\bar{s}}}\mathbb{C}[t^*_{d,g,p}(h_n), t^*_{d',g',p+1}(b_n)]$$

where $m_n = \min\{h_n, b_n\}$. Further define $V^{bc}_{d,g,d',g',p,p+1}(h_n,b_n) = V^{bc}_{d,g,p,p+1}(h_n,b_n) + V^{bc}_{d',g',p,p+1}(h_n,b_n) - 2C^{bc}_{d,g,d',g',p,p+1}(h_n,b_n)$ where

$$\begin{aligned}
V^{bc}_{d,g,p,p+1}(h_n,b_n) &= \frac{1}{nh_n^{\bar{s}}}e_1^T\bar{\Gamma}^{-1}_{d,g,p}(h_n)\bar{\Psi}_{d,g,p}(h_n)\bar{\Gamma}^{-1}_{d,g,p}(h_n)e_1 \\
&+ \frac{1}{nb_n^{\bar{s}}}\frac{h_n^{2p+2}}{b_n^{2+2p}}e_{p+1}^T\bar{\Gamma}^{-1}_{d,g,p+1}(b_n)\bar{\Psi}_{d,g,p+1}(b_n)\bar{\Gamma}^{-1}_{d,g,p+1}(b_n)e_{p+1}) \times (e_1^T\bar{\Gamma}^{-1}_{d,g,p+1}(b_n)\bar{\theta}_{d,g,p,p+1}(h_n))^2 \\
&- 2\frac{m_n^{\bar{s}}}{n(h_nb_n)^{\bar{s}}}\frac{h_n^{p+1}}{b_n^{p+1}}(e_1^T\bar{\Gamma}^{-1}_{d,g,p}(h_n)\bar{\Psi}_{d,g,p,p+1}(h_n,b_n)\bar{\Gamma}^{-1}_{d,g,p+1}(b_n)e_{p+1}) \\
&\times (e_1^T\bar{\Gamma}^{-1}_{d,g,p+1}(h_n)\bar{\theta}_{d,g,p,p+1}(h_n)) \\
V^{bc}_{d',g',p,p+1}(h_n,b_n) &= \frac{1}{nh_n^{\bar{s}}}e_1^T\bar{\Gamma}^{-1}_{d',g',p}(h_n)\bar{\Psi}_{d',g',p}(h_n)\bar{\Gamma}^{-1}_{d',g',p}(h_n)e_1 \\
&+ \frac{1}{nb_n^{\bar{s}}}\frac{h_n^{2p+2}}{b_n^{2+2p}}e_{p+1}^T\bar{\Gamma}^{-1}_{d',g',p+1}(b_n)\bar{\Psi}_{d',g',p+1}(b_n)\bar{\Gamma}^{-1}_{d',g',p+1}(b_n)e_{p+1} \times (e_1^T\bar{\Gamma}^{-1}_{d',g',p}(h_n)\bar{\theta}_{d',g',p,p+1}(h_n))^2 \\
&- 2\frac{m_n^{\bar{s}}}{n(h_nb_n)^{\bar{s}}}\frac{h_n^{p+1}}{b_n^{p+1}}(e_1^T\bar{\Gamma}^{-1}_{d',g',p}(h_n)\bar{\Psi}_{d',g',p,p+1}(h_n,b_n)\bar{\Gamma}^{-1}_{d',g',p+1}(b_n)e_{p+1} \\
&\times (e_1^T\bar{\Gamma}^{-1}_{d',g',p}(h_n)\bar{\theta}_{d',g',p,p+1}(h_n))
\end{aligned}$$

The first two terms represent the asymptotic variance, for $n\min\{h_n^{\bar{s}}, b_n^{\bar{s}}\} \to \infty$ of the (centered) bias-corrected estimator to the right and left of the cutoff respectively, which includes the variance of the original centered estimator, the variance of the centered bias correction, and their covariance. $C^{bc}_{d,g,d',g',p,p+1}(h_n,b_n)$ is given by

$$\begin{aligned}C^{bc}_{d,g,d',g',p,p+1}(h_n,b_n) &= C_{d,g,d',g',p}(h_n) + h_n^{2(p+1)}C_{d,g,d',g',p+1}(b_n)B_{d,g,p,p+1}(h_n)B_{d',g',p,p+1}(h_n)\\ &\quad - h_n^{p+1}C_{d,g,d',g',p+1,p,p+1}(h_n,b_n)B_{d,g,p,p+1}(b_n)\\ &\quad - h_n^{p+1}C_{d,g,d',g',p+1,p,p+1}(b_n,h_n)B_{d,g,p,p+1}(h_n)\end{aligned}$$

where

$$\begin{aligned}C_{d,g,d',g',p}(h_n) &= \frac{1}{nh_n^{\bar{s}}}e_1^T\bar{\Gamma}^{-1}_{d,g,p}(h_n)\bar{\Psi}_{d,g,d',g',p}(h_n)\bar{\Gamma}^{-1}_{d',g',p}(h_n)e_1\\ C_{d,g,d',g',p+1,p,p+1}(h_n,b_n) &= \frac{m_n^{\bar{s}}}{n(h_nb_n)^{\bar{s}}}\frac{1}{b_n^{p+1}}(p+1)!e_1^T\bar{\Gamma}^{-1}_{d,g,p}(h_n)\bar{\Psi}_{d,g,d',g',p,p+1}(h_n,b_n)\bar{\Gamma}^{-1}_{d,g,p+1}(b_n)e_{p+1}\\ C_{d,g,d',g',p+1,p,p+1}(b_n,h_n) &= \frac{m_n^{\bar{s}}}{n(h_nb_n)^{\bar{s}}}\frac{1}{b_n^{p+1}}(p+1)!e_{p+1}^T\bar{\Gamma}^{-1}_{d,g,p+1}(b_n)\bar{\Psi}_{d,g,d',g',p,p+1}(b_n,h_n)\bar{\Gamma}^{-1}_{d',g',p}(h_n)e_1\end{aligned}$$

By similar arguments as Lemma S.3.5, for $n\min\{h_n^{\bar{s}},b_n^{\bar{s}}\}\to\infty$ and $\max\{h_n,b_n\}<\kappa$

$$\bar{\Psi}_{d,g,p}(h_n),\bar{\Psi}_{d',g',p}(h_n) = O\left(\frac{1}{nh_n^{\bar{s}}}\right),\qquad \bar{\Psi}_{d,g,p}(b_n),\bar{\Psi}_{d',g',p}(b_n) = O\left(\frac{1}{nb_n^{\bar{s}}}\right).$$

and the cross–bandwidth terms satisfy

$$\bar{\Psi}_{d,g,p,q}(h_n,b_n),\ \bar{\Psi}_{d',g',p,q}(h_n,b_n) = O\left(\frac{m_n^{\bar{s}}}{n(h_nb_n)^{\bar{s}}}\right),\qquad \bar{\Psi}_{d,g,d',g',p,q}(h_n,b_n) = O\left(\frac{m_n^{\bar{s}+1}}{n(h_nb_n)^{\bar{s}}}\right),$$

Theorem S.3.4. *Suppose Assumptions 1–6, S.3.1, S.3.2, and S.3.3 hold. If* $n\min\{h_n^{\bar{s}},b_n^{\bar{s}}\}\to\infty$, $n\min\{h_n^{2p+2+\bar{s}},b_n^{2p+2+\bar{s}}\}\max\{h_n^2,b_n^2\}\to 0$ *and* $\max\{h_n,b_n\}<\kappa$*:*

$$\frac{\hat{\tau}^{bc}_{d,g|d',g',p,p+1}(h_n,b_n)-\tau_{d,g|d',g'}\left(\bar{\mathcal{X}}_{i\mathcal{S}_i}(d,g\,|\,d',g')\right)}{\sqrt{V^{bc}_{d,g,d',g',p,p+1}(h_n,b_n)}}\xrightarrow{d}\mathcal{N}(0,1)$$

Proof. Consider $Z_{i,d,g,d',g',p}(h_n,b_n) = Z_{i,d,g,p}(h_n,b_n) - Z_{i,d',g',p}(h_n,b_n)$, where $Z_{i,d,g,p}(h_n) = Z_{i,d,g,p,1}(h_n,b_n) - Z_{i,d,g,p,2}(h_n,b_n)$ with

$$\begin{aligned}Z_{i,d,g,p,1}(h_n,b_n) =& e_1^T\bar{\Gamma}^{-1}_{d,g,p}(h_n)I_{i,d,g}K\left(\frac{\tilde{X}_i}{h_n}\right)r_p\left(\frac{\tilde{X}_i}{h_n}\right)\nu_{i,d,g,p}(h_n)/(nh_n^{\bar{s}}),\\ Z_{i,d,g,p,2}(h_n,b_n) =& \frac{h_n^{p+1}b_n^{-p-1}}{nb_n^{\bar{s}}}B_{d,g,p,p+1}(h_n)\times e_{p+1}^T\bar{\Gamma}^{-1}_{d,g,p+1}(b_n)I_{i,d,g}K\Big(\frac{\tilde{X}_i}{b_n}\Big)r_{p+1}\Big(\frac{\tilde{X}_i}{b_n}\Big)\nu_{i,d,g,p+1}(b_n)\end{aligned}$$

and $Z_{i,d',g',p}(h_n,b_n)$ is defined analogously. Here we denote $\nu_{i,\bullet,r}(h) = Y_i - \boldsymbol{r}_r(\tilde{X}_i)\beta_{\bullet,r}(h)$, the residual obtained from the outcome linear approximation using the population linear projection coefficient $\beta_{\bullet,r}(h)$. Then

$$\mathbb{V}\Big[\sum_i Z_{i,d,g,d',g',p}(h_n,b_n)\Big] \;=\; V^{bc}_{d,g,d',g',p,p+1}(h_n,b_n) = O_p\Big(\frac{1}{nh_n^{\bar{s}}}\Big) + O_p\Big(\frac{h_n^{2(p+1)}}{nb_n^{2(p+1)+\bar{s}}}\Big).$$

Let $\xi_n = \sum_i Z_{i,d,g,d',g',p}(h_n,b_n)/\sigma_n$ with $\sigma_n^2 = V^{bc}_{d,g,d',g',p,p+1}(h_n,b_n)$. By Assumption 5, $\{Z_{i,d,g,d',g',p}(h_n,b_n)\}_{i=1}^n$ has dependency graph $\boldsymbol{W}_n$. Stein's method and Leung (2020, Theorem A.4) then yield

$$\begin{aligned}\Delta(\xi_n,\mathcal{N}(0,1)) \le{}& \frac{1}{\sigma_n^3}\mathbb{E}[|Z_{i,d,g,d',g',p}(h_n,b_n)|^3]\sum_i |\boldsymbol{N}_{i,n}|^2 \\ &+ \frac{1}{\sigma_n^2}\Big(\frac{4}{\pi}\mathbb{E}[Z_{i,d,g,d',g',p}(h_n,b_n)^4]\Big)^{1/2}\Big(4\sum_i |\boldsymbol{N}_{i,n}|^3 + 3\sum_{i,j}(\boldsymbol{W}_n^3)_{ij}\Big)^{1/2}\end{aligned} \tag{S.3.16}$$

By the c_r-inequality,

$$\mathbb{E}[|Z_{i,d,g,d',g',p}(h_n,b_n)|^3] \;\le\; 4\big(\mathbb{E}[|Z_{i,d,g,p}(h_n,b_n)|^3] + \mathbb{E}[|Z_{i,d',g',p}(h_n,b_n)|^3]\big).$$

where by decomposing $Z_{i,d,g,p}(h_n,b_n)$

$$\mathbb{E}[|Z_{i,d,g,p}(h_n,b_n)|^3] \;\le\; 4\big(\mathbb{E}[|Z_{i,d,g,p,1}(h_n,b_n)|^3]+\mathbb{E}[|Z_{i,d,g,p,2}(h_n,b_n)|^3]\big) = O\Big(\tfrac{1}{n^3h_n^{2\bar{s}}}\Big)+O\Big(\tfrac{h_n^{3(p+1)}}{n^3b_n^{3(p+1)+2\bar{s}}}\Big),$$

and $\mathbb{E}[|Z_{i,d',g',p}(h_n,b_n)|^3]$ has a bound of the same order. Similarly,

$$\mathbb{E}[Z_{i,d,g,d',g',p}(h_n,b_n)^4] = O\Big(\tfrac{1}{n^4h_n^{3\bar{s}}}\Big) + O\Big(\tfrac{h_n^{4(p+1)}}{n^4b_n^{4(p+1)+3\bar{s}}}\Big).$$

Let $\rho_n = h_n/b_n$. Since $\sum_i |\boldsymbol{N}_{i,n}|^2 = O(n)$ and $\big(4\sum_i |\boldsymbol{N}_{i,n}|^3 + 3\sum_{i,j}(\boldsymbol{W}_n^3)_{ij}\big)^{1/2} = O(n^{1/2})$ by Assumption 6, the first and second terms in (S.3.16) are

$$O\Big((nh_n^{\bar{s}})^{-1/2}\min\{1,\rho_n^{-3(p+1)-\frac{3}{2}\bar{s}}\}\Big) + O\Big((nb_n^{\bar{s}})^{-1/2}\min\{1,\rho_n^{3(p+1)+\frac{3}{2}\bar{s}}\}\Big) = o(1),$$

and

$$O_p\Big((nh_n^{\bar{s}})^{-1/2}\min\{1,\rho_n^{-2(p+1)-\bar{s}}\}\Big) + O_p\Big((nb_n^{\bar{s}})^{-1/2}\min\{1,\rho_n^{2(p+1)+\bar{s}}\}\Big) = o(1).$$

Hence $\xi_n \xrightarrow{d} \mathcal{N}(0,1)$. The condition $n\min\{h_n^{\bar{s}}, b_n^{\bar{s}}\} \to \infty$ combined with Lemma S.3.1 and Lemma S.3.3 gives $\frac{\hat{\tau}^{bc*}_{d,g|d',g',p,p+1}(h_n,b_n)}{\sqrt{V^{bc}_{d,g,d',g',p,p+1}(h_n,b_n)}} = \xi_n + o_p(1)$, so $\hat{\tau}^{bc*}_{d,g|d',g',p,p+1}(h_n, b_n)$ (rescaled) has the same limiting distribution as ξ_n. By $n\min\{h_n^{\bar{s}}, b_n^{\bar{s}}\} \to \infty$ and Lemmas S.3.1 S.3.3 we have $T_{d,g,d'g'}(h_n) = O(h_n^{p+2})$, $h_n^{p+1}(B_{d,g,d',g',p,p+1}(h_n) - \hat{B}_{d,g,d',g',p,p+1}(h_n)) = o_p(h_n^{p+1})$, $h_n^{p+1}b_n B^{bc}_{d,g,d',g',p,p+1}(h_n, b_n) = O_p(h_n^{p+1}b_n)$ and $T^{bc}_{d,g,d',g'}(h_n, b_n) = o_p(h_n^{p+1}b_n)$. The conclusion follows from decomposition (S.3.15) and $n\min\{h_n^{2p+2+\bar{s}}, b_n^{2p+2+\bar{s}}\}\max\{h_n^2, b_n^2\} \to 0$. $\square$

An estimator of the asymptotic variance of $\hat{\tau}^{bc}_{d,g|d',g',p,p+1}(h_n, b_n)$ can be obtained as follows by plugging the following estimators

$$\hat{\hat{\Psi}}_{d,g,p,q}(h_n, b_n) = \mathcal{M}_{d,g,p}(h_n)\boldsymbol{W}_n\mathcal{M}_{d,g,q}(b_n)^T/n$$
$$\hat{\hat{\Psi}}_{d',g',p,q}(h_n, b_n) = \mathcal{M}_{d',g',p}(h_n)\boldsymbol{W}_n\mathcal{M}_{d',g',q}(b_n)^T/n$$
$$\hat{\hat{\Psi}}_{d,g,d',g',p,q}(h_n, b_n) = \mathcal{M}_{d,g,p}(h_n)\boldsymbol{W}_n\mathcal{M}_{d',g',q}(b_n)^T/n$$

as well as the estimators defined in (S.3.10) for the corresponding quantities in the expression for $V^{bc}_{d,g,d',g',p,p+1}(h_n, b_n)$.

S.4 Estimation of Boundary Overall Direct Effects

We now provide the asymptotic theory for the estimator $\hat{\tau}_{1|0}(h_n)$ defined in Eq. (B.3). The outcome regression functions of interest are

$$\tilde{\mu}_1(x_i) = \mathbb{E}[Y_i \mid X_i = x_i], \quad x_i \geq 0, \qquad \tilde{\mu}_0(x_i) = \mathbb{E}[Y_i \mid X_i = x_i], \quad x_i < 0,$$

with cutoff $c = 0$ without loss of generality.

Let $\hat{\tau}_{1|0,p}(h_n)$ denote the generic pth-order local polynomial estimator of $\tau_{1|0}$. Because this estimator can be viewed as a local polynomial estimator on a boundary with codimension $\bar{s} = 1$, its asymptotic analysis follows similar steps as in Section S.3. For brevity, we only sketch the arguments.

S.4.1 Notation

We define the boundary overall direct effect of pth-order local polynomial RDD estimator:

$$\begin{aligned}
\hat{\tau}_{1|0,p}(h_n) &= e_1^T \hat{\beta}_{1,p}(h_n) - e_1^T \hat{\beta}_{0,p}(h_n), \\
\hat{\beta}_{1,p}(h_n) &= \underset{b \in \mathbb{R}^{p+1}}{\arg\min} \sum_i \mathbb{1}(X_i \geq 0)(Y_i - r(X_i)b)^2 K_h(X_i), \\
\hat{\beta}_{0,p}(h_n) &= \underset{b \in \mathbb{R}^{p+1}}{\arg\min} \sum_i \mathbb{1}(X_i < 0)(Y_i - r(X_i)b)^2 K_h(X_i),
\end{aligned}$$

where $h_n > 0$, $r_p(\cdot)$, $K_h(\cdot)$, and e_1 are defined as in Section S.3.

We set $\mathbb{1}(X_i \geq 0) = I_{i,1}$ and $\mathbb{1}(X_i < 0) = I_{i,0}$, $\boldsymbol{Y} = (Y_1, \ldots, Y_n)^T$, and define

$$\begin{aligned}
X_p(h_n) &= [r(X_1/h_n), \ldots, r(X_n/h_n)]^T, \\
S_p(h_n) &= [(X_1/h_n)^p, \ldots, (X_n/h_n)^p]^T, \\
W_1(h_n) &= \mathrm{diag}(\mathbb{1}(X_1 \geq 0)K_h(X_1), \ldots, \mathbb{1}(X_n \geq 0)K_h(X_n)), \\
W_0(h_n) &= \mathrm{diag}(\mathbb{1}(X_1 < 0)K_h(X_1), \ldots, \mathbb{1}(X_n < 0)K_h(X_n)).
\end{aligned}$$

Then set

$$\begin{aligned}
\Gamma_{1,p}(h_n) &= X_p(h_n)^T W_1(h_n) X_p(h_n)/n, \qquad & t_{1,p}(h_n) &= X_p(h_n)^T W_1(h_n) \boldsymbol{Y}/n, \\
\Gamma_{0,p}(h_n) &= X_p(h_n)^T W_0(h_n) X_p(h_n)/n, \qquad & t_{0,p}(h_n) &= X_p(h_n)^T W_0(h_n) \boldsymbol{Y}/n,
\end{aligned}$$

We have

$$\hat{\beta}_{1,p}(h_n) = H(h_n)\Gamma_{1,p}(h_n)^{-1} t_{1,p}(h_n), \quad \hat{\beta}_{0,p}(h_n) = H(h_n)\Gamma_{0,p}(h_n)^{-1} t_{0,p}(h_n).$$

Finally, we define the linear projection coefficients

$$\beta_{1,p}(h_n) = H(h_n)\bar{\Gamma}_{1,p}(h_n)\bar{t}_{1,p}(h_n), \qquad \beta_{0,p}(h_n) = H(h_n)\bar{\Gamma}_{0,p}(h_n)\bar{t}_{0,p}(h_n) \tag{S.4.1}$$

and define the centered quantities $t^*_{1,p}(h_n), t^*_{0,p}(h_n), \hat{\beta}^*_{1,p}(h_n), \hat{\beta}^*_{0,p}(h_n)$, and $\hat{\tau}^*_{1|0,p}(h_n)$ obtained by replacing Y_i with $\nu_{i,d} = Y_i - r_p(X_i)\beta_{d,p}(h_n)$, $d \in \{0, 1\}$.

S.4.2 Asymptotic Theory

Under Assumptions 1-4

$$\tilde{\mu}_1(x_i) = \sum_{g\in\mathcal{G}_i}\int_{\mathcal{X}_{s_i}(g)} m_{1,g}(x_i,\boldsymbol{x}_{s_i})\cdot\frac{f(x_i,\boldsymbol{x}_{s_i})}{f(x_i)}d\boldsymbol{x}_{s_i}, \quad \tilde{\mu}_0(x_i) = \sum_{g\in\mathcal{G}_i}\int_{\mathcal{X}_{s_i}(g)} m_{0,g}(x_i,\boldsymbol{x}_{s_i})\cdot\frac{f(x_i,\boldsymbol{x}_{s_i})}{f(x_i)}d\boldsymbol{x}_{s_i}$$

are continuous in $x_i = 0$, where $\mathcal{X}_{s_i}(g)$ is the set of elements $\boldsymbol{x}_{s_i}$ such that $e(\boldsymbol{x}_{s_i}) = g$. We further adopt the assumptions from Section S.3, replacing S.3.1.c with:

Assumption S.4.4. *$\tilde{\mu}_1(x_i)$ and $\tilde{\mu}_0(x_i)$ are S-times continuously differentiable with $S \geq p+2$.*

Under Assumption S.4.4, we obtain the decomposition

$$\hat{\tau}_{1|0,p}(h_n) = \tau_{1|0} + h_n^{p+1}\underbrace{\Big(\frac{\tilde{\mu}_1^{(p+1)}(0)}{(p+1)!}B_{1,p,p+1}(h_n) - \frac{\tilde{\mu}_0^{(p+1)}(0)}{(p+1)!}B_{0,,p,p+1}(h_n)\Big)}_{B_{1,0,p,p+1}(h_n)} + T_{1,0}(h_n) + \hat{\tau}^*_{1|0,p}(h_n) \tag{S.4.2}$$

where $B_{1,p,p+1}(h_n) = e_1^T\bar{\Gamma}_{1,p}^{-1}(h_n)\bar{\theta}_{1,p,p+1}(h_n)$ and $B_{0,,p,p+1}(h_n) = e_1^T\bar{\Gamma}_{0,p}^{-1}(h_n)\bar{\theta}_{0,p,p+1}(h_n)$, with

$$\bar{\theta}_{\bullet,p,q}(h_n) = \mathbb{E}\big[X_p(h_n)^T W_\bullet(h_n)\, S_q(h)/n\big], \quad S_q(h_n) = [(X_1/h_n)^q, ..., (X_n/h_n)^q]$$

for $\bullet \in \{0,1\}$, and $T_{1,0}(h_n)$ depends on the Taylor reminders.

Because the estimator uses only observations with $|X_i| \leq h_n$, we have

$$\begin{aligned}\mathbb{E}\left[\frac{1}{nh_n}\sum_i I_{i,1}K\Big(\frac{X_i}{h_n}\Big)\Big(\frac{X_i}{h_n}\Big)^k\right] &= \frac{1}{n}\sum_i\int_0^1 K(u)u^k\int_{\boldsymbol{X}_{s_i}} f(uh_n,\boldsymbol{x}_{s_i})\,d\boldsymbol{x}_{s_i}\,du\\ &= \int_0^1 K(u)u^k f(uh_n)\,du,\end{aligned}$$

for nonnegative integer k, where $f(x_i) = f_{X_i}(x_i)$ is the marginal density of X_i, and analogously for $\mathbb{E}\left[\frac{1}{nh_n}\sum_i I_{i,0}K\Big(\frac{X_i}{h_n}\Big)\Big(\frac{X_i}{h_n}\Big)^k\right]$. Moreover, by similar arguments to Lemma S.3.1, one obtains

$$\mathbb{V}\left[\frac{1}{nh_n}\sum_i I_{i,\bullet}K\Big(\frac{X_i}{h_n}\Big)\Big(\frac{X_i}{h_n}\Big)^k\right] = O\Big(\frac{1}{nh_n}\Big).$$

for $\bullet \in \{0,1\}$, from which for $nh_n \to \infty$ and $h_n \to 0$, $\Gamma_{\bullet,p}(h_n) = f(0)\,\Gamma^1_p + o_p(1)$ and

$$t_{\bullet,p}(h_n) = \theta^1_{p,0} \cdot \sum_{g \in \mathcal{G}_i} \int_{\mathcal{X}_{\mathcal{S}_i}(g)} m_{\bullet,g}(x_i, \boldsymbol{x}_{\mathcal{S}_i}) f(x_i, \boldsymbol{x}_{\mathcal{S}_i}) d\boldsymbol{x}_{\mathcal{S}_i} + o_p(1),$$

with

$$\Gamma^1_p = \int_0^1 K(u) r_p(u)\, du, \qquad \theta^1_{p,q} = \int_0^1 K(u) u^{p+q}\, du,$$

recalling the notation in Subsection S.3.1. Additionally, similarly to S.3.3 $\bar{\theta}_{\bullet,p,q} = f(0)\theta^1_{p,q} + o(1)$.

Finally, $nh_n \mathbb{V}\big[t^*_{1,0,p}(h_n)\big] = \big(\bar{\omega}_1(0) + \bar{\omega}_0(0)\big)\Psi^1_p + o(1)$ where for $\bullet \in \{0,1\}$

$$\bar{\omega}_\bullet(0) = \sum_{g \in \mathcal{G}_i} \int_{\mathcal{X}_{\mathcal{S}_i}(g)} \big(\sigma_{\bullet,g}(0, \boldsymbol{x}_{\mathcal{S}_i}) + (m_{\bullet,g}(0, \boldsymbol{x}_{\mathcal{S}_i}) - \tilde{\mu}_\bullet(0))^2\big) f(0, \boldsymbol{x}_{\mathcal{S}_i}) d\boldsymbol{x}_{\mathcal{S}_i}$$

Theorem S.4.1. *Suppose Assumptions 1–6, S.3.1, S.3.2, and S.3.3 hold (with Assumption S.3.1.c replaced by Assumption S.4.4, $S \geq p+2$). If $nh_n \to \infty$, $h_n \to 0$, and $h_n = O(n^{-1/(2p+3)})$, then*

$$\sqrt{nh_n} \frac{\Big(\hat{\tau}_{1|0,p}(h_n) - \tau_{1|0} - h_n^{p+1} B_{1,0,p,p+1}(h_n)\Big)}{\sqrt{V_{1,0,p}(h_n)}} \xrightarrow{d} \mathcal{N}(0,1),$$

where

$$B_{1,0,p,p+1}(h_n) = \Big(\frac{\tilde{\mu}_1^{(p+1)}(0) - \tilde{\mu}_0^{(p+1)}(0)}{(p+1)!}\Big) e_1^T (\Gamma^1_p)^{-1} \theta^1_{p,p+1} + o(1), \quad V_{1,0,p}(h_n) = \frac{\bar{\omega}_1(0) + \bar{\omega}_0(0)}{f(0)^2} e_1^T (\Gamma^1_p)^{-1} \Psi^1_p (\Gamma^1_p)^{-1} e_1$$

Proof. The proof parallels Theorem S.3.1. Define

$$Z_{i,1,p}(h_n) = e_1^T \bar{\Gamma}^{-1}_{1,p}(h_n) I_{1,i} K\Big(\tfrac{X_i}{h_n}\Big) r_p\Big(\tfrac{X_i}{h_n}\Big) \nu_{i,1}/n, \quad Z_{i,0,p}(h_n) = e_1^T \bar{\Gamma}^{-1}_{0,p}(h_n) I_{0,i} K\Big(\tfrac{X_i}{h_n}\Big) r_p\Big(\tfrac{X_i}{h_n}\Big) \nu_{i,0}/n,$$

and set $Z_{i,1,0,p}(h_n) = Z_{i,1,p}(h_n) - Z_{i,0,p}(h_n)$.

Then, $nh_n \mathbb{V}\big[\sum_i Z_{i,1,0,p}(h_n)\big] = V_{1,0,p}(h_n) = (\bar{\omega}_1(0) + \bar{\omega}_0(0))\Psi^1_p / f(0)^2 + o(1)$. Denote $\sigma_n^2 = V_{1,0,p}(h_n)/nh_n$ and $\xi_n = \sum_i Z_{i,1,0,p}(h_n)/\sigma_n$. By Assumption 6 and applying Stein's method with the bounds of Leung (2020, Theorem A.4), one obtains $\Delta(\xi_n, \mathcal{N}(0,1)) = O\big((nh_n)^{-1}\big) \to 0$. Thus $\xi_n \xrightarrow{d} \mathcal{N}(0,1)$.

Since $\sqrt{nh_n} \frac{\hat{\tau}_{1|0,p}(h_n)^*}{\sqrt{V_{1,0,p}(h_n)}} = \xi_n + o_p(1)$, the decomposition (S.4.2) and convergence of $\bar{\Gamma}_{d,p}(h_n)$ and $\bar{\theta}_{d,p,p+1}(h_n)$, for $d \in \{0,1\}$ to $f(0)\Gamma^1_p$ and $f(0)\theta^1_{p,p+1}$ gives the conclusion. $\square$

S.4.3 Variance Estimation and Bias Correction

Define

$$\begin{aligned}\mathcal{M}_{1,p}(h_n)^T &= \Big[I_{1,1}K\left(\frac{\tilde{X}_1}{h_n}\right)r_p\left(\frac{\tilde{X}_1}{h_n}\right)\hat{\xi}_{1,1}\ \cdots\ I_{n,1}K\left(\frac{\tilde{X}_n}{h_n}\right)r_p\left(\frac{\tilde{X}_n}{h_n}\right)\hat{\xi}_{n,1}\Big],\\ \mathcal{M}_{0,p}(h_n)^T &= \Big[I_{1,0}K\left(\frac{\tilde{X}_1}{h_n}\right)r_p\left(\frac{\tilde{X}_1}{h_n}\right)\hat{\xi}_{1,0}\ \cdots\ I_{n,0}K\left(\frac{\tilde{X}_n}{h_n}\right)r_p\left(\frac{\tilde{X}_n}{h_n}\right)\hat{\xi}_{n,0}\Big],\end{aligned} \tag{S.4.3}$$

where $\hat{\xi}_{i,1}$ and $\hat{\xi}_{i,0}$ are the regression residuals to the right and left of the cutoff, respectively.

An estimator of the asymptotic variance $\hat{\tau}_{1|0,p}(h_n)$ denoted by $\mathcal{V}_{1,0,p}(h_n)$ is

$$\hat{\mathcal{V}}_{1,0,p}(h_n) = \frac{1}{n}\, e_1^T\Big(\hat{V}_{1,p}(h_n) + \hat{V}_{0,p}(h_n) - 2\hat{V}_{1,0,p}(h_n)\Big)e_1, \tag{S.4.4}$$

with

$$\begin{aligned}\hat{V}_{1,p}(h_n) &= \Gamma_{1,p}^{-1}(h_n)\hat{\hat{\Psi}}_{1,p}(h_n)\Gamma_{1,p}^{-1}(h_n),\\ \hat{V}_{0,p}(h_n) &= \Gamma_{0,p}^{-1}(h_n)\hat{\hat{\Psi}}_{0,p}(h_n)\Gamma_{0,p}^{-1}(h_n),\\ \hat{V}_{1,0,p}(h_n) &= \Gamma_{1,p}^{-1}(h_n)\hat{\hat{\Psi}}_{1,0,p}(h_n)\Gamma_{0,p}^{-1}(h_n),\end{aligned} \tag{S.4.5}$$

where

$$\begin{aligned}\hat{\hat{\Psi}}_{1,p}(h_n) &= \mathcal{M}_{1,p}(h_n)\boldsymbol{W}_n\mathcal{M}_{1,p}(h_n)^T/n,\\ \hat{\hat{\Psi}}_{0,p}(h_n) &= \mathcal{M}_{0,p}(h_n)\boldsymbol{W}_n\mathcal{M}_{0,p}(h_n)^T/n,\\ \hat{\hat{\Psi}}_{1,0,p}(h_n) &= \mathcal{M}_{1,p}(h_n)\boldsymbol{W}_n\mathcal{M}_{0,p}(h_n)^T/n.\end{aligned} \tag{S.4.6}$$

Finally, we give the expression for the bias-corrected estimator of $\tau_{1|0}^{(v)}(0)$:

$$\hat{\tau}_{1|0,p,q}^{bc}(b_n, h_n) = \hat{\tau}_{1|0,p}(h_n) - \hat{\mathcal{B}}_{1,0,p,p+1}(h_n, b_n)$$

where $\hat{\mathcal{B}}_{1,0,p,p+1}(h_n, b_n)$ uses $e_{p+1}^T\hat{\beta}_{1,p+1}(b_n)$ and $e_{p+1}^T\hat{\beta}_{0,p+1}(b_n)$, where $\hat{\beta}_{1,p+1}(b_n)$ and $\hat{\beta}_{0,p+1}(b_n)$ are the $(p+1)$-order local polynomial estimators to the right amd to the left of the cutoff with bandwidth b_n.

S.5 Proof of Results in Online Appendix

S.5.1 Heterogeneous Effects

In this section, we show the convergence properties allowing for heterogeneous interference sets, effective treatment boundaries and outcome and score distributions. Hence, notable quantities including, $|\mathcal{S}_{i,n}|$ and $\bar{\mathcal{X}}_{i\mathcal{S}_{i,n}}(d,g,\,|\,d,g')$ are i-specific and indexed by n through their dependence on the network.

Let

$$f_{i,n,d,g,d',g'}(0) = \int_{\bar{\mathcal{X}}_{i\mathcal{S}_{i,n}}(d,g,\,|\,d,g')} f_i(x_i, \boldsymbol{x}_{\mathcal{S}_{i,n}}) d\mathcal{H}^{|\mathcal{S}_i|+1-\bar{s}}$$

be the boundary density, and denote for short $m_{i,n,\bullet}(0) = \mathbb{E}_i[Y_i(\bullet)\,|\,(X_i, \boldsymbol{X}_{\mathcal{S}_{i,n}}) \in \bar{\mathcal{X}}_{i\mathcal{S}_{i,n}}(d,g,\,|\,d,g')]$ for $\bullet \in \{(d,g),(d',g')\}$. We require the following assumptions to establish convergence of the estimator under heterogeneity.

Assumption S.5.5. *The interference sets satisfy* $\sup_{i,n}|\mathcal{S}_{i,n}| < \infty$. *Moreover, for some integer* $\bar{n}$, $\bar{s}_n = \bar{s}$ *for* $n \geq \bar{n}$, *where* $\bar{s}_n = \inf_i \bar{s}_{i,n}$.

Assumption S.5.6. *For some* $\kappa > 0$ *the following holds for* $(x_i, \boldsymbol{x}_{\mathcal{S}_i}) \in \mathcal{B}_\kappa(\bar{\mathcal{X}}_{i\mathcal{S}_{i,n}}(d,g,\,|\,d,g'))$:

a) $f_i(x_i, \boldsymbol{x}_{\mathcal{S}_{i,n}})$ *is bounded away from zero and continuous (and thus uniformly continuous) with common modulus of continuity over* i *and* n. *Moreover, as* $n \to \infty$

$$\frac{1}{n}\sum_{i:\bar{s}_i=\bar{s}} f_{i,n,d,g,d',g'}(0) \to \bar{f}^{\bar{s}}_{d,g,d',g'}(0).$$

b) $\mathbb{V}_i\big[Y_i(d,g)\mid X_i = x_i, \boldsymbol{X}_{\mathcal{S}_{i,n}} = \boldsymbol{x}_{\mathcal{S}_{i,n}}\big]$ *and* $\mathbb{V}_i\big[Y_i(d',g')\mid X_i = x_i, \boldsymbol{X}_{\mathcal{S}_{i,n}} = \boldsymbol{x}_{\mathcal{S}_{i,n}}\big]$ *are uniformly bounded and bounded away from zero over* i, n.

c) $m_{i,d,g}(x_i, \boldsymbol{x}_{\mathcal{S}_{i,n}})$ *and* $m_{i,d'g'}(x_i, \boldsymbol{x}_{\mathcal{S}_{i,n}})$ *are continuous (and thus uniformly continuous) with common modulus of continuity over* i *and* n. *Moreover, as* $n \to \infty$

$$\frac{1}{n}\sum_{i:\bar{s}_i=\bar{s}} m_{i,\bullet}(0) \to \bar{m}^{\bar{s}}_{\bullet}(0).$$

Theorem S.5.1. *Suppose Assumptions 1–3, 5–6, S.3.3, andS.5.5 S.5.6 hold. If* $nh_n^{\bar{s}} \to \infty$ *and* $h_n \to 0$, *then*

$$\hat{\tau}_{d,g|d',g'}(h_n) \xrightarrow{p} \frac{\bar{m}^{\bar{s}}_{d,g}(0) - \bar{m}^{\bar{s}}_{d',g'}(0)}{\bar{f}^{\bar{s}}_{d,g,d',g'}(0)}.$$

Proof. **Expectation of** $\Gamma_{d,g,p}(h_n)$**.** For $n \geq \bar{n}$,

$$= \frac{1}{nh_n^{\bar{s}}} \sum_{i \in V_g} \sum_{\ell_{i,n}} h_n^{s_{\ell_{i,n}} - \bar{s}} \int_{\mathcal{R}_{\ell_{i,n}}} \int_{N^{s_{\ell_{i,n}}}} K(\|\boldsymbol{u}\|) r_p(\|\boldsymbol{u}\|) r_p(\|\boldsymbol{u}\|)^T f(h_n \boldsymbol{u}, \boldsymbol{x}_{R_{\ell_i}})\, d\boldsymbol{u}\, d\boldsymbol{x}_{R_{\ell_i}} + \frac{1}{nh_n^{\bar{s}}} I_{ih_n}$$

where we recall V_g is the set of units for which g is achievable. For brevity, we will just use the subscript i in summation and leave the belonging in this set implicit.

Partition the sample into $i \in \mathcal{I}_{\bar{s}} := \{i : \bar{s}_{i,n} = \bar{s}\}$ and $i \in \mathcal{I}_{>\bar{s}} := \{i : \bar{s}_{i,n} > \bar{s}\}$.

$$\begin{aligned}\mathbb{E}[\Gamma_{d,g,p}(h_n)] = &\frac{1}{n} \sum_{\mathcal{I}_{\bar{s}}} \sum_{\ell_{i,n}} h_n^{s_{\ell_{i,n}} - \bar{s}} \int_{\mathcal{R}_{\ell_{i,n}}} \int_{N^{s_{\ell_{i,n}}}} K(\|\boldsymbol{u}\|) r_p(\|\boldsymbol{u}\|) r_p(\|\boldsymbol{u}\|)^T f(\boldsymbol{u} h_n, \boldsymbol{x}_{R_{\ell_i}})\, d\boldsymbol{u}\, d\boldsymbol{x}_{R_{\ell_i}} + \frac{1}{nh_n^{\bar{s}}} I_{ih_n} \\ &+ \frac{1}{n} \sum_{\mathcal{I}_{>\bar{s}}} \sum_{\ell_{i,n}} h_n^{s_{\ell_{i,n}} - \bar{s}} \int_{\mathcal{R}_{\ell_{i,n}}} \int_{N^{s_{\ell_{i,n}}}} K(\|\boldsymbol{u}\|) r_p(\|\boldsymbol{u}\|) r_p(\|\boldsymbol{u}\|)^T f(\boldsymbol{u} h_n, \boldsymbol{x}_{R_{\ell_i}})\, d\boldsymbol{u}\, d\boldsymbol{x}_{R_{\ell_i}} + \frac{1}{nh_n^{\bar{s}}} I_{ih_n}\end{aligned}$$

The terms in the summation over $\mathcal{I}_{>\bar{s}}$ are $O(h_n)$ by Assumption S.5.6.a, S.3.3, and because $h_n^{s_{\ell_{i,n}} - \bar{s}} = O(h_n)$ and $\sum_{\ell_{i,n}} \mathrm{Vol}(\mathcal{R}_{\ell_{i,n}})$ is uniformly bounded (Assumption S.5.5). Hence, it suffices to study the first summation over $\mathcal{I}_{\bar{s}}$. By an analogous decomposition as in Lemma S.3.1

$$\frac{1}{n} \sum_{\mathcal{I}_{\bar{s}}} \sum_{\ell_{i,n} : s_{\ell_{i,n}} = \bar{s}} \int_{\mathcal{R}_{\ell_{i,n}}} \int_{N^{\bar{s}}} K(\|\boldsymbol{u}\|) r_p(\|\boldsymbol{u}\|) r_p(\|\boldsymbol{u}\|)^T f(\boldsymbol{u} h_n, \boldsymbol{x}_{R_{\ell_i}})\, d\boldsymbol{u}\, d\boldsymbol{x}_{R_{\ell_i}} + \frac{1}{nh_n^{\bar{s}}} I_{ih_n} + I(s_{\ell_{i,n}} > \bar{s})$$

where $I(s_{\ell_{i,n}} > \bar{s})$ collects terms depending on higher-codimension pieces, each $O(h_n)$ uniformly in i and n.

By Assumption S.5.6.a, there exists a common modulus of continuity $\omega : [0, \infty] \to [0, \infty]$ such that, uniformly over i, over pieces ℓ_i and over $\boldsymbol{x}_{\mathcal{R}_{\ell_{i,n}}}$,

$$\left| f_i(h_n \boldsymbol{u}, \boldsymbol{x}_{\mathcal{R}_{\ell_{i,n}}}) - f_i(\boldsymbol{0}, \boldsymbol{x}_{\mathcal{R}_{\ell_{i,n}}}) \right| \leq \omega(\, h_n \|\boldsymbol{u}\|\,).$$

Hence,

$$\frac{1}{n}\sum_{\mathcal{I}_{\bar{s}}}\sum_{\ell_{i,n}:s_{\ell_{i,n}}=\bar{s}}\int_{\mathcal{R}_{\ell_{i,n}}}\int_{N^{\bar{s}}} K(\|\boldsymbol{u}\|)\, r_p(\|\boldsymbol{u}\|) r_p(\|\boldsymbol{u}\|)^T \left| f_i(h_n\boldsymbol{u}, \boldsymbol{x}_{\mathcal{R}_{\ell_{i,n}}}) - f_i(\boldsymbol{0}, \boldsymbol{x}_{\mathcal{R}_{\ell_{i,n}}})\right| d\boldsymbol{u}\, d\boldsymbol{x}_{\mathcal{R}_{\ell_{i,n}}}$$
$$\leq \frac{\omega(\,h_n\|\boldsymbol{u}\|\,)}{n}\sum_{\mathcal{I}_{\bar{s}}}\mathrm{Vol}(\bar{\mathcal{X}}_{i\mathcal{S}_{i,n}}(d,g\,|\,d',g'))\int_{N^{\bar{s}}} K(\|\boldsymbol{u}\|)\,\|\boldsymbol{u}\|^k\, d\boldsymbol{u} \;\to\; 0,$$

as $n \to \infty$ and $h_n \to 0$ since $\mathrm{Vol}(\bar{\mathcal{X}}_{i\mathcal{S}_{i,n}}(d,g\,|\,d',g')) = \sum_{\ell_{i,n}:s_{\ell_{i,n}}=\bar{s}} \mathrm{Vol}(\mathcal{R}_{\ell_{i,n}})$ is bounded uniformly over i, n by Assumption S.5.5. Moreover,

$$\frac{1}{n}\sum_{\mathcal{I}_{\bar{s}}}\sum_{\ell_{i,n}:s_{\ell_{i,n}}=\bar{s}}\int_{\mathcal{R}_{\ell_{i,n}}} f(\boldsymbol{0}, \boldsymbol{x}_{\mathcal{R}_{\ell_{i,n}}})\, d\boldsymbol{x}_{R_{\ell_i}} \;\longrightarrow\; \bar{f}^{\bar{s}}_{d,g,d',g'}(0) \quad \text{by Assumption S.5.6.a.}$$

Therefore,

$$\frac{1}{n}\sum_{\mathcal{I}_{\bar{s}}}\sum_{\ell_{i,n}:s_{\ell_{i,n}}=\bar{s}}\int_{\mathcal{R}_{\ell_{i,n}}}\int_{N^{\bar{s}}} K(\|\boldsymbol{u}\|)\, r_p(\|\boldsymbol{u}\|) r_p(\|\boldsymbol{u}\|)^T\, f_i(h_n\boldsymbol{u}, \boldsymbol{x}_{\mathcal{R}_{\ell_{i,n}}})\, d\boldsymbol{u}\, d\boldsymbol{x}_{\mathcal{R}_{\ell_{i,n}}}$$
$$\to \bar{f}^{\bar{s}}_{d,g,d',g'}(0)\int_{N^{\bar{s}}} K(\|\boldsymbol{u}\|)\,\|\boldsymbol{u}\|^k\, d\boldsymbol{u}.$$

Hence, $\mathbb{E}[\Gamma_{d,g,p}(h_n)] = \bar{f}^{\bar{s}}_{d,g,d',g'}(0)\Gamma^{\bar{s}}_p + o(1)$.

Expectation of $t_{d,g,p}(h_n)$. We expand $\mathbb{E}[t_{d,g,p}(h_n)]$

$$= \frac{1}{nh_n^{\bar{s}}}\sum_{i\in V_g}\sum_{\ell_{i,n}} h_n^{s_{\ell_{i,n}}-\bar{s}}\int_{\mathcal{R}_{\ell_{i,n}}}\int_{N^{s_{\ell_{i,n}}}} K(\|\boldsymbol{u}\|) r_p(\|\boldsymbol{u}\|) m_{d,g}(h_n\boldsymbol{u}, \boldsymbol{x}_{R_{\ell_i}}) f(h_n\boldsymbol{u}, \boldsymbol{x}_{R_{\ell_i}})\, d\boldsymbol{u}\, d\boldsymbol{x}_{R_{\ell_i}} + \frac{1}{nh_n^{\bar{s}}} I_{ih_n}$$

Dividing and multiplying by $f_{i,n,d,g,d',g'}(0)$, which is positive by Assumption S.5.6.a, and using common modulus of continuity of $m_{i,d,g}(x_i, \boldsymbol{x}_{\mathcal{S}_{i,n}})$ and $f_i(x_i, \boldsymbol{x}_{\mathcal{S}_{i,n}})$ yields

$$\mathbb{E}[t_{d,g,p}(h_n)] \to \quad \theta^{\bar{s}}_{p,0}\cdot \bar{m}^{\bar{s}}_{d,g}(0)$$

Convergence in probability Under Assumptions 5–6 and bounded conditional variances (Assumption S.5.6.b) the element-wise variance of $\Gamma_{d,g,p}(h_n)$ and $t_{d,g,p}(h_n)$ is $O((nh_n^{\bar{s}})^{-1})$ by analgous arguments as in Lemma S.3.1) and S.3.2

$$\Gamma_{d,g,p}(h_n) \;=\; \bar{f}^{\bar{s}}_{d,g,d',g'}(0)\Gamma^{\bar{s}}_p \;+\; o_p(1), \qquad t_{d,g,p}(h_n) \;=\; \theta^{\bar{s}}_{p,0} \;+\; o_p(1),$$

Limit of the estimator. By continuous mapping and the identity $e_1^\top(\Gamma^{\bar{s}}_p)^{-1}\theta^{\bar{s}}_{p,0} = 1$,

$$e_1^T \hat{\beta}_{d,g,p}(h_n) = e_1^\top \Gamma_{d,g,p}(h_n)^{-1} t_{d,g,p}(h_n) \xrightarrow{p} \frac{\bar{m}^{\bar{s}}_{d,g}(0)}{\bar{f}_{d,g,d',g'}(0)}$$

Repeating the argument for (d', g') and taking the difference gives the stated probability limit for $\hat{\tau}_{d,g,d',g',p}(h_n)$. □

References

Simon, L. (1984). Lectures on geometric measure theory. In *Proceedings of the Centre for Mathematical Analysis*, volume 3.